Novel Heat-Bath Algorithmic Cooling methods

by

Nayeli Azucena Rodríguez Briones

A thesis
presented to the University of Waterloo
in fulfillment of the
thesis requirement for the degree of
Doctor of Philosophy
in
Physics (Quantum Information)

Waterloo, Ontario, Canada, 2020

Examining Committee Membership

The following served on the Examining Committee for this thesis. The decision of the Examining Committee is by majority vote.

External Examiner:	Jonathan Oppenheim Professor, Dept. of Physics, University of College London
Supervisor(s):	Raymond Laflamme Professor, Dept. of Physics and Astronomy, University of Waterloo
	Eduardo Martín-Martínez Associate Professor, Dept. Applied Math, University of Waterloo
	Achim Kempf Professor, Dept. Applied Math, University of Waterloo
Internal Member:	Crystal Senko Professor, Dept. of Physics and Astronomy, University of Waterloo
Internal-External Member:	Christopher Wilson Professor, Dept. of Electrical and Computer Engineering, University of Waterloo
Internal-External Member:	Jonathan Baugh Professor, Dept. of Chemistry, University of Waterloo

Author's Declaration

This thesis consists of material all of which I authored or co-authored: see Statement of Contributions included in the thesis. This is a true copy of the thesis, including any required final revisions, as accepted by my examiners.

I understand that my thesis may be made electronically available to the public.

Statement of Contributions

NOTE: Supervision from Prof. Raymond Laflamme should be assumed in all of the below. Contributors to the work with non-overlapping contributions with N. Rodríguez Briones are not mentioned.

- Chapter 3.
  - N. Rodríguez Briones derived the analytical results of the achievable cooling limits for the PPA-HBAC protocol.
  - N. Rodríguez Briones gave the analytic form of system state in the cooling limit when the initial state is maximally mixed.
  - N. Rodríguez Briones obtained an upper bound on the number of steps required to get a certain polarization.
- Chapter 4.
  - N. Rodríguez Briones, T. Mor, Y. Weinstein and R. Laflamme described for the first time the NOE effect in terms of processing of information.
  - N. Rodríguez Briones presented explicit improved cooling algorithms (the SRΓ_n-HBAC protocols) which lead to an increase of purity beyond all the previous work.
  - N. Rodríguez Briones, T. Mor, Y. Weinstein and R. Laflamme introduced a new tool for cooling algorithms(the 'state-reset' operation).
  - N. Rodríguez Briones derived the new achievable cooling limits for the SRΓ_n-HBAC protocols.
- Chapter 5
  - Supervision and collaboration from Professors E. Martín-Martínez, A. Kempf and R. Laflamme should be assumed in all the results of this chapter.
  - N. Rodríguez Briones and E. Martín-Martínez proposed the quantum energy teleportation protocol for increasing the purity of interacting quantum systems that takes advantage of correlations present due to the internal interaction.
  - N. Rodríguez Briones performed the simulations of the new protocol

- Chapter 6
  - N. Rodríguez Briones and Robert Spekkens conceived the idea of using ideas and concepts from resource theory to study the limits of HBAC.
  - N. Rodríguez Briones derived all the results of this chapter.
- Appendix C
  - N. Rodríguez Briones performed the simulations of CP-local passivity in explicit quantum systems.
  - N. Rodríguez Briones proved that the sufficient physical conditions to have a system in a CP-local passive state are not necessary (supported with numerical examples)

The work presented contains material from the following publications and preprints:

- N. Rodríguez Briones, and R. Laflamme, "Achievable polarization for Heat-Bath Algorithmic Cooling", Phys. Rev. Lett. 116, 170501 (2016) [93, 91]
- N. Rodríguez Briones, E. Martín-Martínez, A. Kempf, and R. Laflamme, "Correlation-Enhanced Algorithmic Cooling", Phys. Rev. Lett. 119 (5), 050502 (2017) [90]
- N. Rodríguez Briones, J. Li, X. Peng, T. Mor, Y. Weinstein, and R. Laflamme, "Heat-Bath Algorithmic Cooling with correlated qubit-environment interactions", New Journal of Physics 19 (11), 113047, (2017) [89]
- A. Alhambra, G. Styliaris, N. Rodríguez Briones, J. Sikora, and E. Martín-Martínez, "Fundamental limitations to local cooling of quantum systems", Phys. Rev. Lett. 123, 190601 (2019) [2]
- N. Rodríguez Briones, R. Spekkens, "N-to-1 distillation of athermality for two-level systems", in progress

Other publications completed during the duration of my PhD but not included in this thesis are:

- E McKay, N. Rodríguez-Briones, and E. Martín-Martínez, "Fluctuations of work cost in optimal generation of correlations", Phys. Rev. E 98, 032132 (2018) [70]
- N. Rodríguez Briones, "Computación cuántica", Science Outreach article. Eek Magazine. Consejo Zacatecano de Ciencia, Tecnología e Innovación (2017) [92]
- D. K. Park, N. Rodríguez Briones, G. Feng, R. Rahimi, J. Baugh, and R. Laflamme, "Heat Bath Algorithmic Cooling with Spins: Review and Prospects", Book Chapter in L. Berliner et al. (eds.), Electron Spin Resonance (ESR) Based Quantum Computing, Biological Magnetic Resonance 31, DOI 10.1007/978-1-4939-3658-8-8, Springer New York 2016) [78]

Abstract

The field of quantum information has inspired new methods for cooling physical systems at the quantum scale by manipulating entropy in an algorithmic way, such as heat-bath algorithmic cooling (HBAC). These methods not only provide fundamental insight into quantum thermodynamics, but they are also at the core of practical applications in quantum science and quantum technologies. Arguably, the most promising practical applications are in quantum computing, for the preparation of pure states. The ability to prepare highly pure states is required both for initializing qubits in most quantum algorithms and for supplying reliable low-noise ancilla qubits that satisfy the fault-tolerance threshold for quantum error correction (achieving the high levels of purity required represents one of the major challenges not only for ensemble implementations but also for technologies with strong but not perfect projective measurements).

The heat bath algorithmic cooling protocols have inspired the work within this thesis, which examines and proposes powerful new techniques that significantly enhance cooling by taking advantage of classical and quantum correlations. These new methods go beyond the limits of conventional cooling techniques, providing a novel way to cool that allows a generalized interaction of the system with the environment, which has not been taken into account in previous work. Concretely, I have contributed to elucidating our understanding of these algorithmic cooling mechanisms by using techniques from quantum information theory and quantum thermodynamics. First, I found the analytical solution of the maximum achievable cooling of these algorithmic cooling methods, which had been a longstanding problem that remained open for almost 15 years. Then, I showed how to circumvent the cooling limits of the conventional algorithmic cooling – which were widely believed to be optimal –, creating novel methods that show how correlations can be used to significantly improve cooling. On the one hand, we fundamentally changed the way previous methods considered the interactions between the system and environment and showed how correlated relaxation processes can be essential for enhancing cooling. On the other hand, we demonstrated that correlations present in the initial state due to internal interactions can be exploited to improve cooling. Finally, we showed how, by using ideas and concepts from resource theory, it is possible to find the optimal entropy compression required for HBAC by studying the n-to-1 distillation of athermality of two level systems.

The main contribution of these thesis is listed as follows:

Obtaining the maximum achievable cooling of algorithmic cooling. The theoretical limit of algorithmic cooling has been a longstanding open problem for more than a decade, after Schulman et al. proved the existence of the physical limits [98], and only bounds and numerical estimations had been provided. In particular, the limits were studied using a specific algorithm, the Partner Pairing Algorithm [98] which is optimal under the assumption that the interaction of the system with the environment causes individual-qubit relaxation. In my research, we completely resolved the problem by finding the analytical solution for the achievable cooling limits and the asymptotic steady state of the system [93].

Enhancing cooling by designing novel techniques that exploit correlated relaxation processes [89]. We generalized the allowed interactions of the quantum system with the environment by including crossed relaxation processes, which is a crucial step that had not been taken into account in previous works. We then designed new tools to refresh qubits with steps where the bath only couples to certain energy transitions during the relaxation process, and presented explicit protocols that go beyond all previous Heat-Bath Algorithmic Cooling techniques.

Characterized the fundamental limitations for local cooling quantum systems [2]. We provided the necessary and sufficient conditions to have in a quantum system the impossibility to extract energy by means of any general local map on a system. We bounded the critical temperature at which below this property appears in the system.

Enhancing cooling by taking advantage of correlations due to internal interactions [90]. These results pushed beyond the cooling limits by combining techniques from quantum field theory to exploiting internal correlations of the system. Concretely, we used quantum energy teleportation protocols to extract energy locally from the target qubit while removing correlations due to internal interactions, considerably improving the final purity of the target qubit.

Explaining optimal operations of HBAC with resource theories tools We showed how, by using ideas and concepts from resource theory, it is possible to find the optimal entropy compression and connect with the distillation of athermality from two level systems.

Acknowledgements

First and foremost I want to thank my supervisor Dr. Raymond Laflamme for his support over the past years. I have been very lucky to have such a fantastic supervisor! Ray, I truly appreciate your kindness and all the guidance during this journey, as well as the freedom to explore my research interests. It is always (always) a pleasure talking to you! Thank you for sharing your wisdom, your amazing stories and your passion for science.

I would also like to express my gratitude for my two other supervisors (yes, I have three supervisors). Eduardo, I cannot thank you enough for motivating me and for sharing your enthusiasm for science (I've always thought your eyes sparkle when you talk about science). Achim, thank you for all your generous support and for piquing my curiosity: listening to your great stories about life and general knowledge of the universe always made me want to keep exploring and learning!

I would like to take this opportunity to acknowledge all my colleagues of IQC and Perimeter Institute. The collaboration and discussions with great members of IQC and PI such as Prof. Rob Spekkens, Lauren Hayward, Alvaro Alhambra, Jamie Sikora, Meenu Kumari, Hemant Katiyar and Junan Lin among others have been extremely stimulating and enriching from a scientific perspective and have also led to long lasting friendships.

During my stay I have had the fortune of meeting amazing people who have become great friends, especially Lauren Hayward, Paulina Corona, Luis Ruiz, Néstor Ortiz and Aida Ahmadzadegan. I value your friendship immensely! Also special thanks and hugs to Maria Papageorgiou, Jose Pipo de Ramon, Pavel Shuldiner and Dainy Manzana for becoming my family far away from home and making Waterloo a fun place.

Yorgo, thank you for your love and for motivating me to become a better version of myself.

I am forever thankful to all my family. Being away from you has been tremendously hard! Mom and Dad, thank you for your unconditional love and support, for which I do not have enough words.

Table of Contents

List of Figures

Chapter 1

Introduction and motivation

Quantum information science gives us a new language to ponder and understand our universe in terms of the evolution of information. This information language not only allows us to reinterpret the laws of nature in an enriched conceptual framework of information, it also provides us with powerful mathematical tools that can be used both to tackle some of the major open questions in physics and to bring novel practical applications. Furthermore, understanding the essence of information in the quantum regime, such as how information is stored, transmitted and processed in quantum systems, allows us to develop tasks of unprecedented capabilities with remarkable applications in quantum science and quantum technologies. One of these tasks is cooling, which has the potential to elucidate fundamental theoretical properties in quantum thermodynamics, lead to new experimental possibilities with genuine quantum effects, and bring applications for quantum technologies [61, 79].

Indeed, the field of quantum information has inspired new methods for cooling physical systems at the quantum scale by manipulating entropy in an algorithmic way [11, 100, 29, 98, 99, 105, 106], verifying that energy transport and information processing are two sides of the same coin. These methods, known as algorithmic cooling protocols, decrease the entropy of quantum systems by applying alternating rounds of suitable internal redistributions of entropy – through reversible entropy compression operations – and contact with a thermal bath to pump entropy out of the system [7, 11, 78, 29]. These cooling methods not only provide an essentially novel way to cool, but can also go beyond the cooling limits of conventional cooling techniques [98, 93], bringing important applications in quantum

science and technologies.

Arguably, the most promising practical applications are in quantum computing.Quantum computing has the potential to revolutionize the way in which we process information and communicate by harnessing the laws of quantum mechanics. Concretely, quantum features, such as quantum superposition and entanglement, enable development of new algorithms that considerably outperform classical algorithms, and promise the possibility of dramatically speeding up computations and simulations. Some of the most important examples are simulating quantum phenomena [31], factoring large numbers [101, 102], and increasing speed in database searching [42] [1]. However, physically constructing a quantum computer crucially requires the ability to prepare qubits in a pure state, which is a big challenge in quantum computing, not only for ensemble implementations but also for strong but imperfect projective measurements. In fact, the importance of the pure state preparation is widely known as part of the DiVicenzo criteria [24], which consists of 5 basic requirements that any experimental platform must meet in order to reliably perform a quantum computer. This preparation of highly pure qubits is required in the initialization stage of most quantum algorithms, and for supplying reliable low-noise ancilla qubits that satisfy the fault-tolerance threshold for quantum error correction [58, 21].

In fact, the preparation of highly pure states is one of the major challenges for quantum computing and quantum thermodynamics. On the one hand, even though, in theory, ideal pure states can be obtained through projective measurements or cooling them to very low temperatures, such luxury is not possible in the lab. As it has been demonstrated in Ref. [43], ideal projective measurements have infinite resource costs, which is also deeply related with the third law of Thermodynamics [69, 33]. On the other hand, for ensemble implementations –such as NMR and ESR [61]– a different technique might be needed, since it is not possible to have individual access to systems, and only average values of certain observables are measurable. This restriction, added to the fact that in typical ensemble systems the qubits are highly mixed at room temperature, constitutes an extremely difficult problem.

Heat-bath algorithmic cooling (HBAC) constitutes a potential solution designed to pu-

[1] More breakthroughs of the quantum revolution are still expected to come, for example to solve mathematical problems once thought to be intractable, develop unbreakable encryption of information, build time-keeping devices with unparalleled precision, and make ultra-sensitive detectors with extraordinary accuracy, among others.

rify qubits by using a different approach that exploits tools from quantum information processing to increase purity by cooling. This approach provides a fresh set of device-independent protocols that work not only for ensemble implementations but also for technologies with strong but imperfect measurements [61, 7, 30, 27, 14, 15, 77, 96, 11, 100, 29, 98, 99, 61].

The question at the heart of this thesis is how to provide more refined algorithmic cooling protocols that take advantage of correlations to enhanced cooling, which has not been taken into account in previous protocols. In particular, I explore relaxation processes where the bath only couples to certain energy transitions in the context of quantum information processing, to go beyond all previous HBAC techniques. Then, we show how correlations present in the initial state due to internal interactions can be exploited to improve cooling. Finally, by using ideas and concepts from resource theory, we show how it is possible to find the optimal entropy compression required for HBAC by studying the n-to-1 distillation of athermality of two level systems.

1.1 Introduction of Heat-Bath Algorithmic Cooling

Ole W. Sørensen [106, 107, 105], while studying the relation between entropy and the bounds on the attainable states for spins [2], observed for the first time how unitary dynamics allows to decrease the entropy of a subset of qubits at the expense of increasing the entropy of the complementary qubits, and also provided bounds to what later would be called reversible entropy compression –one of the building blocks for the algorithmic cooling protocols.

An explicit way to implement this redistribution of entropy, in the context of quantum information, was given by Schulman and Vazirani [100], who proposed cooling algorithms for ensemble quantum computers. Their protocol, which they called the "quantum mechanical heat engine" [100], carries out a reversible process in which an input of energy to the system results in a separation of cold and hot regions. This method, particularly inspired by Peres's recursive algorithm [83], was a reinterpretation in thermodynamic terms of a

[2] Sørensen provided the so-called "universal bound on spin dynamics". This theorem gives the maximum possible projection of a final state in the Liouville space on any state vector, starting from an arbitrary initial state, under only unitary transformations [107, 105]

simple step introduced by von Neumann to extract fair coin flips from sequences of biased coin flips [112]. Schulman and Vazirani showed that it is possible to reach polarization (purity – see Chapter 2, for the definitions) of order unity in the cold region using only a number of identical qubits in the system which is polynomial in the initial polarization ϵ_b (where the polarization ϵ is related to the purity $\mathcal{P}$ by $\epsilon = \sqrt{2\mathcal{P}-1}$, for ϵ in the eigenbasis of ρ, see background in Chapter 2). Specifically, the number of qubits scales as $1/\epsilon_b^2$ for very low initial polarizations $\epsilon_b \ll 1$.

This scheme, later named "reversible algorithmic cooling", was improved by adding contact with a heat bath to cool the qubits that were heated during the process [11]. This improved method – called "Heat-Bath Algorithmic Cooling" (HBAC) – allows entropy to keep being pumped out of the system to the heat-bath after each irreversible entropy-compression step in an iterative way. Beyond theoretical interest, proof-of-principle experiments have demonstrated reversible algorithm cooling [17] and heat-bath algorithm cooling [30, 7, 96, 27, 15, 77]. These studies have shown improvement in polarization for a few qubits after a few rounds of HBAC were performed, and some studies have even included the impact of noise [55]. Based on this idea, many other cooling algorithms have been designed and proposed experimentally [29, 73, 98, 26, 99, 28, 55, 15].

Furthermore, while originally algorithmic cooling was mainly focused on ensemble quantum computing implementations [17, 30, 27, 15, 7, 96, 77, 78], it can also be used to increase the purity of quantum states up to the fault-tolerance threshold for technologies with strong but imperfect projective measurements (e.g. in superconducting qubits, quantum optics, etc). This technique could also be used to complement randomized benchmarking techniques by distinguishing state and measurement errors. Another potential use of algorithmic cooling is for improving the signal to noise ratio in NMR and MRI applications [30, 72] (see also the corresponding limitations analyzed in [15]). Finally, algorithmic cooling is of interest to the community of quantum thermodynamics.

Cooling bounds for the Algorithmic cooling protocols

Even though HBAC had already been performed in the lab for several rounds and had been studied through numerical simulations, the cooling limits of these techniques remained an open problem for almost 15 years. The first attempts for providing bounds and numerical evidence of the limits of the cooling algorithms were given by Schulman et al. [98, 99], and

Moussa [73]. Moussa and Schulman observed that if the polarization of the bath (ϵ_b) is much smaller than 2^{-n}, where n is the total number of qubits, the asymptotic polarization reached would be $\sim 2^{n-2}\epsilon_b$. However, when ϵ_b is greater than 2^{-n}, a polarization of order one can be reached. Nevertheless, the actual limits of the HBAC protocols were not well understood.

The limits of HBAC have been studied using a specific algorithm, the Partner Pairing Algorithm (PPA), which was introduced by Schulman, Mor and Weinstein [98], and claimed to be optimal among all possible HBAC protocols [99]. Based on this statement, it has been claimed that the fundamental limits for all HBAC techniques under general conditions should be given by the limits of the PPA protocol [88]. The exact steady state of the cooling limit of PPA was recently found and presented in Refs. [93, 88]. However, we later found and proved that the claim about the "fundamental cooling limits" is incorrect [89, 94], and this is where the story of our contributions, presented in this thesis, begins.

1.2 Main contributions and organization of this thesis

After we solved the problem of finding the analytical solution for the achievable cooling of the PPA method [91, 93, 79] [3], we found an implicit assumption within Schulman et al.'s optimization of the PPA protocol , which can be removed to give a more general interaction with the bath and improve the achievable cooling. Concretely, in Schulman's et. al's proof, it was assumed that the optimal use of the heat bath was to fully thermalize the qubits that are allowed to make contact with the bath. However, we found that better purification can be achieved by removing the restriction of individual relaxation and include correlation between qubits as they reset, also known as cross-relaxation.

In more detail, we introduced a novel tool that thermalizes only selected pairs of energy

[3] We analytically solved for the achievable cooling of the PPA HBAC method for the generalized case of cooling a target qubit from a system setup of dimension $2d$ (for instance, for a target qubit withing a string of n qubits, we have $2d = 2^n$) and m extra qubits that come in contact with a bath. [91, 93, 79].

The analytic result for the maximum achievable cooling of PPA can be reached for a totally mixed initial state, which gives an achievable bound as we can always efficiently turn a state into the maximally mixed one, while some other initial states do lead to higher polarizations.

The asymptotic polarization of order one can be reached doubly exponentially in the number of qubits (or exponential as a function of the size of the Hilbert space of the system). See chapter 3 for a more detailed description.

levels of the system, instead of completely thermalizing the qubits as in previous protocols. This operation, which we have called the "reset-state operation", can occur when the coupling to the environment includes correlations between the qubits of the system, making cross-relaxation processes possible. The reset-state operation uses correlated decay processes, in contrast to the full thermalization, which requires only single qubits decay. Furthermore, we give a physical description for how such correlations exist in real physical systems and relate this new technique to the Nuclear Overhauser Effect (NOE).

We present explicit new cooling algorithms that lead to an increased purity beyond the achievable cooling of the PPA, as the coupling to the environment is not limited to independent qubit-relaxation. In our first model, we remove the restriction of individual relaxation and include correlation between qubits as they reset to have cross-relaxation processes. We generalize our algorithm to the case where we use both cross relaxations and independent qubit-relaxations and show an improvement on cooling. We present the analytical maximum achievable polarization for our methods as a function of the dimension of the system used and the heat-bath polarization.

Our results show how by taking advantage of correlations during the refresh step, the long standing upper bound on the limits of algorithmic cooling [98] can be surpassed. Indeed, recent work has suggested that quantum correlations are important in work extraction and entropy flows in cooling protocols [34, 16, 81, 94, 66, 36, 40, 23].

Furthermore, in our second main contribution, we relaxed another assumption underlying all previous HBAC methods, which is that the qubits are not interacting or initially correlated [29, 73, 98, 26, 99, 28, 55]. In practice, the qubits typically possess correlations of both classical and quantum origin, generated, respectively, thermally and through interaction-induced entanglement. Nevertheless, algorithms such as the PPA do not make use of correlations in the system; what is more, these PPA-like algorithms include steps (rethermalization with the environment for resetting qubits) that break quantum and classical correlations in the system.

In our second model, we generalize HBAC to allow the presence of correlations, and we show that these correlations provide a resource that can be used to improve the efficiency of HBAC methods beyond previously-established limits, in particular when this interaction is sufficiently strong. The underlying principle behind the improvement requires the notion of local passivity, i.e. the impossibility to extract energy by using general local operations.

Our method improves cooling by using pre-existing correlations to remove energy instead of breaking them during the thermalization processes. In particular, we implement ideas from the so-called Quantum Energy Teleportation (QET) protocol [51, 35, 53, 34, 50, 48, 109, 49, 52, 111].This protocol allows us to break the local passivity of a part of the system by taking advantage of pre-existing correlations in an interacting system together with classical communication (or quantum communication [52]).

Finally, we show how to combine ideas and concepts from resource theories in which the thermodynamic processes are characterized by the attainable states under a restricted set of physical operations. Concretely, we present the analytic expression of the athermal Lorenz curve for N identical qubits. Then, we approximated it for the case of large N. We related our result with the entropy compression needed for algorithmic cooling, and we obtained the maximum achievable purity for a target qubit in a single shot. In particular, we considered two different scenarios that allow the following operations: in one scenario the thermal operations, and in the other global unitary operations. We present a proof of the best entropy compression under the aforementioned allowed operations by using the Thermo-majorization curves and Lorenz curves, respectively.

Other results, not included here, are the cooling limitations to local energy extraction in quantum systems [2]. We found the necessary and sufficient conditions for CP-local passivity, i.e. the impossibility to extract energy under the the most general type of local access to quantum systems, which is given by the completely positive trace-preserving (CPTP) maps. These conditions take the form of a simple inequality of operators. We also derived simpler sufficient conditions that show definite physical situations in which this phenomenon appears, and we provide numerical examples illustrating the general picture. We also strengthened a previous result of Frey et al. [34] by showing a physically relevant quantitative bound on the threshold temperature at which this passivity appears. Furthermore, we showed how this no-go result also holds for thermal states in the thermodynamic limit, provided that the spatial correlations decay sufficiently fast, and we give numerical examples.

Furthermore, our new techniques and protocols have inspired and influenced other works to further improve cooling techniques. An example is the work of Alhambra et al. [1], who pushed to its limits our idea of considering relaxation processes that act only on certain energy transitions of the ancillas coupled to the bath. Alhambra et al. optimized the corresponding strategies under general thermalization processes and found HBAC protocols

that can obtain ground state cooling with an exponential convergence with the number of rounds. Interestingly, the cooling enhancements are due to non-Markovian thermalisation dynamics, which suggests that memory effects can be exploited to improve cooling, which has been recently explored in Ref. [108]

In summary, this thesis' main contribution can be summarized as a significant improvement to previous algorithmic cooling techniques, which were believed to be optimal, by taking advantage of correlations in two different ways. In the first protocol, the correlations that we take advantage of are due to correlated relaxation processes between the qubit and environment when we refresh the qubits. In the second protocol, we take advantage of the correlations present in the initial state due to internal interactions. Furthermore, we give a physical description of how such correlations exist in real physical systems and provide a realistic algorithm to exploit them.

Contents of the Thesis

In this thesis, I will first review the basic ideas of algorithmic cooling (Chapter 2) and give analytical results for the achievable cooling limits for the PPA heat-bath protocol (Chapter 3). Then, I will show how the limits can be circumvented by using correlations. In one algorithm I take advantage of correlations that can be created during the rethermalization step with the heat-bath (Chapter 4) and in another I use correlations present in the initial state that are induced by the internal interactions of the system (Chapter 5). These two algorithms show how correlations can be used to improve cooling. Then, I will show how, by using ideas and concepts from resource theory, it is possible to find the optimal entropy compression and connect with the distillation of athermality from two level systems (Chapter 6).

- **Chapter 2:** Review of the basic ideas of algorithmic cooling
- **Chapter 3:** Analytical results for the achievable cooling limits for the PPA heat-bath protocol
- **Chapter 4:** How the cooling limits of the PPA method can be circumvented by using correlations. Explicit novel cooling algorithms that take advantage of correlations created during the rethermalization step with the heat-bath

- **Chapter 5** A generalization of the HBAC methods to interacting systems. Explicit cooling techniques that use correlations present in the initial state that are induced by the internal interactions of the system
- **Chapter 6** How, by using ideas and concepts from resource theory, it is possible to find the optimal entropy compression and connect with the distillation of athermality from two level systems
- **Chapter 7** Conclusions

Supplemental material is presented in the appendices at the end of the thesis.

Chapter 2

Background

In this chapter, first I provide the background needed to understand the connection between energy, information and the purity of qubits. The profound connection between the aforementioned concepts provided insights for a novel generation of cooling techniques which manipulate information in a controlled way to reproduce cooling effects. In particular, I present here one of these methods, known as the PPA protocol, which was introduced by Schulman, Mor and Weinstein [98]. This protocol gives the optimal cooling algorithm with respect to entropy extraction when the interaction with the bath is restricted to individual qubit-relaxation.

2.1 Cooling physical systems with tools from quantum information processing

A key concept for understanding how the tools from quantum information science can be used to cool physical systems is *entropy*. Entropy plays a fundamental role in information theory and is also an essential concept in thermodynamics – deeply related to the physical properties of the system, such as temperature and energy. In fact, understanding the relationship between entropy, energy and purity in quantum systems, allows us to design strategies to manipulate the internal entropy of the quantum system to reproduce effects such as energy transfer. In the next subsections, I show how the aforementioned properties

are connected in quantum systems in general, and then in particular for a target qubit and ensembles of qubits in a thermal state.

2.1.1 Entropy and purity of a quantum system

Entropy gives a measure of the unpredictability of a state, or equivalently, of the mixedness of a quantum state. In quantum information theory, the von Neumann entropy for a quantum system with state ρ is defined as $S(\rho) \equiv -\mathrm{tr}(\rho \log \rho)$. This expression can be rewritten in terms of the eigenvalues $\{\lambda_x\}_x$ of the density matrix ρ as $S(\rho) = -\sum_x \lambda_x \log \lambda_x$. As a result, for a diagonal density matrix, the von Neumann entropy is reduced to the Shannon entropy of the probability distribution given by the diagonal entries of ρ.

Entropy equal to 0 corresponds to the case when the state of the system is perfectly known, i.e. when the system has a probability 1 of being in a given state. This quantum system whose state is perfectly known is said to be in a *pure state*.

The level of purity of a quantum system is commonly measured as $\mathcal{P}(\rho) := \mathrm{Tr}(\rho^2)$, which for a system of dimension d goes from $1/d$ to 1, i.e. from the maximally mixed state to a pure state. Thus, a simple criterion for determining whether a state ρ is pure or not, is to check whether the state satisfies exactly the condition $\mathrm{Tr}(\rho^2) = 1$; for $\mathrm{Tr}(\rho^2) < 1$ the state is said to be in a mixed state. The purity is conserved under unitary transformations acting on the density matrix. In general for a state ρ the purity can be calculated on the corresponding diagonalized density matrix and expressed in terms of its eigenvalues $\{\lambda_x\}_x$ as $\mathcal{P}(\rho) = \sum_x \lambda_x^2$.

In particular for our interests, it is important to identify what part of the system will be the *target subsystem* to be cooled, and to which we will try to increase its purity. Given the special simplicity and significance of systems made of qubits, in the next subsection I start to derive the relationships between entropy and purity for the simple case of a general individual qubit, followed by similar derivations for an ensemble of qubits in a thermal state.

Target qubit

Let us consider the case of having a single qubit as the target to be cooled (in general this target qubit is assumed to be a subsystem of a larger system). A qubit, which is a two-level quantum system, has a density matrix with two eigenvalues λ_0 and λ_1, that are related as $\lambda_0 + \lambda_1 = 1$, since the state should be trace 1. Then, the corresponding entropy and purity evaluates to

$$S(\rho_{1q}) = -\lambda_0 \log[\lambda_0] - (1-\lambda_0)\log[1-\lambda_0] \quad \text{and} \quad \mathcal{P}(\rho_{1q}) = \lambda_0^2 + (1-\lambda_0)^2. \tag{2.1.1}$$

For the qubit case, the entropy an purity are parameterized based on the same parameter λ_0, which goes from zero to 1. Fig. 2.1 shows the entropy and purity as a function of the eigenvalue λ_0 of the target qubit. Note that, decreasing entropy is equivalent to increasing the purity of the target qubit.

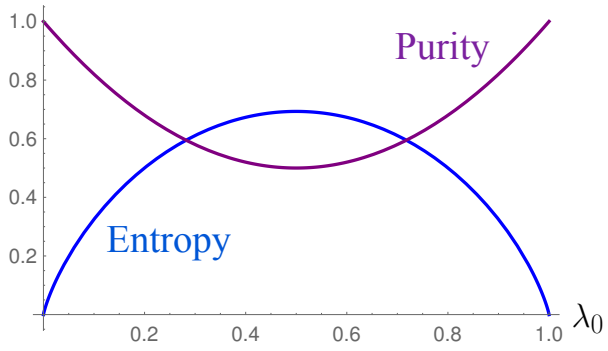

Figure 2.1: Entropy and purity of a single qubit as a function of its eigenvalue λ_0, in blue and purple, respectively. This illustrates the mapping described between the entropy and purity, parameterized with λ_0. For a state with the bath polarization ϵ_b, $\lambda_0 = (1+\epsilon_b)/2$.

To describe this change of entropy (purity) in terms of the energy of the target qubit, let us consider the local Hamiltonian of the target qubit, which in general can be written as

$$H = E_0|E_0\rangle\langle E_0| + E_1|E_1\rangle\langle E_1|, \tag{2.1.2}$$

where $|E_0\rangle$ and $|E_1\rangle$ are the eigenstates of the Hamiltonian, with eigenenergies E_0, and E_1, respectively (without loss of generality, let us assume that $E_0 < E_1$). Then, the state

of the qubit in the eigen-energy basis is

$$\rho_{1q} = \sum_{i,j} \rho_{ij} |E_i\rangle\langle E_j| = \begin{pmatrix} \rho_{00} & \rho_{01} \\ \rho_{01}^* & 1-\rho_{00} \end{pmatrix}, \tag{2.1.3}$$

where the properties of ρ_{1q} (being a positive semidefinite and Hermitian operator of trace 1 [1]) were used on the right side of Eq. (2.1.3).

To decrease the energy of the target qubit, we have to increase the probability that the target qubit is in its local ground state $|E_0\rangle$, i.e. we should increase the value of ρ_{00}. Then, from the Schur–Horn theorem, the largest value than ρ_{00} can take, under local unitary operations, corresponds to the biggest eigenvalue of ρ_{1q}. So, let us allow a rotation to diagonalize the qubit, in such a way that ρ_{00} takes the largest λ_x (let $\rho_{00} = \lambda_0 \geq 1/2$ without loss of generality).

Then, as it has been mentioned in order to cool it is necessary to increase the probability ρ_{00} of being in the ground state, which in the basis where the target qubit is diagonal, is equivalent to the problem of increasing the eigenvalue $\lambda_0 \geq 1/2$. Increasing the value of $\lambda_0 \geq 1/2$, is equivalent to decreasing the entropy of the target qubit, while the purity increases (eq.(2.1.1), and see Fig. 2.1).

2.1.2 Temperature and polarization of an ensemble of qubits

Consider an ensemble of qubits, i.e. a collection of independent, identical two-level quantum systems. Let $|0\rangle$ and $|1\rangle$ be the two levels, with corresponding energy eigenvalues E_0 and E_1. When the system is left undisturbed for a long time, in contact with the molecular surroundings, it reaches a state of thermal equilibrium with that environment. In thermal equilibrium at temperature T, the following properties hold for the system [63]:

1. The probability of occupancy of a given energy level $|i\rangle$ is given by the Boltzmann distribution, $n(E_i) = \exp[-E_i/kT]/Z$, where Z is the partition function ($Z = \exp[-E_0/kT] + \exp[-E_1/kT]$).

2. The coherences between the states are all zero.

[1] Also, the off-diagonal elements of the density matrix are bounded as $|\rho_{ij}| \leq \sqrt{|\rho_{ii}||\rho_{jj}|}$, then in this case $|\rho_{01}|^2 \leq |\rho_{00}||1-\rho_{00}|$.

Accordingly, the average-density matrix over all members of the ensemble is given by

$$\rho^{eq} = \begin{pmatrix} n(E_0) & 0 \\ 0 & n(E_1) \end{pmatrix} = \frac{1}{Z} \begin{pmatrix} \exp[-E_0/kT] & 0 \\ 0 & \exp[-E_1/kT] \end{pmatrix}. \tag{2.1.4}$$

This density matrix is used to represent the state of any qubit of the ensemble in thermal equilibrium [63]. In ensemble implementations only expectation values are measurable, there is no access to individual qubits. Moreover, in most cases the state of the system is highly mixed.

In ensemble implementations, the excess population in the energetically-favorable $|0\rangle$ state, is commonly measured with the bias $\epsilon = \mathrm{Tr}(\sigma_z \rho)$, also called ***polarization***. Then, the polarization of of the ensemble of qubits in the thermal state is as follows:

$$\epsilon = n(E_0) - n(E_1) = \frac{e^{-E_0/kT} - e^{-E_1/kT}}{e^{-E_0/kT} + e^{-E_1/kT}}, \tag{2.1.5}$$

$$\epsilon = \tanh\left(\frac{E_0 - E_1}{2kT}\right) \equiv \tanh(\xi), \tag{2.1.6}$$

where $\xi \equiv \frac{E_\delta}{kT}$, and E_δ is the energy splitting between the two levels, $E_\delta = (E_0 - E_1)/2$. Note that, from eq.(2.1.6), decreasing the temperature of the system leads to increasing its polarization for a fixed energy gap (E_δ). In the limit when the temperature is zero, the polarization is 1, taking its maximum value (the absolute value of the polarization $|\epsilon_b|$ ranges from 0 to 1). Explicitly, the inverse temperature β is related to polarization by $\beta = T^{-1} = \frac{k}{2E_\delta} \ln(\frac{1+\epsilon}{1-\epsilon})$.

Then, the density matrix of the qubits at thermal equilibrium with the bath takes the

following simple form, in terms of the polarization of the bath ϵ_b [2] ,

$$\rho_{\epsilon_b} = \frac{1}{2}\begin{pmatrix} 1+\epsilon_b & 0 \\ 0 & 1-\epsilon_b \end{pmatrix}. \tag{2.1.8}$$

The corresponding entropy and purity for an ensemble of qubits with polarization ϵ_b, then take the form given by Eq.(2.1.1) with $\lambda_0 = (1+\epsilon_b)/2$, namely,

$$S(\rho_{\epsilon_b}) = -\frac{1+\epsilon_b}{2}\log_2\left(\frac{1+\epsilon_b}{2}\right) - \frac{1-\epsilon_b}{2}\log_2\left(\frac{1-\epsilon_b}{2}\right), \tag{2.1.9}$$

and the purity evaluates to

$$\mathcal{P}\left(\rho_{\epsilon_b}\right) = \mathrm{Tr}\left(\rho_{\epsilon_b}^2\right) = \frac{1}{2}\left(1+\epsilon_b^2\right). \tag{2.1.10}$$

Polarization ϵ is related to purity by $\epsilon = \sqrt{2\mathcal{P}-1}$, in the eigenbasis of ρ (ϵ is basis dependent). From here that the following relationships between the concepts of purity, entropy and polarization hold,

$$\text{Decreasing } T \Leftrightarrow \text{Increasing } \mathcal{P} \Leftrightarrow \text{Decreasing } S \Leftrightarrow \text{Increasing } |\epsilon_b|$$

Fig.(2.1) and Fig.(2.2) show the entropy and purity as a function of the polarization of the system ($\lambda_0 = (1+\epsilon_b)/2$) and as function of the inverse temperature β. A system with high polarization corresponds to a system with high purity and low entropy.

Note that purification of a quantum system is not equivalent to extracting energy from it. Indeed, by warming the target qubit to the excited state ($\epsilon_b \to -1$), it can give also a pure state pointing in a different direction in the bloch sphere.

[2] Some authors, such as Schulman et al. [98, 99], use a different definition of polarization, given by $\epsilon = \mathrm{arctanh}\,(\epsilon_b)$. For this case, the corresponding density matrix at thermal equilibrium takes the following form

$$\rho_{\epsilon_b} = \frac{1}{e^{-\epsilon}+e^{\epsilon}}\begin{pmatrix} e^{\epsilon} & 0 \\ 0 & e^{-\epsilon} \end{pmatrix}. \tag{2.1.7}$$

Note that in the high-temperature regime, the two aforementioned definitions of polarization, ϵ_b and ϵ, are very close to each other, $\epsilon_b \approx \epsilon$. However, for the low-temperature regime, ϵ_b and ϵ differ to each other considerably (ϵ goes to infinity as the temperature reaches zero, while the maximum value of ϵ_b is 1).

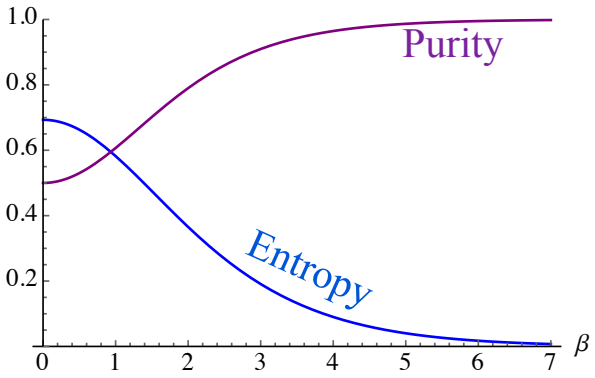

Figure 2.2: Entropy and purity of the target qubit, of Hamiltonian $H = -\frac{1}{2}\omega\sigma_z$ without loss of generality, as a function of inverse temperature β, with $\omega = 1$. As the temperature of the target qubit decreases, its purity increases and its entropy decreases.

2.2 Ensemble of qubits in NMR and cooling methods

In the context of NMR quantum information processing [20, 110], the ensemble consists of a bulk sample of identical molecules, each with n distinguishable nuclear spins. Each molecule is considered as an individual n-qubit processor.

The interaction of a spin-$\frac{1}{2}$ with an external static magnetic field, gives the two eigenstates required for a qubit. The energy splitting, Zeeman splitting, between those two levels is proportional to the field strength, B, and is much smaller than thermal energy, kT, at room temperature, where k is the Bolztmann constant. The corresponding polarization, calculated using eq.(2.1.6), is

$$\epsilon_b \approx \frac{\mu B}{2kT} \approx \epsilon, \tag{2.2.1}$$

where μ is the magnetic moment of the spin in question. For the case of larger spin, l, the analysis is similar [63].

For protons at room temperature, in a $B = 7T$ field, the polarization is of the order of magnitud of 10^{-5}. It has been shown that even with such a low polarization, it is possible to get computational advantages over classical computation in some cases (for example, for simulating some physical systems [57], measuring the average fidelity decay [86], among others). However, for general purposes of quantum computing, purification

remains necessary [3].

Different techniques have been implemented to boost the polarization of the nuclear spins in NMR to solve the initialization problem. Most of these methods are based on pseudo-pure state (PPS) preparation techniques [19, 38], nevertheless these procedures have an exponential loss of signal-to-noise with the number of qubits [11]. It is still conceivable that in conjunction with other methods, the PPS techniques would play a role in initializing scalable ensemble quantum computing. Therefore, finding ways to produce highly polarized states (or at least with a polarization level where it would be feasible to use PPS) remains indispensable.

In general, decreasing the temperature, to extremely low values, is experimentally hard. In the one side, the equation of the polarization, $\epsilon_b = \tanh(E_\delta/kT)$, suggests that we can decrease the temperature by changing the parameter of polarization, or increasing the energy gap E_δ of the target qubit. However, these approaches are technological dependent; for example, in NMR, that would mean increasing the magnetic field (eq.(2.2.1)), which nevertheless, to be increased at least one order of magnitude, from the typical current magnetic field values would require a big technological advancement.

The concepts introduced in this background establish a close interrelationship between increasing the polarization, lowering the temperature, decreasing the entropy, and purifying the system. From this, it is possible to plan different strategies to purify the qubits in ensemble implementations. Algorithmic cooling techniques propose strategies that can obtain cooling effects by directly redistributing the internal entropy of the system, which is possible using the tools of quantum information processing. Remarkably, these procedures are not device dependent as it is explained in the next sections. First, I will introduce the explicit entropy compression methods used by Schulman and Vazirani [100], and then present the standard heat-bath algorithmic cooling [11], in particular the PPA protocol.

2.3 Algorithmic Cooling (AC)

An internal redistribution of the entropy over all the qubits in the system can be obtained through quantum logic operations to get a subset of highly-polarized qubits from an initial set of weakly-polarized ones [11, 100, 29, 98, 99]. This carries out a reversible entropy compression process in which the system results in a separation of cold and hot regions.

Schulman and Vazirani [100], presented an explicit cooling method which recursively applies majority gates, inspired by the Von Neumann's ideas of the extraction of fair coin flips from a sequence of biased ones.

The system setup consists of a string of identical qubits, one of them being our *target qubit*, i.e. the qubit which is going to be cooled. Without loss of generality, the first qubit of the string will be set as the target qubit. Then, the idea of AC is to first re-distribute the entropy among the string of qubits by applying an entropy compression operation U. This is a reversible unitary process that extracts entropy from the target qubit as much as possible and concentrates entropy in the reset qubits of the system. This process results in the cooling of the target qubit while warming the rest of the qubits (see Fig. 2.3).

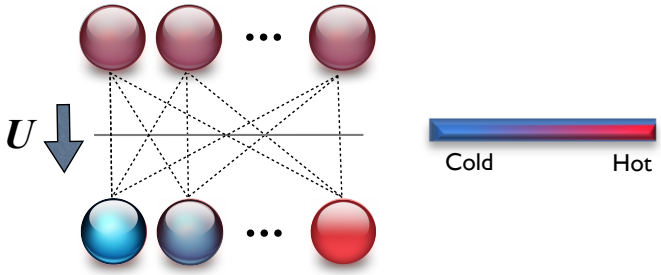

Figure 2.3: Entropy compression step. The idea is to redistribute the entropy within a group of qubits using a unitary operation U. This redistribution should be optimized in such a way that the entropy from the target qubit is extracted as much as possible and compressed in the rest of the qubits. In the figure, the top part represents the string of qubits before the compression. Dotted lines indicate re-distribution of entropy among all qubits, resulting in the separation of cold and hot regions as shown in the bottom part.

2.3.1 Illustrative simple example of the AC

Let us consider the three-qubit case of identical qubits, starting in a product state each of them with the polarization of the bath. Namely, the state of the three-qubit system is given by $\rho_{3q} = \rho_b^{\otimes 3}$, where $\rho_{\epsilon_{\rho_b}} = \frac{1}{2}\begin{pmatrix} 1+\epsilon_b & 0 \\ 0 & 1-\epsilon_b \end{pmatrix}$ is the state of a qubit from the thermal bath. This state can be describe by its diagonal, in the computational basis, as

$$\mathrm{diag}(\rho_0 = \rho_b^{\otimes 3}) = \frac{1}{8}\begin{bmatrix} (1+\epsilon_b)^3 \\ (1+\epsilon_b)^2(1-\epsilon_b) \\ (1+\epsilon_b)^2(1-\epsilon_b) \\ (1+\epsilon_b)(1-\epsilon_b)^2 \\ (1+\epsilon_b)^2(1-\epsilon_b) \\ (1+\epsilon_b)(1-\epsilon_b)^2 \\ (1+\epsilon_b)(1-\epsilon_b)^2 \\ (1-\epsilon_b)^3 \end{bmatrix} \xrightarrow{U(\rho_0)} \frac{1}{8}\begin{bmatrix} (1+\epsilon_b)^3 \\ (1+\epsilon_b)^2(1-\epsilon_b) \\ (1+\epsilon_b)^2(1-\epsilon_b) \\ (1+\epsilon_b)^2(1-\epsilon_b) \\ (1+\epsilon_b)(1-\epsilon_b)^2 \\ (1+\epsilon_b)(1-\epsilon_b)^2 \\ (1+\epsilon_b)(1-\epsilon_b)^2 \\ (1-\epsilon_b)^3 \end{bmatrix} \tag{2.3.1}$$

To cool the first qubit, we should increase its probability to be in the ground state. Namely, we should give the largest values to the probabilities of the first half elements of the diagonal of ρ_0, and the smallest values to the second half. Thus, in this case we can find a very simple unitary operation that rearranges the order of the diagonal elements in decreasing order.

The diagonal elements of ρ_0 are already arranged in non-increasing order, with the exception of the fourth and fifth elements, corresponding to the probabilities of being in the states $|011\rangle$ and $|100\rangle$ respectively – represented in red and blue in Eq. (2.3.1). Thus, a useful entropy compression $U(\rho_0)$ of the PPA is the unitary operation that permutes the probability amplitudes of the states $|011\rangle$ and $|100\rangle$. The explicit form of this unitary $U(\rho_0)$ is presented in Fig. 2.4, with its corresponding circuit.

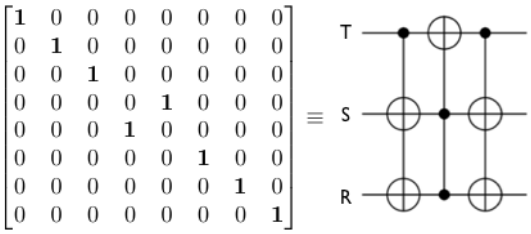

Figure 2.4: Matrix and circuit symbol representing the unitary operation for the entropy compression of the PPA for the 3-qubit case. This iteration boosts the target qubit polarization from ϵ_b to $\frac{3}{2}\epsilon_b - \frac{1}{2}\epsilon_b^3$.

After this entropy compression, the polarization of the first qubit increases from ϵ_b

to $\frac{3}{2}\epsilon_b - \frac{1}{2}\epsilon_b^3$, while the polarization of the scratch qubit and the reset qubit decreases to $\frac{1}{2}\epsilon_b + \frac{1}{2}\epsilon_b^3$.

In the high temperature regime, by applying this entropy compression in the system changes the local temperature of the target from T_b to $2T_b/3$, at the expense of warming the second and third qubit from T_b to $2T_b$.

2.3.2 Limitations of the AC

This AC method allows purify $\frac{1}{20}\epsilon^2 n$ qubits to a polarization of $1 - 2n^{-10}$, from an initial set of n qubits with polarization ϵ. They proved that the optimal adiabatic compression is achieved with this algorithm; however, it is impractical with current technology. For room temperature biases ($\epsilon_b \approx 10^{-5}$), approximately 2x$10^{12}$ qubits are required to boost the polarization close to 1. The cooling limits of this method are imposed by the bound Shannon entropy and the preservation of the eigenvalues.

The aforementioned limitations of AC come from having a closed system. Thus, a natural improvement on the idea of AC, which was proposed by Boykin et al.[11], is obtained by allowing contact to a heat-bath of partially polarized qubits. The access to a thermal bath allows the original system to be open and be able to pump entropy out into the thermal bath. This new kind of methods are called heat-bath algorithmic cooling, and they can transcend the previously mentioned shortcomings. In the next section, I present them in more detail and give in particular the explicit form of the PPA protocol.

2.4 Heat Bath Algorithmic Cooling (HBAC)

Heat-bath algorithmic cooling (HBAC) purifies qubits by applying alternating rounds of entropy compression and pumping entropy into a thermal bath of partially polarized qubits.

Setup of the system – The system setup consists of a string of qubits: one qubit which is going to be cooled (called *target qubit*); one general qudit which aids in the entropy compression (this qudit, called the *scratch system*, can be a spin$-l$ in general [3], or a string

[3]Having the spin$-l$ is equivalent to having n' qubits if the dimension of their Hilbert spaces is the same, i.e. if $d = 2l + 1 = 2^{n'}$.

of qubits as in the standard system setup); and m reset qubits that can be brought into thermal contact with a heat-bath of polarization ϵ_b. We will also refer to the target qubit and the scratch qudit as the computational qubits (see Fig. 2.5).

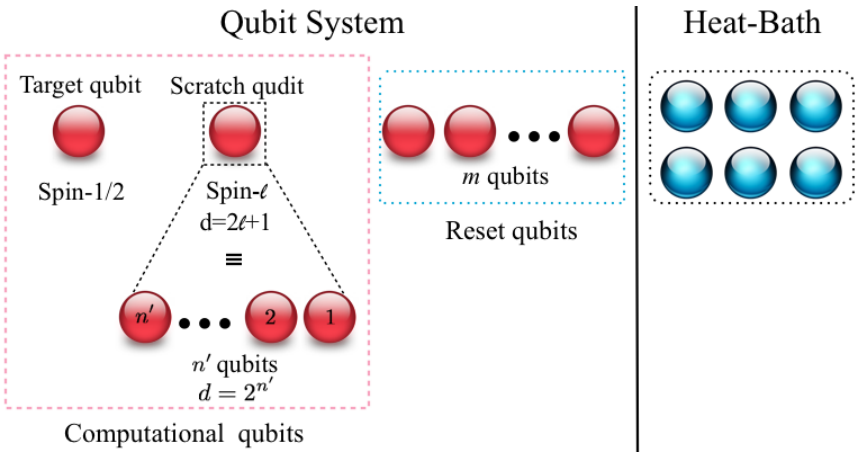

Figure 2.5: System setup for HBAC protocol. The qubit system consists of (from left to right) a target qubit, which is going to be cooled, a general $d-$dimensional quantum system as a scratch qudit (this can be a string of n' qubits, for example) and m reset qubits which can make contact with a thermal bath (which is illustrated on the right).

The idea of HBAC is to first re-distribute the entropy within the qubit system by applying an entropy compression operation that extracts entropy from the target qubit as much as possible, at the expense of heating up the m reset qubits, as explained in the previous section (Fig. 2.3). Then, the reset qubits can be refreshed by using the heat-bath for removing entropy (Fig. 2.6). The heat-bath is assumed to have infinite heat capacity, such that the action of qubit-bath interaction on the bath is negligible.

HBAC consists of the iterations of these two steps: reversible entropy compression (which depends on the state of the system and therefore must be optimized in each round) followed by a refreshed step with the bath. These two steps can be applied until the target qubit reaches the desired temperature or until the cooling limit is reached. In the next subsection, I present the explicit form of this two steps for the PPA protocol.

In the conventional HBAC, the refresh operation re-thermalizes the reset qubits to the heat-bath temperature, which is equivalent to swapping the reset qubits with qubits of the heat-bath. This particular refresh procedure is used in the PPA method, as explained in

the next section (Fig. 2.6).

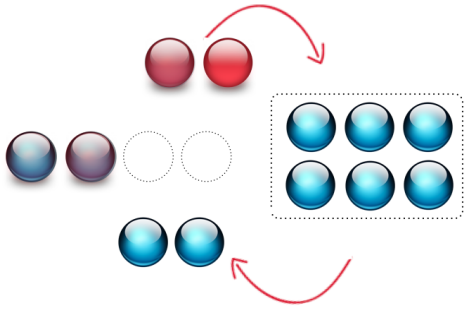

Figure 2.6: Refresh step. The m reset qubits are brought into thermal contact with a heat-bath to pump entropy out from the qubit system into the bath. In the figure, two reset qubits are used as an example.

Note that the physical requirements for the computational and the reset qubits are different. A computational qubit should have long relaxation time to remain polarized after being cooled through entropy compression, and a reset qubit should strongly interact with the bath in order to rapidly relax and attain the bath temperature.

2.4.1 The Partner Pairing Algorithm (PPA)

The Partner Pairing Algorithm (PPA) protocol was invented by Schulman et al. [98, 99], and it is optimal under the assumption that during the reset step the qubits are thermalized individually with a Markovian process. Under these restrictions, the best use of the bath is to fully re-thermalized individually the m reset qubits to the temperature of the heat-bath.

For the PPA protocol, the initial state of the system is assumed to be in the totally mixed state, followed by a preliminary preparation before implementing the rounds of the PPA algorithm. This preliminary step consists of refreshing all the qubits with the bath. Thus, the state of the system, before the first round of PPA, is in a product state with all the qubits at the same bath temperature. For the case of a string of qubits (a target, n' scratch qubits and m reset qubits), this state is given by

$$\rho_0 = \rho_b^{\otimes n} = \rho_b^{1+n'+m}$$

where $\rho_{\epsilon_b} = \frac{1}{2}\begin{pmatrix} 1+\epsilon_b & 0 \\ 0 & 1-\epsilon_b \end{pmatrix}$ is the state of a qubit from the thermal bath, and ϵ_b is the heat-bath polarization [4]. Note that this state is diagonal in the computational basis, and will remain diagonal under the steps of the PPA, which are explained as follows:

The PPA protocol

The PPA protocol is made of iterating rounds, each round consisting of the next two steps

1. PPA entropy compression step. An optimal reversible entropy compression operation on the qubit system, $U(\rho)$. Concretely, this is a unitary operations that rearranges the diagonal elements of the state ρ of the qubit system in a descending sort order:

$$\rho \xrightarrow{Compression} \rho' = U(\rho)\,\rho U^{\dagger}(\rho).$$

2. PPA Refresh step. The m reset qubits are brought into thermal contact with the bath to be fully thermalized with the heat-bath. This step is equivalent to tracing-over the m reset qubits, and replacing them with qubits in a thermal state at the bath temperature:

$$\rho' \xrightarrow{Refresh} \rho'' = \mathrm{Tr}_{m_{qubits}}[\rho'] \otimes \rho_{\epsilon_b}^{\otimes m}.$$

The PPA entropy compression step rearranges the diagonal elements of the system state ρ, such that the probability amplitude of its states starting with 0 (i.e. states like $|0...00\rangle$, $|0...01\rangle$, etc.) will take the highest possible values, while the states starting with 1 will take the lowest ones. Namely, this operation aims to increase the population of the ground state of the first qubit, which corresponds to the target qubit. The entropy compression can no longer improve the polarization of the first qubit once the states are already ordered as described above. In Chapter 6, the optimization of this step is explained in the context of resource theories.

[4] Some authors, such as Schulman et al. [99], use the bath polarization as $\mathrm{arctanh}[\epsilon_b]$.

The particular computations required in this entropy compression step vary in a complex way, since they depend on the number of qubits, the heat-bath polarization, and the particular state of the system at that moment.

Note that with this type of reset step, the maximum polarization that the reset qubits are able to obtain is the polarization of the heat-bath, ϵ_b, which is assumed to have a large heat capacity such that the action of qubit-bath interaction is negligible on the bath temperature.

The total effect of applying a round of PPA on a system with state ρ can be expressed as follows:

$$\Phi_{\mathrm{PPA}}(\rho) = \mathrm{Tr}_{m_{qubits}}\left[U(\rho)\,\rho\,U^{\dagger}(\rho)\right] \otimes \rho_{\epsilon_b}^{\otimes m} \tag{2.4.1}$$

Illustrative example: PPA for three qubits

In order to illustrate how the PPA method works, here it is applied on a particular system of three qubits (one reset qubit, one scratch qubit and one reset qubit). The initial state of the system is assumed to be in the totally mixed state, followed by a preliminary step, before applying the rounds of the PPA. This preliminary step brings the three qubits to a thermal state at the temperature of the heat-bath. Namely, the system will be in the product state of the three qubits, each of the with the bath polarization, before the first PPA round: $\rho_0 = \rho_b^{\otimes 3}$, where $\rho_{\epsilon_b} = \frac{1}{2}\begin{pmatrix} 1+\epsilon_b & 0 \\ 0 & 1-\epsilon_b \end{pmatrix}$ is the state of a qubit at the thermal equilibrium with the heat-bath polarization ϵ_b.

0) Preliminary preparation step for the PPA

The aforementioned state $\rho_0 = \rho_b^{\otimes 3}$ is obtained by refreshing the reset qubit and swapping it with the computational qubits until all the qubits of the system are in a thermal state.

Note that, even though, the standard initial state is assumed to be in the totally mixed state, any general initial state will be left in the state $\rho_b^{\otimes 3}$.

1) First round of the PPA

First, the entropy compression operation $U(\rho_0)$ permutes the diagonal elements of the total state, sorting them in a non-increasing order. This particular step corresponds to the entropy compression example presented in the subsection 2.3.1, eq. (2.3.1). This first entropy compression increases the target qubit polarization from ϵ_b to $\frac{3}{2}\epsilon_b - \frac{1}{2}\epsilon_b^3$, while decreases the polarization of the scratch qubit and reset qubit to $\frac{1}{2}\epsilon_b + \frac{1}{2}\epsilon_b^3$.

Then, a refreshing step can pump out the excess of entropy of the reset qubit into the thermal bath to fully thermalize the reset qubit to the temperature of the bath. This step is equivalent to trace out the reset qubit from the system and replace it with a qubit in state ρ_b. Then diagonal of the total state under this step changes as follows:

$$\frac{1}{8}\begin{bmatrix} (1+\epsilon_b)^3 \\ (1+\epsilon_b)^2(1-\epsilon_b) \\ (1+\epsilon_b)^2(1-\epsilon_b) \\ (1+\epsilon_b)^2(1-\epsilon_b) \\ (1+\epsilon_b)(1-\epsilon_b)^2 \\ (1+\epsilon_b)(1-\epsilon_b)^2 \\ (1+\epsilon_b)(1-\epsilon_b)^2 \\ (1-\epsilon_b)^3 \end{bmatrix} \xrightarrow{Refresh} \text{diag}\left(\Phi_{\text{PPA}}(\rho_0)\right) = \frac{1}{4}\begin{bmatrix} (1+\epsilon_b)^2 \\ (1+\epsilon_b)^2(1-\epsilon_b) \\ (1+\epsilon_b)(1-\epsilon_b)^2 \\ (1-\epsilon_b)^2 \end{bmatrix} \otimes \frac{1}{2}\begin{bmatrix} 1+\epsilon_b \\ 1-\epsilon_b \end{bmatrix} \tag{2.4.2}$$

After this refresh step, we have completed a round of PPA on the state ρ_0.

2) Second round of PPA

If the state of the system after the first round allows a new entropy compression, i.e if the diagonal elements of the state are not in a non-increasing order, then we can apply a new round of PPA.

The diagonal elements of $\Phi_{\text{PPA}}(\rho_0)$, by expanding the eq. (2.4.2), and then permuting them in non-increasing order under a reversible entropy compression operation, are as follows:

$$\operatorname{diag}\left(\Phi_{\mathrm{PPA}}\left(\rho_0\right)\right) = \frac{1}{8}\begin{bmatrix} (1+\epsilon_b)^3 \\ (1+\epsilon_b)^2(1-\epsilon_b) \\ (1+\epsilon_b)^3(1-\epsilon_b) \\ (1+\epsilon_b)^2(1-\epsilon_b)^2 \\ (1+\epsilon_b)^2(1-\epsilon_b)^2 \\ (1+\epsilon_b)(1-\epsilon_b)^3 \\ (1+\epsilon_b)(1-\epsilon_b)^2 \\ (1-\epsilon_b)^3 \end{bmatrix} \xrightarrow{U(\Phi_{\mathrm{PPA}}(\rho_0))} \frac{1}{8}\begin{bmatrix} (1+\epsilon_b)^3 \\ (1+\epsilon_b)^3(1-\epsilon_b) \\ (1+\epsilon_b)^2(1-\epsilon_b) \\ (1+\epsilon_b)^2(1-\epsilon_b)^2 \\ (1+\epsilon_b)^2(1-\epsilon_b)^2 \\ (1+\epsilon_b)(1-\epsilon_b)^2 \\ (1+\epsilon_b)(1-\epsilon_b)^3 \\ (1-\epsilon_b)^3 \end{bmatrix} \tag{2.4.3}$$

The unitary $U\left(\Phi_{\mathrm{PPA}}\left(\rho_0\right)\right)$ arranges the diagonal elements in non-increasing order. Concretely, the compression unitary should swap the probabilities of the states $|001\rangle$ and $|010\rangle$ – represented in red and blue in eq. (2.4.3) – and the probabilities of the states $|101\rangle$ and $|110\rangle$ – represented in pink and cyan. Note that exchanging this this elements is equivalent to swap the the whole scratch qubit with the reset qubit. The explicit form of this unitary is presented in Fig. 2.7, with the corresponding circuit.

$$\begin{bmatrix} \mathbf{1} & 0 & 0 & 0 & 0 & 0 & 0 & 0 \\ 0 & 0 & \mathbf{1} & 0 & 0 & 0 & 0 & 0 \\ 0 & \mathbf{1} & 0 & 0 & 0 & 0 & 0 & 0 \\ 0 & 0 & 0 & \mathbf{1} & 0 & 0 & 0 & 0 \\ 0 & 0 & 0 & 0 & \mathbf{1} & 0 & 0 & 0 \\ 0 & 0 & 0 & 0 & 0 & 0 & \mathbf{1} & 0 \\ 0 & 0 & 0 & 0 & 0 & \mathbf{1} & 0 & 0 \\ 0 & 0 & 0 & 0 & 0 & 0 & 0 & \mathbf{1} \end{bmatrix} \equiv$$

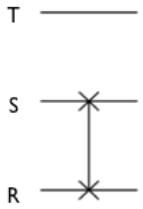

Figure 2.7: Entropy compression of the second round of PPA for the 3-qubit case. This operation effectively swaps the scratch qubit and the reset qubit.

Note that this entropy compression does not improve the polarization of the target qubit, however it removes entropy from the scratch qubit and compresses it into the reset qubit. This excess of entropy in the reset qubit is then sent to the thermal bath during the refresh step of this PPA round, returning the reset qubit to the thermal state of the bath.

n) The next rounds

Upon repeating two more rounds of PPA, it is found that the entropy compression

operations, corresponding to the third and fourth rounds, will be the exactly the same of the ones from the first and second rounds, respectively. Indeed, for the 3-qubit case, all the subsequent pair of rounds have the same form of the first and second rounds. Then, the quantum circuit required to perform the PPA on the three qubits is illustrated in Fig. 2.8, just for the first rounds (subsequent rounds are just the iteration of the first and second round).

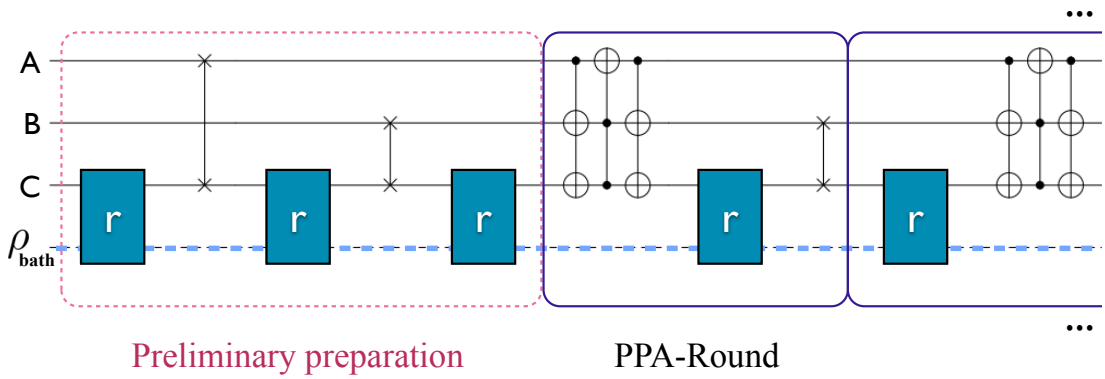

Figure 2.8: Quantum circuit for the PPA protocol on a system of three qubits. In the circuit diagram, the target, the scratch and the reset qubits are denoted by T, S, and R, respectively; the dotted line at the bottom represents the heat-bath. The r gate stands for the refresh operation. The figure shows only the first five rounds of the circuit (a round consists of an entropy compression step followed by a refresh step), subsequent rounds are just the repetition of the first two rounds.

Despite the simplicity and periodicity of the PPA quantum circuit for the 3-qubit case, it is complicated to generalize the PPA for a bigger number of qubits, $n > 3$. Indeed, in general the explicit form of the unitary operations for the entropy compression is different in each round of PPA when $n > 3$, and depends on the specific state of the system in each round.

The polarization evolution of the target qubit under several rounds of the PPA is shown in Fig. 2.9, for the low polarization case. The circuit asymptotically boosts the polarization on the target qubit up to twice the heat-bath polarization (for $\epsilon_b \ll 1$); this limit is discussed and explained in the next section.

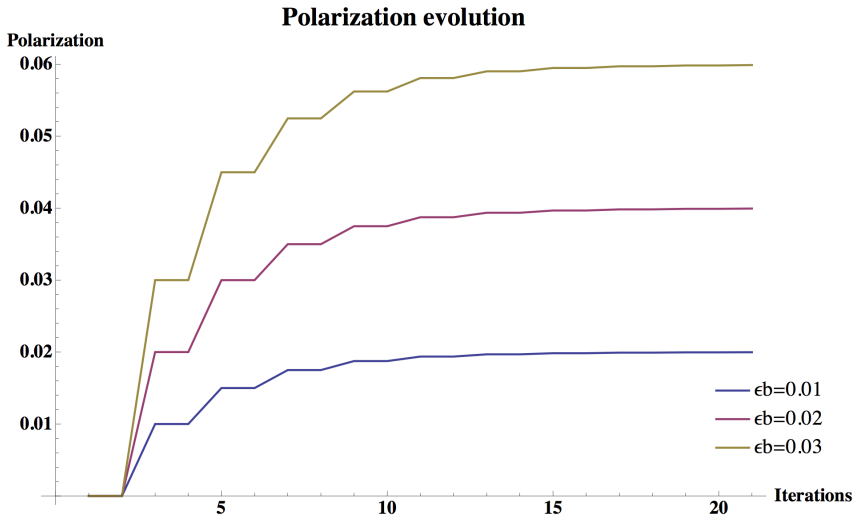

Figure 2.9: Polarization evolution of the target qubit obtained by the PPA protocol for the three-qubit case as a function of the number of rounds, in the low polarization regime ($\epsilon_b \ll 1/2$) for three different bath polarization values. Note that the asymptotic polarization goes to $2\epsilon_b$.

PPA for the two-qubit case

The 2-qubit case was not presented as the simplest illustrative example of the PPA, since for this case the protocol does not give gain beyond the bath temperature, obtained in the preliminary step.

After the preliminary step, when the two qubits are in a product state both with the bath temperature, there is no entropy compression that can cool the target qubit since the diagonal elements of the state are already sorted in a non-increasing order:

$$\mathrm{diag}\left(\rho_{\epsilon_b}^{\otimes 2}\right) = \frac{1}{4}\begin{bmatrix}(1+\epsilon_b)^2\\ 1-\epsilon_b^2\\ 1-\epsilon_b^2\\ (1-\epsilon_b)^2\end{bmatrix},$$

Therefore, the PPA protocol stops at this point, and there are no further improvements beyond the bath temperature.

2.5 Experimental implementation of HBAC

HBAC has already been experimentally tested and implemented to show improved polarization in small qubit systems [30, 7, 96, 27, 14, 15, 77], where a few rounds of HBAC were achieved, and a more realistic implementation has been studied in Ref. [55]. Furthermore, the fact that the HBAC protocols are device independent has made them successfully tested on different platforms. In particular, it was successfully demonstrated in liquid state NMR [30, 27, 14, 15], solid state NMR [7, 96], quantum optics [116], and ion traps [6], and electron spin resonance (ESR) at high polarization [77], among others. In the next subsection, I present a brief review of the HBAC experiments in liquid state NMR, in solid state NMR and in ESR.

2.5.1 Implementing HBAC on NMR and ESR

The experiments in NMR and ESR were significant milestones towards the implementation of HBAC. In fact, they showed and outlined the physical requirements to realize HBAC, demonstrating high control fidelity to prepare an ancilla qubit whose polarization is higher than the cold bath polarization [7, 96, 30, 27, 14, 15]. Nevertheless, even though they have the required control tools, these two platforms are limited by the challenges of finding a system (molecules) with enough qubits, and finding a stronger way to couple the qubits to the heat-bath to remove entropy.

The experimental realization of algorithmic cooling requires high fidelity control and the ability to reset qubits. Liquid State NMR Quantum Information Processing (LSNMR QIP) has demonstrated precise quantum control up to 12 qubits; however, it presents difficulties to refresh qubits. The only way to refresh qubits relies on spin-lattice relaxation, characterized by the time scale of relaxation time T1. For a successful HBAC, the reset qubits must have very short T1 to rapidly relax and attain the bath temperature. On the other hand, this short T1 on the reset qubit limits its T2 and the fidelity of control. Despite these limitations, the first preliminary steps towards full PPA was experimentally realized in LSNMR by using protons (^{1}H nuclei) as reset qubits and ^{13}C nuclei as computational qubits [14]. These experiments showed selective reset operations to polarize all three spin qubits close to the bath temperature for the preliminary step of PPA (nevertheless, the compression step that polarizes a target qubit colder than the heat bath was not

implemented in this experiment). Meanwhile, Chang et al. implemented cooling solely by the final compression gate on three fluorines in C_2F_3BR using LSNMR. Full implementation of HBAC in LSNMR was accomplished much later in Ref. [4].

On the other hand, Solid State NMR (SSNMR) offers a reset step that does not require a relaxation process in the system of interest by using a network of dipolar coupled spins as a spin bath. The decoherence rates can be made slow using refocusing techniques, while spin-spin couplings, which are much larger than in LSNMR, can be exploited to realize faster quantum gates [20]. Moreover, SSNMR experiments can be operated at low temperature, providing a higher bath polarization than LSNMR. The first experimental demonstration of HBAC using SSNMR was done by Baugh et al. in 2005 [7]. Baugh et al. implemented the PPA for three qubits using a single crystal of malonic acid $CH_2(COOH)_2$ as a quantum processor at $B_0 = 7.1T$ and room temperature. In 2008, Ryan et al. experimentally demonstrated nine iterations of algorithmic cooling in the same experimental system (malonic acid) [96]. Ryan et al. achieved a polarization in the target qubit of $1.69\epsilon_b$, while the corresponding theoretical polarization is $1.94\epsilon_b$. Here, the experimental error was dominated by two factors: the imperfection of ^{1}H decoupling and a non-ideal process of spin diffusion in the network of dipolar coupled protons in the bath.

The fundamentals of electron spin resonance (ESR) quantum computing are analogous to NMR quantum computing, and many of the techniques used for manipulating nuclear spins can also be applied to control electrons. The combination of electron and nuclear spin resonance in hyperfine-coupled quantum processors can provide more advantages. One obvious advantage is that the higher gyromagnetic ratio of an electron γ_e (about 660 times greater than that of proton) leads to higher polarization. Decoherence and relaxation rates also scale with γ and hence electron T1 relaxation rate is about 3 orders of magnitude larger than that of nuclei. Thus, the electron spin is an excellent candidate for the reset qubit, which can be refreshed simply by waiting for a time of about 5T1. The anisotropic hyperfine interaction gives an advantage for designing nuclear quantum gates, since it provides a control handle for fast manipulations of nuclear spins. On the other hand, if the anisotropic hyperfine interaction is strong, it could represent a problem given that the electron T1 relaxation process induces nuclear polarization decay in the presence of anisotropic hyperfine interaction. Fortunately, the crystal orientation can be chosen to reduce the anisotropic hyperfine coupling strength so that the nuclear spin decay induced by electron T1 is small enough to allow cooling of a target spin below bath temperature.

The control universality of an electron and a nuclear spin coupled system via anisotropic hyperfine interaction was proved in Ref. [56], and demonstrated experimentally in Ref. [44] for a single nuclear spin qubit gate and in Ref. [119] for a gate involving two nuclear spin qubits.

Chapter 3

Achievable cooling of the PPA

The results presented in this Chapter have been published in Ref. [93].

The theoretical limit of heat-bath algorithmic cooling was a longstanding open problem for more than a decade, after Schulman et al. proved the existence of its physical limits [98], and only bounds and numerical estimations had been provided (see, for example, Refs. [73, 98, 99]). In particular, the limits of heat-bath algorithmic cooling were studied using a specific algorithm, known as the Partner Pairing Algorithm, which is optimal under the assumption that the interaction of the system with the thermal bath fully thermalizes the reset qubits to the bath temperature – as described in the previous Chapter. In this Chapter, I show how we completely resolve the problem of finding the analytical solution for the achievable cooling limits and the asymptotic steady state of the system [91, 93].

We investigate the achievable polarization by analyzing the limit when no more entropy can be extracted from the system under the rounds of the PPA. Concretely, we provide the cooling limit conditions of the steady states of the PPA in the asymptotic limit. From these conditions, we obtain the exact analytical solution of the maximum polarization achievable for the case when the initial state of the qubits is totally mixed (i.e. for the case of having the lowest initial purity), which is the assumed initial state of the PPA. We also found that it is possible to reach higher polarization while starting with certain states other than a mixed state, and thus our result provides an achievable polarization. Finally, we provide the number of steps needed to get a specific required purity.

3.1 Cooling Limit Condition of the PPA

The PPA-HBAC, as discussed in section 2.4, purifies qubits by applying alternating rounds of entropy compression and pumping entropy into a thermal bath of partially polarized qubits. The assumptions under which the cooling limits were calculated are as follows:

System setup's assumptions and allowed operations – The system setup, as described in the Fig. 2.5, consists of a target qubit, which is assumed to have a fixed energy gap; a general $d-$dimensional quantum system as a scratch qudit (which is not restricted to return to its initial state after the rounds of PPA); and m identical reset qubits that are allowed to interact with the heat-bath (in particular the PPA-HBAC assumes that the reset qubits will be fully thermalized after interacting with the bath). It is assumed that the reset qubits can have a different energy gap than the target qubit energy gap, but also fixed. The allowed operations are global unitaries on the system (not including the bath), and the reset qubits can be fully thermalized with the heat-bath.

The cooling limit of the PPA protocol corresponds to the moment at which it is not possible to continue pumping entropy out of the qubit system into the bath and there is no entropy compression that can extract more entropy from the target qubit. Namely, this cooling limit would happen *when the state of the qubit system is not changed by the entropy compression step, with its reset qubits already at the thermal temperature of the bath*. The system achieves this limit asymptotically, converging to a steady state which is an attractive fix point of the PPA protocol. Thus, to find the state that satisfies the cooling conditions, it is necessary to solve for the state ρ^{∞} such that

$$\rho^{\infty} = \Phi_{\mathrm{PPA}}\left(\rho^{\infty}\right), \tag{3.1.1}$$

where $\Phi_{\mathrm{PPA}}\left(\rho\right)$ is the state of the qubit system after a round of the PPA on ρ (see eq. (2.4.1)).

We characterized this condition in terms of the diagonal elements of the computational qubits state ρ_{com}, i.e. the state of the target qubit and a scratch qudit of dimension d: $diag(\rho_{com}) = (A_1, A_2, A_3, ..., A_{2d})$. Then, using this notation, the state of ρ after applying a round of PPA can be described as

$$diag\left(\Phi\left(\rho\right)\right) = (A_1, A_2, ..., A_{2d}) \otimes \frac{1}{2^m}\left(1+\epsilon_b, 1-\epsilon_b\right)^{\otimes m}. \tag{3.1.2}$$

Cooling limit condition

In the cooling limit there is no reversible entropy compression operation that can extract any further entropy from the computational qubits. Equivalently, after applying a new round of PPA, the diagonal elements of the computational qubits state are already sorted in non-increasing order. This happens when the condition

$$A_i \left(1-\epsilon_b\right)^m \geq A_{i+1} \left(1+\epsilon_b\right)^m, \quad \forall \quad i = 1, 2, 3, ..., 2d-1 \tag{3.1.3}$$

is satisfied, corresponding to an attractive fixed point of the rounds of PPA.

The details of the proof are in Appendix A. The condition in Eq.(3.1.3) is achieved asymptotically when the system starts in the totally mixed state, and also for the case when all qubits are initially in a thermal state at bath temperature (as prepared in the preliminary step of the PPA). In fact, it is possible to find different final states as a function of the initial state of the system when the preliminary step of PPA is skipped and allows for general initial states. Arguably, the most interesting steady state is given when the initial state is totally mixed, since it corresponds to the extreme case when the initial polarization is zero, and also because it is always possible to efficiently randomize a state experimentally. Therefore, that asymptotic state can always be asymptotically reached.

In the next section, I present the maximum achievable cooling and the explicit form of the state in the cooling limit.

3.2 Maximally mixed initial state

When the PPA-HBAC protocol was originally proposed by Schulman et al. [97], the cooling limits were studied assuming that the initial state of the system should be in the maximally mixed state. This assumption was motivated by the NMR systems, whose qubits are highly mixed (with initial polarization of the order of 10^{-5}). Furthermore, the corresponding limits would give a general achievable bound, since any initial state can be driven efficiently to a maximally mixed state before applying the PPA-HBAC protocol.

In this chapter, we solve the open question of finding the cooling limits of the PPA-

HBAC not only for the maximally mixed initial state, but also for a larger family of initial states that satisfy the cooling limit condition of eq. (3.1.1).

If we start with a maximally mixed state, or the product state of all the qubits in the thermal state at the bath temperature, it is possible to show that after applying t rounds of PPA, the diagonal elements of the computational qubits state will satisfy

$$A_i^t \left(1-\epsilon_b\right)^m \leq A_{i+1}^t \left(1+\epsilon_b\right)^m , \tag{3.2.1}$$

for all $i = 1, 2, 3, ..., 2d-1$. This can be proved by induction, since it is true for the initial step, as for the maximally mixed state ($t = 0$) all the $A_i = \frac{1}{2d}$. Then, after applying a round of PPA on a state that satisfies the aforementioned order, it turns out that returns a new state that satisfy again the inequalities of eq. (3.2.1). Therefore, the same is true for all subsequent iterations. See Appendix A, for a detailed proof.

Similarly, it is also possible to show that at each step of the protocol the polarization of the target qubit never decreases; while the entropy of the reset qubits always increases beyond the one from the bath after each entropy compression step. Thus, the reset qubits always pump entropy out of the system into the bath, converging to a limit.

Comparing eq. (3.1.3) with eq. (3.2.1) indicates that the asymptotic state of the computational qubits can only go towards the equality

$$A_i^\infty \left(1-\epsilon_b\right)^m = A_{i+1}^\infty \left(1+\epsilon_b\right)^m , \quad \forall \quad i = 1, 2, 3, ..., 2d-1. \tag{3.2.2}$$

From this condition (3.2.2) and the property $\mathrm{Tr}\left(\rho_{com}\right) = 1$, it is possible to find all the diagonal elements of the computational qubits that are in that asymptotic state, which are as follows: $A_i^\infty = \frac{1-Q}{1-Q^{2d}} Q^{i-1}$, where $Q = \left(\frac{1-\epsilon_b}{1+\epsilon_b}\right)^m$. This result gives the exact solution of the steady state of the computational qubits, ρ_{com}^∞, for all values of the bath polarization:

$$diag\left(\rho_{com}^\infty\right) = A_1^\infty \left(1, Q, Q^2, ..., Q^{2d-1}\right). \tag{3.2.3}$$

Achievable cooling for PPA-HBAC

The maximum achievable polarization for the target qubit, for the PPA-HBAC protocol with maximally mixed initial state, is given by

$$\epsilon_{\mathbb{1}}^{\infty} = \frac{(1+\epsilon_b)^{md} - (1-\epsilon_b)^{md}}{(1+\epsilon_b)^{md} + (1-\epsilon_b)^{md}}, \tag{3.2.4}$$

where ϵ_b is the bath polarization, d the dimension of the scratch qudit, and m the number of reset qubits.

Then, the corresponding lowest achievable temperature of the target qubit, in the cooling limit, is as follows:

$$T_{steady} = \frac{1}{md}\, T_b\, \frac{\Delta E_t}{\Delta E_r} \tag{3.2.5}$$

Here T_b is the temperature of the bath, and ΔE_t and ΔE_r are the energy gaps between the two energy levels of the target qubit, and the reset qubits, respectively. Note that, since d is the dimension for the subsystem between the target qubit and the reset qubits ($d = 2^{n'}$ when the scratch qudit is a string of n' qubits), the final temperature decreases exponentially with the number of qubits used in the string. This results agree with the third law of thermodynamics [64, 68], since they would require a system of infinite dimension to achieve temperature zero.

The detailed proof of the achievable polarization and achievable temperature for the target qubit can be found in Appendix A.

The achievable polarization for a target qubit when the system consists of a string of n qubits, i.e the scratch qudit is a string of n' qubits, is given by eq. 3.2.4 with $d = 2^{n'}$:

$$\epsilon_{\mathbb{1}}^{\infty}\left(d = 2^{n'}\right) = \frac{(1+\epsilon_b)^{m2^{n'}} - (1-\epsilon_b)^{m2^{n'}}}{(1+\epsilon_b)^{m2^{n'}} + (1-\epsilon_b)^{m2^{n'}}}, \tag{3.2.6}$$

Furthermore, the asymptotic polarization of each of the qubits in the string (numbered from right to left, as in Fig. 2.5), has a similar form and depends on the position j^{th} of the

qubit in the string (going from hotter to colder as we move from right to left) as follows:

$$\epsilon_{max}^{(j)} = \frac{(1+\epsilon_b)^{m2^{j-1}} - (1-\epsilon_b)^{m2^{j-1}}}{(1+\epsilon_b)^{m2^{j-1}} + (1-\epsilon_b)^{m2^{j-1}}}$$

In the limit for low bath polarization, $\epsilon_b << 1/md$, the achievable asymptotic polarization is proportional to the dimension of the Hilbert space of the scratch qudit (or n' qubits), i.e. $\epsilon_{\mathbb{1}}^{\infty} \approx md\epsilon_b (= m2^{n'}\epsilon_b)$. As the value of ϵ_b increases beyond $1/md$, we observe a transition for the asymptotic polarization. This is shown in Fig. 3.1, as a function of the bath polarization for different number of qubits, using eq. (3.2.4). We can observe the transition noted by [73] and [98] at $\epsilon_b \sim 2^{-n}$, for $m = 1$, agreeing with simulations.

In order to see how $\epsilon_{\mathbb{1}}^{\infty}$ approaches 1, we use $\Delta_{max} = 1 - \epsilon_{\mathbb{1}}^{\infty}$, and eq (3.2.4). Then,

$$\Delta_{max} = \frac{2}{e^{md\ln\left(\frac{1+\epsilon_b}{1-\epsilon_b}\right)} + 1} = \frac{2}{e^{m2^{n'}\ln\left(\frac{1+\epsilon_b}{1-\epsilon_b}\right)} + 1}. \tag{3.2.7}$$

This expression shows that the asymptotic polarization goes to 1 doubly exponentially in the number of qubits n' (or exponential as a function of the size of the Hilbert space d). In Fig. 3.1, we show $\epsilon_{\mathbb{1}}^{\infty}$ as a function of ϵ_b for different values of d, with $m = 1$.

Even though, the asymptotic polarization $\epsilon_{\mathbb{1}}^{\infty}$ was obtained assuming the system qubits started in the completely mixed state, the same asymptotic polarization would be obtained by different initial states as long as they obey eq. (3.2.1). Numerical simulation indicates that this could also happens with some initial states not obeying eq. (3.2.1), but having a target qubit which after the first entropy compression gets a polarization below the value of $\epsilon_{\mathbb{1}}^{\infty}$. On the other hand, we found explicit examples of initial states that lead to asymptotic polarizations that are higher than $\epsilon_{\mathbb{1}}^{\infty}$, when the preliminary preparation of the PPA is skipped (i.e. the standard preliminary step that thermalizes all the qubits to the bath temperature of PPA) and we allow the protocol starts directly with an entropy compression operation on a general initial state. Nevertheless, as any state can be efficiently maximally randomized, it is always possible to reach the polarization given by $\epsilon_{\mathbb{1}}^{\infty}$ and maybe do better if the initial state is different – without applying the preliminary step of the PPA.

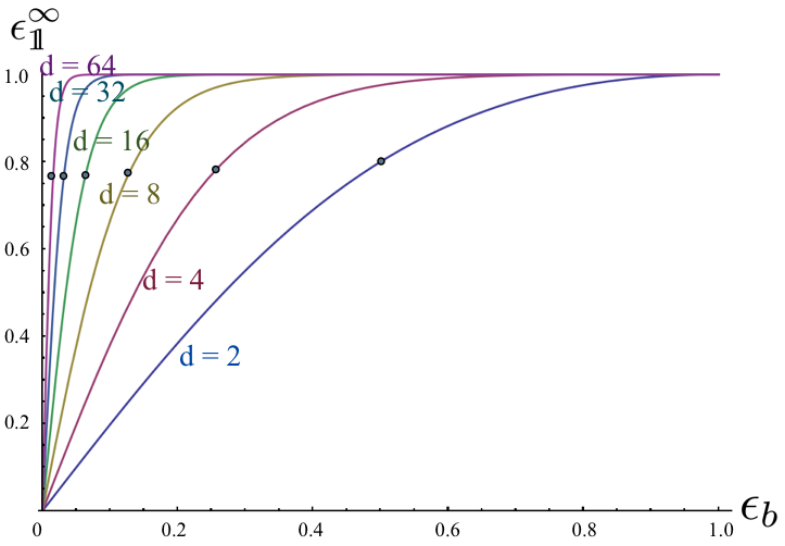

Figure 3.1: Asymptotic achievable polarization for the target qubit. This polarization increases double exponentially in the number of qubits as the scratch qudit, n'. The dots are located at the point of $\epsilon_{\mathbb{1}}^{\infty}$ which corresponds to the $\epsilon_b = \frac{1}{md}$, where the transition can be observed, for $d = 2$, 4, 8, 16, 32, and 64, and $m = 1$. (For ϵ_b smaller than that value, $\epsilon_{\mathbb{1}}^{\infty}$ is linear in ϵ_b.)

3.2.1 Schulman's Physical-Limit Theorem

The steady state, eq. (3.2.3), is consistent with the bounds given by the theorem of Schulman et al. [99]. Their theorem provides an upper bound of the probability of having any basis state, concluding that no heat-bath method can increase that probability from its initial value, 2^{-n}, to more than $min\{2^{-n}e^{\epsilon 2^{n-1}}, 1\}$. Where ϵ is related to the polarization of the heat-bath as $\epsilon_b = \tanh\epsilon$, and n is the total number of qubits ($n = n' + 2$: $n' + 1$ computational qubits and one reset qubit).

We improved the aforementioned theorem by finding the corresponding exact maximum probability, p_{max} of having the basis state $|00...0\rangle$, namely at the cooling limit. This polarization can be calculated from the steady state, eq. (3.2.3), and $\rho = \rho_{com}^{\infty} \otimes \rho_{\epsilon_b}$. Then,

$p_{max} = A_1^{\infty}\left(1+\epsilon_b\right)/2$, which can be written as a function of n and ϵ_b as follows:

$$p_{max} = \frac{\epsilon_b}{1-\left(\frac{1-\epsilon_b}{1+\epsilon_b}\right)^{2^{n-1}}}$$

Fig. 3.2 shows both the upper bound proposed by Schulman (dashed lines) and the asymptotic value obtained here (thick lines), for different values of n. We can see that the bound is very close to the exact solution for small values of ϵ_b, but differ for large values of ϵ_b.

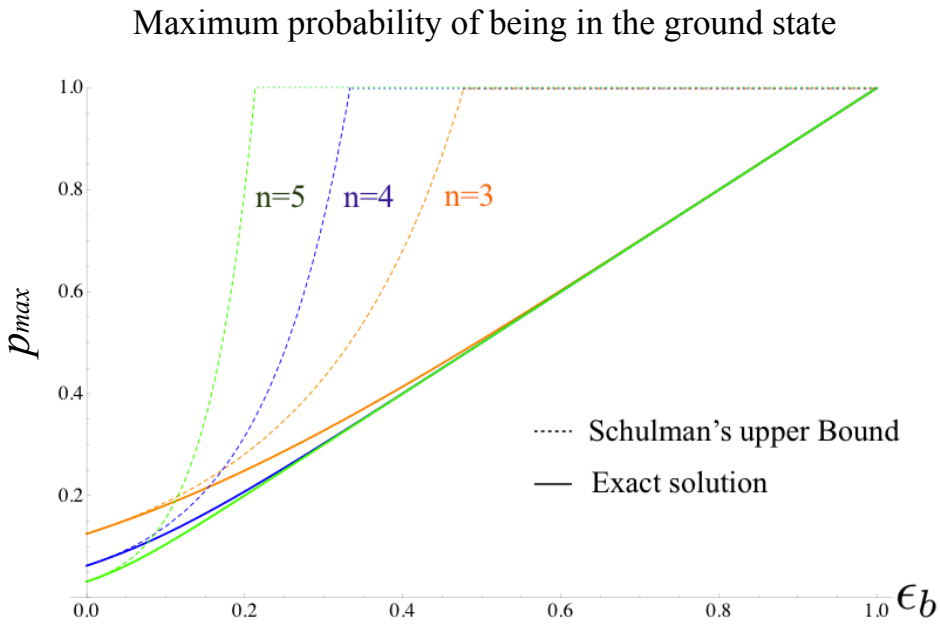

Figure 3.2: Comparison between the exact maximum achievable cooling and the Schulman's upper bounds. Upper limit of the probability of any basis state for the total n qubit system ($n = n'+2$: $n'+1$ computational qubits and one reset qubit). The dashed line corresponds to the Schulman's upper bound and the thick line to the exact asymptotic probability. Orange for $n = 3$, purple for $n = 4$, and green for $n = 5$.

3.2.2 Number of rounds required to get a polarization $\epsilon = \epsilon_{\mathbb{1}}^{\infty} - \delta$

For the three qubit case, it is easy to derive the exact number of steps required to get a certain polarization $\epsilon = \epsilon_{\mathbb{1}}^{\infty} - \delta$, since the quantum circuit to perform the PPA method for this case repeats the same entropy compression operation in all the iterations of the PPA (which consists of different subsequent rounds), see Fig. 2.8. By taking the initial target polarization as $\epsilon^{t=0} = \epsilon_0$, after j rounds of the PPA, the polarization will be

$$\epsilon^t = \epsilon_{\mathbb{1}}^{\infty} - q^j \left(\epsilon_{\mathbb{1}}^{\infty} - \epsilon_b\right), \tag{3.2.8}$$

where $q = \frac{1-\epsilon_b^2}{2}$. Then, by replacing the corresponding achievable polarization of this case, i.e. $\epsilon_{\mathbb{1}}^{\infty} = \frac{2\epsilon_b}{1+\epsilon_b^2}$ (eq. (3.2.4) with $d = 2$ and $m = 1$), it is obtained that the number of rounds needed to get to $\epsilon = \epsilon_{\mathbb{1}}^{\infty} - \delta$ for the three-qubit case is as follows (See Appendix A for details):

$$N_{3q}(\delta, \epsilon_b) = 2\frac{\log\left(\frac{\delta}{\epsilon_{\mathbb{1}}^{\infty} - \epsilon_b}\right)}{\log q}.$$

On the other hand, despite the simplicity and periodicity of the PPA's quantum circuit for the 3-qubit case, it is complicated to generalize the quantum circuit for a bigger number of qubits. First, the entropy compression operation depends on the state of the system and, thus, is different in each iteration. Second, the number of gates needed in each iteration grows with the number of qubits.

Then, for the n-qubit case, with $n > 3$, we only provide an upper bound on the number of steps required to get polarization $\epsilon_{h,\delta} < \epsilon_{max}$ (with $n' = n - 2$, $m = 1$) is

$$N_{upper-bound} = \prod_{k=1}^{k=[n'/2]} N(\delta_k, \epsilon_k), \tag{3.2.9}$$

where $\epsilon_{max} = \frac{(1+\epsilon_b)^{d/2} - (1-\epsilon_b)^{d/2}}{(1+\epsilon_b)^{d/2} + (1-\epsilon_b)^{d/2}}$; $\epsilon_k := f(\epsilon_{k-1}) - \delta_k$; $\epsilon_{h,\delta} = \epsilon_h$, with $h = [n'/2]$ (the integer part of $n'/2$); $f(\epsilon) = \frac{2\epsilon}{1+\epsilon^2}$; $N(\delta, \epsilon) = 2\frac{\log\left(\frac{\delta}{f(\epsilon_b) - \epsilon_b}\right)}{\log q}$; and $\epsilon_0 = \epsilon_b$. (See Appendix A for more details.)

Fig. 3.3 shows numerical simulations of the number of steps as a function of $\delta_{rel} = \frac{\epsilon_{\mathbb{1}}^{\infty} - \epsilon}{\epsilon_{\mathbb{1}}^{\infty}} = \delta/\epsilon_{\mathbb{1}}^{\infty}$. The simulations are consistent with the upper bound of the number of steps

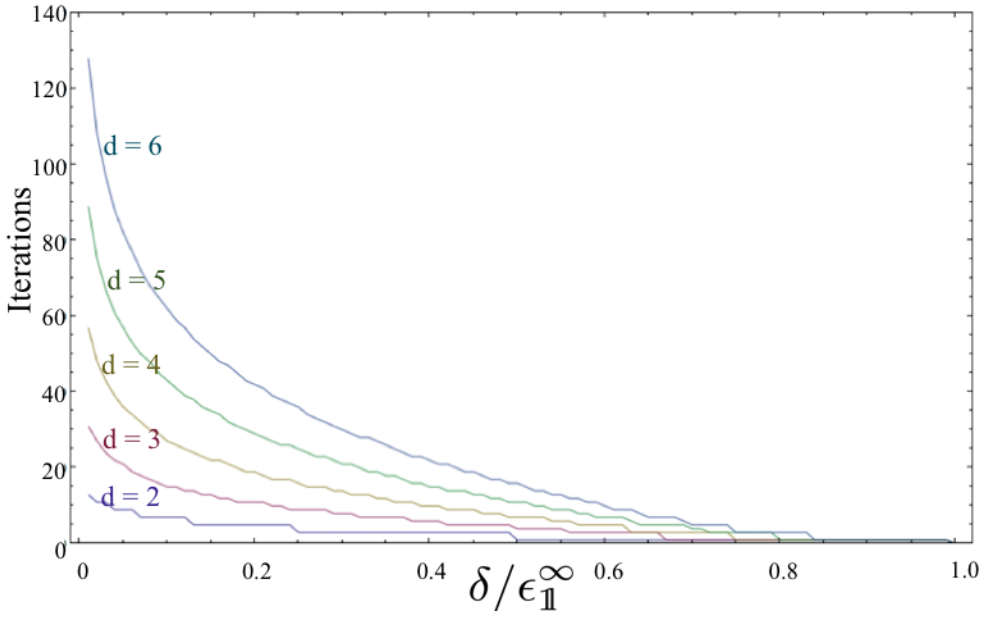

Figure 3.3: Number of PPA-iterations that are required to have polarization $\epsilon = \epsilon_{\mathbb{1}}^{\infty} - \delta$ as a function of $\delta/\epsilon_{\mathbb{1}}^{\infty}$, for d=2, 3, 4, 5, and 6.

and with the exact solution for the case of three qubits.

3.3 Is this the ultimate cooling limit?

After we solved the problem of finding the analytical solution for the PPA achievable cooling, we realized that the implicit assumption about the optimization of the PPA protocol can be removed to give a more general interaction with the bath and improve the achievable cooling. In particular, we found that better purification can be achieved by using correlated relaxation processes between the system and the thermal bath during the refresh steps, as explained in the next chapter.

Chapter 4

Heat-Bath Algorithmic Cooling with correlated qubit-environment interactions

The limits of HBAC have been studied using, in particular, the PPA algorithm, which was widely believed to be optimal among all possible heat-bath algorithmic cooling protocols [88, 98, 99]. These cooling limits were claimed to be the fundamental limit for all HBAC techniques under general conditions [88]. In this Chapter, however, I show that the long standing upper bound on the limits of the PPA algorithm [98] can be surpassed by using a more general reset operation that takes advantage of correlations during the relaxation processes. Our results provide a novel set of tools for the cooling techniques, which we use to design explicit algorithms that circumvent the cooling limit by taking advantage of correlations when the coupling to the environment is not limited to independent qubit-relaxation. The content of this chapter was published in the Ref. [89].

4.1 The PPA cooling limit for the 2-qubit case

The maximum achievable cooling of the PPA protocol, Eq.(3.2.4), indicates that, in particular for the case of two identical qubits, there is no improvement in polarization beyond

the bath polarization. Namely, from Eq.(3.2.4), for a 2-qubit system made up of one target qubit and one reset qubit, the maximum achievable polarization is $\epsilon_{\mathbb{1}}^{\infty}(n=2, m=1, d=2^0) = \epsilon_b$. However, in a recent paper [65], Jun Li and collaborators found cases/experiments where utilizing relaxation effects does offer a polarization enhancement while they were studying the efficiency of polarization transfer in the presence of a bath, using the *vector of coherence representation*. In looking at the maximum polarization (or purity), they (re)-discovered that it is possible to enhance the polarization of one of two qubits beyond the bath polarization in the presence of relaxation and cross-relaxation for the quantum system. The surprising improvement turns out to be related to the Nuclear Overhauser Effect (NOE), discovered in 1953 [76]. This effect, even though it has been known for a long time, had never been explicitly connected as a tool for algorithmic cooling before. [1]

NOE appears in the presence of cross-relaxation and results in the boost of polarization of one qubit when the second one is saturated, i.e. rotated rapidly so that in the relevant timescale its polarization averages to zero (in the next section I present a description of the NOE using the Solomon equations). So, what was the PPA method missing? In particular, in the PPA method, the refresh step fully re-thermalizes the reset qubits to the heat-bath temperature, which is equivalent to swapping these qubits with qubits from the bath. This full thermalization was assumed to be the optimal refresh operation, with respect to the entropy extraction from the system per contact with the thermal bath, which is true when the interaction is limited to single qubit decay processes. However, there are different ways to couple the quantum system with the heat-bath to remove entropy.

In this chapter, I show how correlated relaxation processes between the system and environment during re-thermalization can be exploited to enhance cooling. Inspired by these effects, we created a more general reset operation that includes correlated-qubits interaction with the bath with cross-relaxation processes, rather than just a single qubit decay. We introduce this reset operation as a new tool for cooling algorithms, which we call "state-reset". Furthermore, we present explicit improved cooling algorithms that lead to an increase of purity beyond all previous work.

[1] In Ref. [15], the NOE is mentioned in the context of HBAC, however the bypass was not noted in that work, nor was it integrated into the protocols.

4.2 Nuclear Overhauser Effect

We have two spins (qubits), we irradiate one and the other one cools down! When first proposed as a contributed paper at an APS meeting in April 1953, the proposal was met with much skepticism by a formidable array of physics talent. Included among these were notables such as: Felix Bloch (recipient of 1952 Physics Nobel Prize), Edward M. Purcell (recipient of Nobel Prize 1952 with Bloch and session chair), Isidor I. Rabi (recipient of Physics Nobel Prize, 1944) and Norman F. Ramsey (recipient of Physics Nobel Prize, 1989). Eventually everyone was won over.

> *Letter from Norman Ramsey to Overhauser.* July 27, 1953
>
> Dear Dr. Overhauser:
> You may recall that at the Washington Meeting of the Physical Society, when you presented your paper on nuclear alignment, Bloch, Rabi, Pearsall, and myself all said that we found it difficult to believe your conclusions and suspected that some fundamental fallacy would turn up in your argument. Subsequent to my coming to Brookhaven from Harvard for the summer, I have had occasion to see the manuscript of your paper. **After considerable effort in trying to find the fallacy in your argument, I finally concluded that there was no fundamental fallacy to be found. Indeed, my feeling is that this provides a most intriguing and interesting technique for aligning nuclei.** After considerable argument, I also succeeded in convincing Rabi and Bob Pound of the validity of your proposal and I have recently been told by Pound that he subsequently converted Pearsall shortly before Pound left for Europe. I hope that you will have complete success in overcoming the rather formidable experimental problems that still remain. I shall be very interested to hear of what success you have with the method.
>
> Sincerely,
> Norman F. Ramsey

In the Nuclear Overhauser Effect (NOE) it is possible the transfer of nuclear spin polarization from one population of spin-active nuclei to another via cross-relaxation. This

effect, although it was discovered in 1953 [76], had never been used in the context of quantum information science, and consequently, had not been connected with algorithmic cooling ideas.

4.2.1 NOE for two qubits

In a system of two qubits, NOE effect appears in the presence of cross-relaxation results in a boost of polarization of one of the qubits when the second one is saturated, i.e. rotated rapidly so that over relevant timescale its polarization averages to zero. This can be seen from the Solomon equations [104], which describe the dipolar relaxation process of a system consisting of two spins. These equations, so named after physicist Ionel Solomon, describe how the population of the different spin states changes in relation to the strength of the self-relaxation rate constant R_1 and the cross-relaxation rate constant R_{12}. The R_1 and R_{12} are combinations of relaxation rates Γ_i for the transition between the four states ($|00\rangle$, $|01\rangle$, $|10\rangle$ and $|11\rangle$), as depicted in Fig. 4.1, as follows:

$$R_1 = \Gamma_2' + 2\Gamma_1 + \Gamma_2 \quad \text{and} \quad R_{12} = \Gamma_2 - \Gamma_2'.$$

In the limit of low polarization, the expectation of the Z Pauli operator for the first spin $\langle Z_1 \rangle = \mathrm{Tr}(\sigma_z \rho_1)$, obeys the following Solomon's equation (see [104]):

$$\frac{d\langle Z_1 \rangle}{dt} = -R_1(\langle Z_1 \rangle - \langle Z_1 \rangle_0) - R_{12}(\langle Z_2 \rangle - \langle Z_2 \rangle_0), \tag{4.2.1}$$

where $\langle Z_i \rangle$ is the polarization of the i^{th} qubit ($\langle Z_i \rangle = \mathrm{Tr}(\sigma_z \rho_i)$), in particular $\langle Z_i \rangle_0$ is the polarization in their equilibrium values, R_1 is the self-relaxation rate constant – the relaxation parameter – for the first spin, and R_{12} is the cross-relaxation rate constant for exchange of magnetization between the two spins (qubits).

The cross relaxation, R_{12}, is the important term which is responsible for transferring magnetization from one spin to the other and gives rise to the nuclear Overhauser effect.

It is possible to drive (rotate) the second spin so that on the relevant timescale (related to R_2 and R_{12}) the expectation of $\langle Z_2 \rangle \approx 0$. Then, the steady state of the Solomon equation

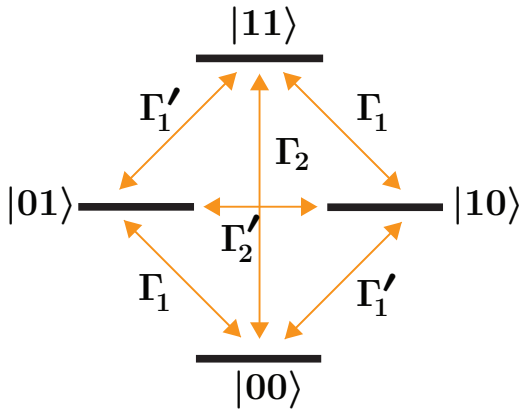

Figure 4.1: Relaxation diagram for a two qubit system. Γ_1, Γ'_1, Γ_2, and Γ'_2 represent the transition probabilities per unit time between the four states, as indicated by the arrows. The process illustrated as Γ_2 ($|00\rangle \leftrightarrow |11\rangle$) cannot be described as a qubit-reset with the bath as in the PPA, and results in the boost of polarization of one qubit when the other is saturated.

Eq.(4.2.1), for that situation, implies that

$$\langle Z_1 \rangle = \langle Z_1 \rangle_0 + \frac{R_{12}}{R_1} \langle Z_2 \rangle_0.$$

Namely, the polarization of the first qubit would go to $\epsilon_{target} = \left(1 + \frac{R_{12}}{R_1}\right) \epsilon_b$, where $\langle Z_1 \rangle_0 = \langle Z_2 \rangle_0 = \epsilon_b$, since both qubits are immersed in the bath. This gives an enhancement beyond PPA for the two-qubit case, as long as R_{12}/R_1 is positive. In particular, when $\Gamma'_2 = \Gamma_1 = 0$ we obtain an enhancement of 2, for two spins with identical thermal-equilibrium polarizations.

This effect relies on cross-relaxation, and cannot be understood as a simple "swap" of the polarization of the reset qubits with the polarization of the bath. In particular, it can occur in NMR when two nuclei (in the same molecule) interact with a same nuclei of the environment [104]. In other technologies such as superconducting qubits or ions traps, they could be engineered by placing the qubits in a leaky cavity which resonantes at the twice the frequency of the qubits leading to a relaxation process which involves two qubits.

Note that the refresh step required in the PPA, which individually thermalizes the

reset qubits to the temperature of the bath, only involves the Γ_1 to reset the second qubit (similarly, the Γ_1' is transition required to fully thermalize the first qubit).

One way to understand the process from an algorithmic point of view is to realize that the cross relaxation effectively provides a state relaxation/equilibration ("state reset") between $|11\rangle$ and $|00\rangle$, without touching the other states, analogous to the qubit reset. This form of reset accompanied by a rotation of the second qubit can however boost the polarization of the first qubit beyond what would be obtained by a qubit reset from the bath as in the PPA. In the next section, I will show how to express this process in the language of quantum information processing, and then create a new tool that can be exploited for the algorithmic protocols. Concretely, the individual qubit relaxation and the crossed relaxation are presented and described in terms of Krauss operators, and then rewrite the NOE effect as an algorithm. Moreover, we present an improved NOE algorithm that goes beyond the polarization enhancement obtainable by the conventional NOE (and by the PPA class).

4.3 Qubit relaxation processes

What operations describe the effect of dissipation to an environment at finite temperature? In this section, I explain the quantum operations of both the individual relaxation process and crossed relaxation processes. These processes have their own unique features, but the general behavior of them is well characterized by a quantum operation known as amplitude damping [74].

4.3.1 Individual relaxation for qubits

The individual relaxation, which describes the type of refresh step used in the PPA protocol can be described with the longitudinal relaxation, T1, also known as spin-lattice relaxation. This longitudinal relaxation is the process through which the state of the nuclei returns to the thermal state due to coupling of spins to their surrounding lattice –a large system which is in thermal equilibrium at a given temperature.

The individual relaxation for a qubit is due to the transitions of the type Γ_1. See for

example, the two-qubit case depicted in Fig. 4.1, where the PPA reset on the second qubit can be understood as a rethermalization due to Γ_1 only (similarly, to Γ_1' for refreshing the first qubit).

The effect of the Γ_1 transitions can be described with a generalized amplitude damping. For single qubits, the Kraus operators that describe the evolution under the individual relaxation Γ_1 [74] are

$$\begin{aligned} A_1 &= \sqrt{p}\begin{pmatrix} 1 & 0 \\ 0 & \sqrt{1-\eta} \end{pmatrix}, \qquad A_2 = \sqrt{p}\begin{pmatrix} 0 & \sqrt{\eta} \\ 0 & 0 \end{pmatrix}, \\ A_3 &= \sqrt{1-p}\begin{pmatrix} \sqrt{1-\eta} & 0 \\ 0 & 1 \end{pmatrix}, \qquad A_4 = \sqrt{1-p}\begin{pmatrix} 0 & 0 \\ \sqrt{\eta} & 0 \end{pmatrix}, \end{aligned} \tag{4.3.1}$$

For $\eta \approx 1$, the evolution gives a fast thermalization, that we will call process $\mathcal{E}_{\Gamma_1}$, which is the one that reproduces the individual qubit-reset needed in the PPA-HBAC.

Qubit-reset operation $\mathcal{E}_{\Gamma_1}$, for individual thermalization

The state of the qubit under the **qubit-reset** operation, due to the individual relaxation Γ_1, can be described as

$$\mathcal{E}_{\Gamma_1}(\rho) = \sum_{i=1}^{4} A_i^{\Gamma_1} \rho \left(A_i^{\Gamma_1}\right)^\dagger,$$

with the set of Kraus operators of the generalized amplitude damping, Eq. (4.3.1). When $\eta = 1$, this operation reproduces the full thermalization of the qubit, with the following operators:

$$\begin{aligned} A_1^{\Gamma_1} &= \sqrt{p_1}|0\rangle\langle 0| \\ A_2^{\Gamma_1} &= \sqrt{p_1}|0\rangle\langle 1|, \\ A_3^{\Gamma_1} &= \sqrt{1-p_1}|1\rangle\langle 1|, \\ A_4^{\Gamma_1} &= \sqrt{1-p_1}|1\rangle\langle 0|. \end{aligned}$$

Here the probability p_1 is chosen to leave the thermal equilibrium distribution over the states $|0\rangle$ and $|1\rangle$, and depends on the energy gap of the reset qubit ΔE_q and the energy gap of the qubits from the bath ΔE_b, as follows:

$$p_1 = \frac{e^{\beta \Delta E_q/2}}{2\cosh\left(\beta \Delta E_q/2\right)},$$

where β_b is the bath's inverse temperature –which is related with the bath polarization as $\epsilon_b = \tanh\left(\beta \Delta E_b/2\right)$.

Thus, for a qubit with same energy gap of the qubits of the bath ($\Delta E_q = \Delta E_b$), p_1 is given by

$$p_1 = \frac{1+\epsilon_b}{2}$$

which provides an effect equivalent to make a simple swap between the qubit we want to reset and a qubit from the bath.

4.3.2 Cross relaxation as a new tool to reset states

The cross-relaxation rate constant, $R_{12} = \Gamma_2 - \Gamma_2'$, allows the exchange of magnetization between the two spins (qubits), which can be exploited for practical applications. For example, the cross-relaxation process gives rise to the nuclear Overhauser effect (NOE), and also makes possible the determination of three-dimensional molecular structures by NMR spectroscopy.

In this section, I show how to integrate the cross relaxation, as a new operation, to the set of tools for algorithmic cooling protocols, and in general to the operations of quantum information for processing the probabilities of states in a correlated way.

Let us consider a two-qubit system ($n = 2$), with occupation numbers N_{00}, N_{01}, N_{10} and N_{11} – i.e., the probabilities corresponding to the states $|00\rangle$, $|01\rangle$, $|10\rangle$ and $|11\rangle$, respectively. The effect of the cross relaxation, due to the double quantum transition Γ_2 (as depicted in Fig. 4.1), drives a direct transfer of populations between the states $|00\rangle$ and $|11\rangle$ while the system thermalizes to an equilibrium. In the extreme case, when Γ_2 is much larger than the other transition probabilities, there will be a fast equilibration between the occupational numbers N_{00} and N_{11}, while the change in the other variables N_{01} and N_{10} can be negligible

during the relaxation process.

This situation can give a different type of reset step that partially thermalizes both qubits, by only relaxing a selected pair of states. Based on this process, we define a reset operation, which we called *"state-reset"* to distinguish it from the conventional *qubit-reset* used in previous algorithmic cooling protocols (i.e. the individual full thermalization of qubits given by Γ_1). The concrete definition of the *state-reset* is presented in the following box. For the state-reset, the Kraus operators that describe the evolution under Γ_2 are analogous to the generalized amplitude damping presented in the previous section.

***State-reset* operation on the states $|00\rangle$ and $|11\rangle$: $\mathcal{E}_{\Gamma_2}$**

We define the ***state-reset*** operation $\mathcal{E}_{\Gamma_2}$, as the process that refreshes the pair of states $|00\rangle$ and $|11\rangle$ with the cross-relaxation Γ_2.

The effect of the state-reset on a two-qubit system ρ, can be described with the following set of operators:

$$\mathcal{E}_{\Gamma_2}(\rho) = \sum_{i=1}^{6} A_i^{\Gamma_2} \rho \left(A_i^{\Gamma_2}\right)^\dagger,$$

$$\begin{aligned} A_1^{\Gamma_2} &= \sqrt{p_2}|00\rangle\langle 00| & A_5^{\Gamma_2} &= |01\rangle\langle 01| \\ A_2^{\Gamma_2} &= \sqrt{p_2}|00\rangle\langle 11| & A_6^{\Gamma_2} &= |10\rangle\langle 10| \\ A_3^{\Gamma_2} &= \sqrt{1-p_2}|11\rangle\langle 11| \\ A_4^{\Gamma_2} &= \sqrt{1-p_2}|11\rangle\langle 00| \end{aligned}$$

where the probability p_2 is chosen to leave the thermal equilibrium distribution over the states $|00\rangle$ and $|11\rangle$, and it is given by

$$p_2 = \frac{e^{2\xi_b}}{2\cosh 2\xi_b},$$

where $\epsilon_b = \tanh \xi_b$, when the qubits of the system have the same energy gap of the qubits from the bath. In the limit of low polarization, this probability takes the simple form of $p_2 = (1 + 2\epsilon_b)/2$.

The state-reset operation $\mathcal{E}_{\Gamma_2}$ transforms the diagonal elements of the density matrix ρ as follows:

$$\mathrm{diag}\,(\rho) = [N_0, N_1, N_2, N_3] \xrightarrow{\mathcal{E}_{\Gamma_2}} [(N_0 + N_3)\,p_2, N_1, N_2, (N_0 + N_3)\,(1 - p_2)]\,,$$

resulting in the rethermalization between $|00\rangle$ and $|11\rangle$. This type of relaxation can be generalized for higher dimensions, and also for different pair of states, as I discuss in next sections.

Note that for qubits with different energy gap than the qubits from the bath, the probability p_2 is given by

$$p_2 = \frac{e^{\beta \Delta E_q}}{2\cosh\left[\beta \Delta E_q\right]},$$

where ΔE_b is the energy gap of the qubits from the bath, and ΔE_q is the energy gap of the reset qubit. The bath polarization is related with ΔE_b and β as $\epsilon_b = \tanh\left[\beta \Delta E_b/2\right]$.

The state-reset operation $\mathcal{E}_{\Gamma_2}$, accompanied by saturation of the second qubit, can boost the polarization of the first qubit, giving rise to the NOE effect. In the next section, I describe this effect as an algorithmic protocol in quat.

4.4 Nuclear Overhauser Effect as an algorithm in QIP

The NOE emerges in a pair of qubits in the presence of cross-relaxation (Γ_2), when one of the qubits is rapidly rotated so that over relevant timescale its polarization averages to zero, resulting in the boost of polarization of the other qubit [76]. In the quantum information processing terminology, as an algorithm, this process consists of the iteration of two operations: one to saturate (totally mix) one of the qubits and a relaxation operation for the cross-relaxation of the system with the bath ($\mathcal{E}_{\Gamma_2}$). In this sense, we assume we have control over non-unitary processes, in the spirit of reservoir engineering (as in [87]) to create the effect of turning on Γ_1 and Γ_2 independently.

We define the "Completely-mixed-state (CMS)" operation, as the operation that saturates the state of a qubit ρ, i.e. $\mathrm{CMS}\,(\rho) = I/2$.

Nuclear Effect Overhauser Algorithm (NOE Algorithm)

The NOE Algorithm for a two-qubit system consists of the alternating iteration of two steps: **1)** A completely-mixed-state operation CMS on the reset qubit. **2)** Cross-relaxation $\mathcal{E}_{\Gamma_2}$ to reset the states $|00\rangle$ and $|11\rangle$ of the system. The corresponding circuit to reproduce the NOE algorithm is depicted as follows:

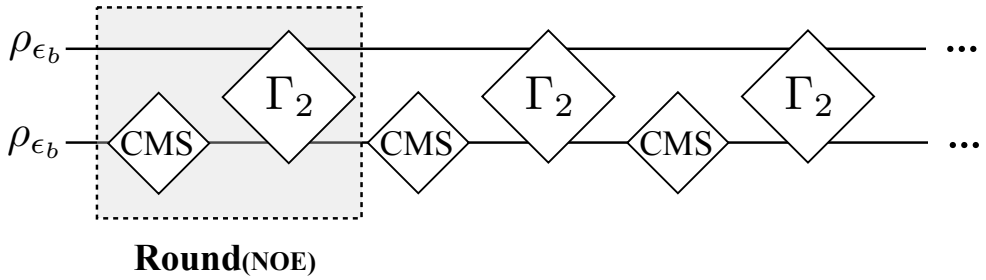

Figure 4.2: NOE Algorithm for the two qubit case. It consists of the iteration of rounds made of a CMS followed by the state-reset of the states $|00\rangle$ and $|11\rangle$. The gray dotted box represents a round. Note that, since the $\mathcal{E}_{\Gamma_2}$ and CMS are not unitary operations, they are not represented with the conventional boxes used for unitaries, but instead they are represented with diamonds for non-unitary processes.

The net effect of applying a round of the NOE Algorithm on a two-qubit system with state ρ can be expressed as follows:

$$\Phi_{\mathrm{NOE-Round}}(\rho) = \mathcal{E}_{\Gamma_2}\left[(\mathbb{1} \otimes \mathrm{CMS})\,\rho\right]$$

The polarization enhancement of the target qubit, under the NOE algorithm, goes asymptotically to a unique and attractive fixed point, which corresponds to the polarization predicted by the Solomon equations for the NOE effect: $2\epsilon_b$. The proof is detailed in the next subsection for low bath polarization and in Appendix B1 for any bath polarization.

4.4.1 Polarization evolution for the NOE Algorithm

Consider a system of two homo-nuclear spins. Let the system start in thermal equilibrium with polarization ϵ_b, i.e. with initial state $\rho_0 = \rho_b^{\otimes 2}$. Let us see how the polarization of the qubits evolves under a round of the NOE algorithm.

For simplicity in this section, Let us consider the low polarization regime (see Appendix B1 for any polarization). The diagonal of the initial state, which can be approximated to

$$\operatorname{diag}(\rho_0) = \operatorname{diag}\left(\frac{1}{4}\begin{bmatrix}1+\epsilon_b & 0\\ 0 & 1-\epsilon_b\end{bmatrix}^{\otimes 2}\right) \approx \frac{1}{4}\left(1+2\epsilon_b, 1, 1, 1-2\epsilon_b\right),$$

evolves under the two steps of the round as follows [2]:

$$\begin{aligned}
\operatorname{diag}(\rho_0) \xrightarrow{\mathbb{1}\otimes\mathrm{CMS}} &\frac{1}{2}\left(1+\epsilon_b, 1-\epsilon_b\right) \otimes \frac{1}{2}\left(1,1\right)\\
=&\frac{1}{4}\left(1+\epsilon_b, 1+\epsilon_b, 1-\epsilon_b, 1-\epsilon_b\right)\\
\xrightarrow{\Gamma_2} &\frac{1}{4}\left(1+2\epsilon_b, 1+\epsilon_b, 1-\epsilon_b, 1-2\epsilon_b\right)\\
\approx &\frac{1}{2}\left(1+\frac{3}{2}\epsilon_b, 1-\frac{3}{2}\epsilon_b\right) \otimes \frac{1}{2}\left(1+\frac{1}{2}\epsilon_b, 1-\frac{1}{2}\epsilon_b\right),
\end{aligned}$$

enhancing the polarization of the target qubit from ϵ_b to $\frac{3}{2}\epsilon_b$ at the expense to decrease the polarization of the second qubit to $\epsilon_b/2$.

Let ϵ_N be the polarization of the target qubit after N rounds of the NOE algorithm, then

$$\begin{aligned}
\operatorname{diag}(\rho_N) \xrightarrow{\mathbb{1}\otimes\mathrm{CMS}} &\frac{1}{2}\left(1+\epsilon_N, 1-\epsilon_N\right) \otimes \frac{1}{2}\left(1,1\right)\\
=&\frac{1}{4}\left(1+\epsilon_N, 1+\epsilon_N, 1-\epsilon_N, 1-\epsilon_N\right)\\
\xrightarrow{\Gamma_2} &\frac{1}{4}\left(1+2\epsilon_b, 1+\epsilon_N, 1-\epsilon_N, 1-2\epsilon_b\right),
\end{aligned}$$

[2] Note that the state of the system will remain in diagonal during the whole protocol.

which gives to the target qubit a polarization of $\epsilon_{N+1} = \frac{1}{2}\epsilon_N + \epsilon_b$. Thus, by induction,

$$\begin{aligned}\epsilon_N =& \frac{\epsilon_0}{2^N} + \sum_{i=0}^{N-1} \epsilon_b \\ =& \frac{\epsilon_0}{2^N} + 2\epsilon_b \left(1 - \frac{1}{2^N}\right)\end{aligned}$$

Thus, the polarization enhancement goes asymptotically to the polarization

$$\epsilon_{\text{NOE}}^{\infty} = \lim_{N\to\infty} \epsilon_N = 2\epsilon_b,$$

giving a unique attractive fix point, which is independent of the initial state of the qubits. This expression corresponds to small ϵ_b, for the low bath-polarization regime. This asymptotic polarization $\epsilon_{\text{NOE}}^{\infty} = 2\epsilon_b$ gives the same enhancement obtained from the Solomon equations that corresponds to the NOE effect, as described in the previous sections.

The asymptotic polarization of the NOE algorithm for any bath-polarization is given by

$$\epsilon_{NOE}^{\infty} = \tanh\left(2\xi_b\right),$$

where ξ_b is related to the polarization of the bath by $\epsilon_b = \tanh\left(\xi_b\right)$ (see Appendix B1 for details). Then, in Appendix B2 you can find a generalization of the NOE algorithm for larger systems of qubits, $n > 2$.

The steady state of the NOE algorithm $\rho_{\infty}^{\text{NOE}}$ corresponds to a diagonal state with the following diagonal

$$\text{diag}\left(\rho_{\text{NOE}}^{\infty}\right) = \frac{1}{2}\left(1 + \epsilon_{\text{NOE}}^{\infty}, 1 - \epsilon_{\text{NOE}}^{\infty}\right) \otimes \frac{1}{2}\left(1, 1\right).$$

In particular, when the initial polarization of the qubits is the same of the bath polarization, i.e. $\epsilon_0 = \epsilon_b$, the target qubit polarization will have an enhancement given by $\epsilon_k = 2\epsilon_b \left(1 - \frac{1}{2^{k+1}}\right)$ after k rounds of the protocol.

4.5 State-Reset HBAC for the two-qubit case

We present a novel cooling algorithm, which we called the "SRΓ_n HBAC" protocol for the n-qubit case, which allows the use of the state-reset as a tool to improve cooling. Concretely, for this novel type of protocols the allowed operations are as follows: 1) general unitary operations on the n-qubit system, 2) CMS operations to send qubits to the complete-mixed state, 3) Reset-state operations which thermalize the pairs of energy levels of the form $|00...0\rangle$ and $|11...1\rangle$ (note that this reset-state includes the individual relaxation when the pair of state are the $|0\rangle$ and $|1\rangle$). Also, it is assumed that the n qubits have the same energy gap, which is fixed.

Under the aforementioned assumptions, we present the optimal protocol for cooling a target qubit. However, note that when you allow the reset-state operation on arbitrary pairs of energy levels (different to the ones of the form $|00...0\rangle$ and $|11...1\rangle$), it could be possible to lead to an even better cooling.

In this section, I introduce the 2-qubit case of our new algorithm..

SRΓ_2-HBAC method

The SRΓ_2 HBAC for a two-qubit system consists of the iteration of the three steps:

1) A flip operation on the second qubit.

2) The cross-relaxation $\mathcal{E}_{\Gamma_2}$ operation to reset the states $|00\rangle$ and $|11\rangle$ of the system.

3) The individual relaxation $\mathcal{E}_{\Gamma_1}$ operation on the second qubit.

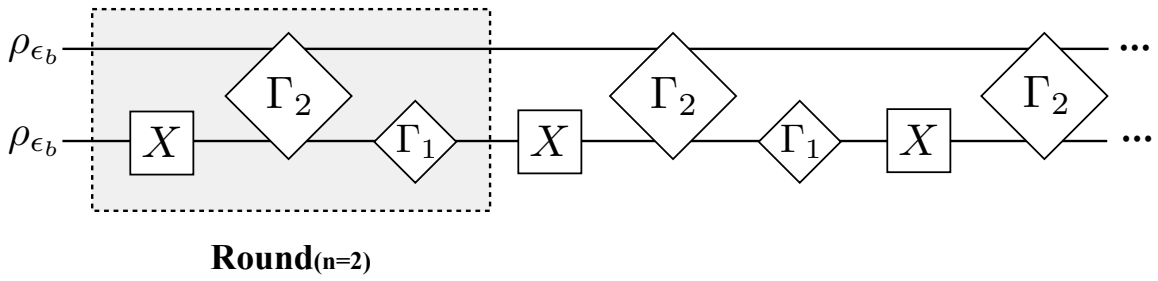

Figure 4.3: Circuit for the SRΓ_2-HBAC method. Γ_1 and Γ_2 are the state-reset operations on one and on two qubits, $\mathcal{E}_{\Gamma_1}$ and $\mathcal{E}_{\Gamma_2}$, respectively. The part inside the dotted box represents a round of the protocol. The entire circuit is just the repetition of that round.

The asymptotic polarization of the SRΓ_2-HBAC algorithm for any bath-polarization is given by

$$\epsilon^{\infty}_{\mathrm{SR}\Gamma_2} = \tanh\left(3\xi_b\right), \tag{4.5.1}$$

where ξ_b is related to the polarization of the bath by $\epsilon_b = \tanh\left(\xi_b\right)$ (see Appendix B3.1 for the precise calculation). Thus, the SRΓ_2-HBAC leads to an improvement on both the NOE ($\epsilon^{\infty}_{\mathrm{NOE}} = \tanh\left(2\xi_b\right)$) and the PPA-HBAC ($\epsilon^{\infty}_{\mathrm{PPA}_2} = \epsilon_b$).

Here, as a simple example, I present the approximation for the low polarization regime. Let us start with two qubits at thermal equilibrium, with polarizations ϵ_b, i.e. with state

$$\rho_0^{n=2} = \rho_{\epsilon_b}^{\otimes 2} = \left[\frac{1}{2}\begin{pmatrix} 1+\epsilon_b & 0 \\ 0 & 1-\epsilon_b \end{pmatrix}\right]^{\otimes 2} = \left[\frac{1}{2\cosh\xi_b}\begin{pmatrix} e^{\xi_b} & 0 \\ 0 & e^{-\xi_b} \end{pmatrix}\right]^{\otimes 2}. \tag{4.5.2}$$

The vector of its diagonal elements in the low polarization regime can be approximated as $\mathrm{diag}\left(\rho_0^{n=2}\right) = \frac{1}{4\cosh^2\xi_b}\left(e^{2\xi_b}, 1, 1, e^{-2\xi_b}\right) \approx \frac{1}{4}\left(1+2\epsilon_b, 1, 1, 1-2\epsilon_b\right)$.

Under the first two steps of the protocol (see Fig. 4.3), the initial state will evolve to $\mathrm{diag}\left(\rho_1\right) = \frac{1}{4}\left(1+2\epsilon_\mathrm{b}, 1+2\epsilon_\mathrm{b}, 1-2\epsilon_\mathrm{b}, 1-2\epsilon_\mathrm{b}\right)$. At this stage, the polarization of the first qubit is doubled and the second qubit has zero polarization, analogous to the NOE [76]. Then, the third gate prepares the second qubit for a new round. The polarization of the first qubit increases in each round. Concretely, after applying k rounds, the first qubit

polarization will be

$$\epsilon_k^{(n=2)} = \left(3 - \frac{1}{2^{k-1}}\right)\epsilon_b,$$

for the low polarization case. This leads to an asymptotic polarization of $3\epsilon_b$, an improvement on both the NOE and the PPA-HBAC for the two-qubit case.

For the general bath polarization, the maximum polarization achievable for the SRΓ_2-HBAC, as has been mentioned in eq. (4.6.3), will be $\epsilon^{\infty}_{\mathrm{SR}\Gamma_2} = \tanh(3\xi_b)$, leading to an improvement on both the NOE and the PPA-HBAC.

See Fig. 4.4 for a comparison of the maximum achievable polarization as a function of the bath polarization for the PPA-HBAC, the NOE algorithm and the SRΓ_2 HBAC, for the two-qubit case.

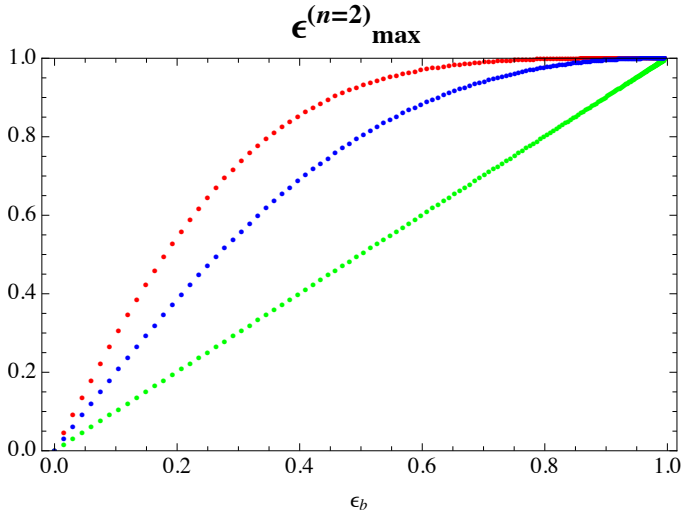

Figure 4.4: Comparison of the maximum achievable polarization for the PPA-HBAC (in green), the NOE algorithm (in blue) and the SRΓ_2 HBAC (in red), for the 2-qubit case, assuming thermal equilibrium polarization ϵ_b.

The enhancement of our methods is only due to the state-reset operations which require cross-relaxation processes, and not to the individual non-unitary processes on the qubits. The control over non-unitary processes to turn on/off Γ_1 and Γ_2 independently is needed to have them individually during the protocol, since the presence of Γ_1 at the same time as Γ_2 would decrease the polarization enhancement.

4.6 Generalized State-Reset

We generalize the state-reset idea to increase the polarization of a target qubit in a larger $n-$qubit system by considering the transition probability Γ_n between the eigenstates $|0\rangle^{\otimes n}$ and $|1\rangle^{\otimes n}$. Similarly, in the limit case, when $\Gamma_n \neq 0$, and the other transition probabilities equal to zero, the cross relaxation Γ_n effectively provides a state-reset between $|0\rangle^{\otimes n}$ and $|1\rangle^{\otimes n}$, without changing the other states. Then, the corresponding Kraus operators for the Γ_n operation are given by:

$$\begin{aligned} A_1^{(n)} &= \sqrt{p_n} \bigotimes_{i=1}^{n} |0\rangle_i\langle 0|_i, \\ A_2^{(n)} &= \sqrt{p_n} \bigotimes_{i=1}^{n} |0\rangle_i\langle 1|_i, \\ A_3^{(n)} &= \sqrt{1-p_n} \bigotimes_{i=1}^{n} |1\rangle_i\langle 1|_i, \\ A_4^{(n)} &= \sqrt{1-p_n} \bigotimes_{i=1}^{n} |1\rangle_i\langle 1|_i, \\ A_{4+j}^{(n)} &= \left(|j_{bin}\rangle\langle j_{bin}|\right), \end{aligned} \tag{4.6.1}$$

for all j integers between 0 and $2^n - 1$, where the subscript i correspond to the i-th qubit, and j_{bin} is the binary representation of j written as a string of n digits. (For instance, for $n = 3$, $A_5^{(n=3)} = (|001\rangle\langle 001|)$, $A_6^{(n=3)} = (|010\rangle\langle 010|)$, ..., and $A_{10}^{(n=3)} = (|110\rangle\langle 110|)$). From here, it is not difficult to generalize for the case of n-qubits, as it is explain as follows.

State-Reset $\mathcal{E}_{\Gamma_n}$ on the states $|s_1\rangle$ and $|s_2\rangle$

In general, the operation to reset any pair of states, $|s_1\rangle$ and $|s_2\rangle$, can be given by a Kraus decomposition with the following operators:

$$
\begin{aligned}
A^{(n)}_{1_{(|s_1\rangle\longleftrightarrow|s_2\rangle)}} &= \sqrt{p_n}|s_1\rangle\langle s_1|, \\
A^{(n)}_{2_{(|s_1\rangle\longleftrightarrow|s_2\rangle)}} &= \sqrt{p_n}|s_1\rangle\langle s_2|, \\
A^{(n)}_{3_{(|s_1\rangle\longleftrightarrow|s_2\rangle)}} &= \sqrt{1-p_n}|s_2\rangle\langle s_2|, \\
A^{(n)}_{4_{(|s_1\rangle\longleftrightarrow|s_2\rangle)}} &= \sqrt{1-p_n}|s_2\rangle\langle s_1|, \\
A^{(n)}_{4+r_{(|s_1\rangle\longleftrightarrow|s_2\rangle)}} &= \left(|r_{bin}\rangle\langle r_{bin}|\right),
\end{aligned}
\tag{4.6.2}
$$

for all the r_{bin} integer binary numbers of a string of n digits such that $r_{bin} \in \{0,1\}^{\otimes n}\backslash\{s_1, s_2\}$, and $r \in \mathbb{N}$ is used for indexing the Kraus operators. When the state-reset is chosen to be between $|0\rangle^{\otimes n}$ and $|1\rangle^{\otimes n}$, the probability p_n is related to the heat bath polarization ϵ_b as $p_n = \frac{e^{n\xi_b}}{2\cosh n\xi_b}$, where $\epsilon_b = \tanh \xi_b$. Thus, for low polarization, $p_n = (1 + n\epsilon_b)/2$. This operation transforms the state ρ to

$$
\mathcal{E}_{\Gamma_n(|s_1\rangle\longleftrightarrow|s_2\rangle)}(\rho) = \sum_i A^{(n)}_{i\,(|s_1\rangle\longleftrightarrow|s_2\rangle)} \rho \left(A^{(n)}_{i\,(|s_1\rangle\longleftrightarrow|s_2\rangle)}\right)^\dagger.
$$

For Γ_n, unless the exact pair of states to be reset is specified, it will be assumed that the equilibration is between the states $|0\rangle^{\otimes n}$ and $|1\rangle^{\otimes n}$.

Similarly, this kind of reset, combined with rotations to totally mix all the qubits with the exception of the qubit that is going to be cooled, can boost the polarization of some qubits. We found a generalization of the NOE on n qubits (see Appendix B2), that gives a final polarization of $n\epsilon_b$, in the approximation of low polarization. Used by itself, the generalized NOE does not always give a better polarization than the PPA-HBAC for large n, but we use this state-reset operation as a tool to create new enhanced HBAC algorithms: the SR-Γ_n HBAC protocols. The 2-qubit case has been already introduced in the previous section, and now that the general $\mathcal{E}_{\Gamma_n}$ state-reset operation is defined, the n-qubit case will be presented, for $n > 2$.

4.6.1 State-Reset HBAC for the three-qubit case

To extend to three qubits we include Γ_3, in addition to Γ_2 which can be applied on any combination of qubit-pairs of the system, and Γ_1 on any of the qubits.

SRΓ_3-HBAC method

The algorithm consists of the iteration of three-step rounds:

1) The polarization of the second qubit (counted from top to bottom in the circuit of Fig. 4.5) is increased by applying the SRΓ_2-HBAC on the second and third qubits, to achieve a polarization close enough to its maximum value (see eq. (4.6.3)), $\tanh 3\xi$ ($3\epsilon_b$ for low polarization).

2) The second and third qubits are flipped.

3) A state-reset Γ_3 on all three qubits is applied to pump additional entropy out of the system.

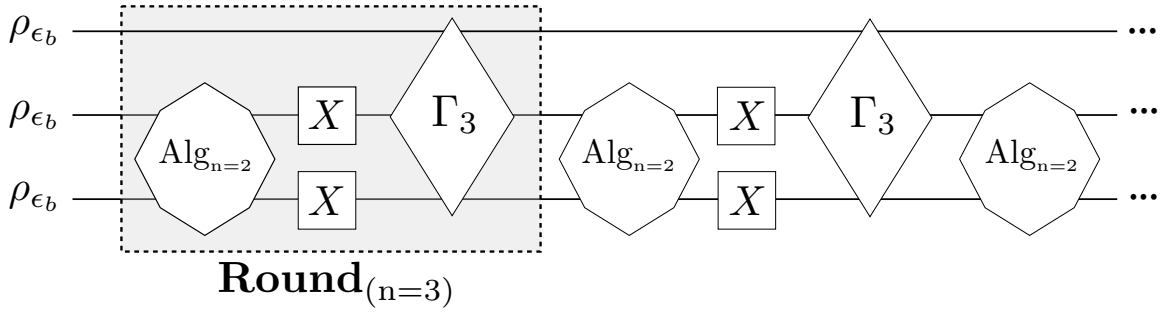

Figure 4.5: Circuit for the SRΓ_3-HBAC method. Γ_3 is the reset-state operation on three qubits that resets the states $|000\rangle$ and $|111\rangle$ to their corresponding equilibrium values. Alg$_{(n=2)}$ is the preparation of the second qubit, using the SRΓ_2-HBAC on the second and third qubits. The dotted box encloses a segment of the circuit which is repeated, which constitutes a Round$_{(n=3)}$.

The asymptotic polarization of the SRΓ_3-HBAC algorithm for any bath-polarization is given by

$$\epsilon^{\infty}_{\mathrm{SR}\Gamma_2} = \tanh\left(7\xi_b\right), \tag{4.6.3}$$

where ξ_b is related to the polarization of the bath by $\epsilon_b = \tanh\left(\xi_b\right)$ (see Appendix B3.2 for the precise calculation), leading to an improvement beyond the PPA-HBAC for the 3-qubit case.

Let us derive the achievable polarization for the three-qubit case in the low heat-bath polarization regimen,

$$\rho_0^{n=3} = \rho_{\epsilon_b}^{\otimes 3} = \left[\frac{1}{2}\begin{pmatrix} 1+\epsilon_b & 0 \\ 0 & 1-\epsilon_b \end{pmatrix}\right]^{\otimes 3} = \left[\frac{1}{2\cosh\xi_b}\begin{pmatrix} e^{\xi_b} & 0 \\ 0 & e^{-\xi_b} \end{pmatrix}\right]^{\otimes 3}. \tag{4.6.4}$$

Then, the vector of the diagonal elements is $\text{diag}\left(\rho_0^{n=3}\right) = \left[\frac{1}{2}\left(1+\epsilon_b, 1-\epsilon_b\right)\right]^{\otimes 3}$. For low polarization, Γ_3 will transform a diagonal state $\text{diag}\left(\rho^{n=3}\right) = (N_0, N_1, N_2, N_3, N_4, N_5, N_6, N_7)$ into $\left(\frac{1+3\epsilon_b}{2}\left(N_0+N_7\right), N_1, N_2, N_3, N_4, N_5, N_6, \frac{1-3\epsilon_b}{2}\left(N_0+N_7\right)\right)$. $\text{Alg}_{(\text{n}=2)}$ will prepare the second qubit by applying the SRΓ_2-HBAC to enhance its polarization close to $3\epsilon_b$. Then, under this algorithm, the polarization of the first qubit, after applying k' $\text{Round}_{(\text{n}=3)}$ (see Fig. 4.5), will be

$$\epsilon_{k'}^{n=3} = \left[7 - 6\left(\frac{3}{4}\right)^{k'}\right]\epsilon_b, \tag{4.6.5}$$

leading to an asymptotic polarization $\epsilon_{max}^{(n=3)} = 7\epsilon_b$, for low bath polarization regime.

4.6.2 State-Reset HBAC for the n-qubit case

For our new algorithm for the n-qubit case, SRΓ_n-HBAC, we assume that we have the ability to apply the set of state-reset operations Γ_m in a controlled way on any subsystem of m qubits, for all $m < n$, in the spirit of reservoir engineering (as in Ref. [87]). Similarly to the algorithm for the 3-qubit case SRΓ_3-HBAC – which makes use of the preparation SRΓ_2-HBAC as one of its steps – the algorithm SRΓ_n-HBAC, uses the preparation of the SRΓ_{n-1}-HBAC. The protocol is presented as follows:

SRΓ_n-HBAC method

The SRΓ_n-HBAC algorithm, for the n-qubit case, consists of the iteration of 3-steps:

1) First, the polarization of the second qubit (counted from top to bottom in the circuit of Fig. 4.6), is increased by using the preparation of the SRΓ_{n-1}-HBAC protocol (denoted by $\text{Alg}_{(\text{n}-1)}$).

2) All the qubits with the exception of the first qubit are flipped.

3) A state-reset operation $\mathcal{E}_{\Gamma_n}$ is applied to pump entropy out of the first qubit.

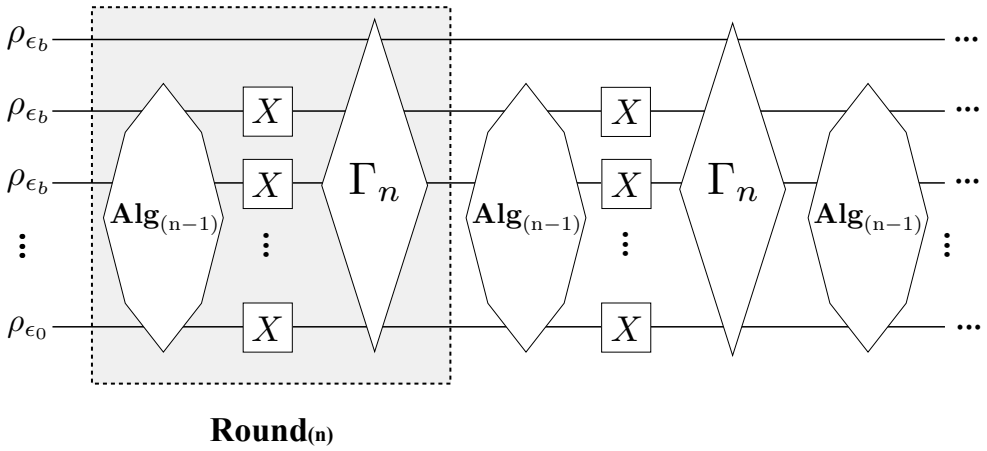

Figure 4.6: Circuit for the SRΓ_n-HBAC algorithm. Γ_n represents the reset-state operation $\mathcal{E}_{\Gamma_n}$ that resets the states $|0\rangle^{\otimes n}$ and $|1\rangle^{\otimes n}$ on n qubits. $\mathrm{Alg}_{\mathrm{n-1}}$ is the polarization preparation of the second qubit by using SRΓ_{n-1}-HBAC. The part of the circuit inside the dotted box represents a round of the protocol, $\mathrm{Round}_{(\mathrm{n})}$. The entire circuit is the repetition of this round.

The maximum polarization achievable for the target qubit is

$$\epsilon^{\infty}_{\mathrm{SR}\Gamma_n} = \tanh\left[(2^n - 1)\xi_b\right], \tag{4.6.6}$$

where $\xi_b = \operatorname{arctanh}(\epsilon_b)$.

The final asymptotic temperature of the target qubit for this SRΓ_n-HBAC protocol is given by

$$T^{\infty}_{\mathrm{SR}\Gamma_n} = \frac{T_b}{2^n - 1},$$

where T_b is the temperature of the heat-bath, and n is the number of qubit in the system.

The final temperature obtained by the SRΓ_n-HBAC is improved by a factor of 4 over the final temperature achieved by the PPA-HBAC on a string of identical qubits, in general

for all n:

$$T^{\infty}_{\mathrm{SR}\Gamma_n} = \frac{T_b}{2^n - 1} \quad < \quad T^{\infty}_{\mathrm{PPA}_n} = \frac{4T_b}{2^n} \qquad \forall n \tag{4.6.7}$$

Similarly, the maximum polarization achievable for the SRΓ_n-HBAC is higher than the achievable polarization obtained by the PPA-HBAC method [93]. Fig. 4.7 shows particular examples of the maximum polarizations achieve by our new method and the PPA-HBAC, as a function of ϵ_b.

The analytical result of the maximum achievable polarization, eq. (4.6.6), can be demonstrated by induction, as described below. The basis case of induction, for $n = 2$ and 3, the maximum polarization for the first qubit is $\epsilon_{\infty}^{(n=2)} = \tanh 3\xi_b$ and $\epsilon_{\infty}^{(n=3)} = \tanh 7\xi_b$, respectively. In the induction step, we assume that for a number $\tilde{n}$, $\epsilon_{\infty}^{(k)} = \tanh\left(2^k - 1\right)\xi_b$, $\forall k \leq \tilde{n}$, and prove this equation for $k = \tilde{n} + 1$. Let us consider a system of $\tilde{n} + 1$ qubits, we are going to calculate the maximum polarization $\epsilon_{\infty}^{(\tilde{n}+1)}$. After applying SR$\Gamma_n$-HBAC all the qubits will be in a product state, with the last $\tilde{n}$ qubits having the corresponding maximum polarization (i.e., the last qubit with polarization $\epsilon_{\infty}^{(n=1)}$, the second last one with polarization $\epsilon_{\infty}^{(n=2)}$, and so on). Let us name $\epsilon_{fix}^{(n+1)}$ to the polarization of the first qubit in the cooling limit. After the second step of the round, flipping the last $\tilde{n}$ qubits, the first element of the diagonal density matrix will be $\beta_1 := \frac{1}{2^{n+1}}(1 + \epsilon_{fix}^{(n+1)}) \prod_{i=1}^{n} \left[1 - \tanh\left[(2^i - 1)\xi_b\right]\right]$. Similarly, the last element of the density matrix will be $\beta_{2^{n+1}} := \frac{1}{2^{n+1}}(1 - \epsilon_{fix}^{(n+1)}) \prod_{i=1}^{n} \left[1 + \tanh\left[(2^i - 1)\xi_b\right]\right]$.

Let us define the sum of these two elements, β_1 and $\beta_{2^{n+1}}$, as B. Then, the state-reset Γ_{n+1} will change these two elements to Bp_{n+1} and to $B(1 - p_{n+1})$, respectively. This state will achieve the fixed point when the first and the last elements are already equal to Bp_{n+1} and to $B(1 - p_3)$, respectively. Namely, $\beta_1 = Bp_{n+1} = (\beta_1 + \beta_{2^{n+1}})(1 + \tanh n\xi_b)/2$. Substituting β_1 and $\beta_{2^{n+1}}$ in this expression, and solving for $\epsilon_{fix}^{(n+1)}$, we get $\epsilon_{fix}^{(n+1)} = \tanh\left[(2^{n+1} - 1)\xi_b\right]$, which proves the claim: The polarization limit, achievable with our algorithm, for the n-qubit case is $\epsilon_{\infty}^{(n)} = \tanh\left[(2^n - 1)\xi_b\right]$, leading to an improvement on both the NOE and the PPA-HBAC. For low polarization, this polarization limit reduces to $(2^n - 1)\epsilon_b$.

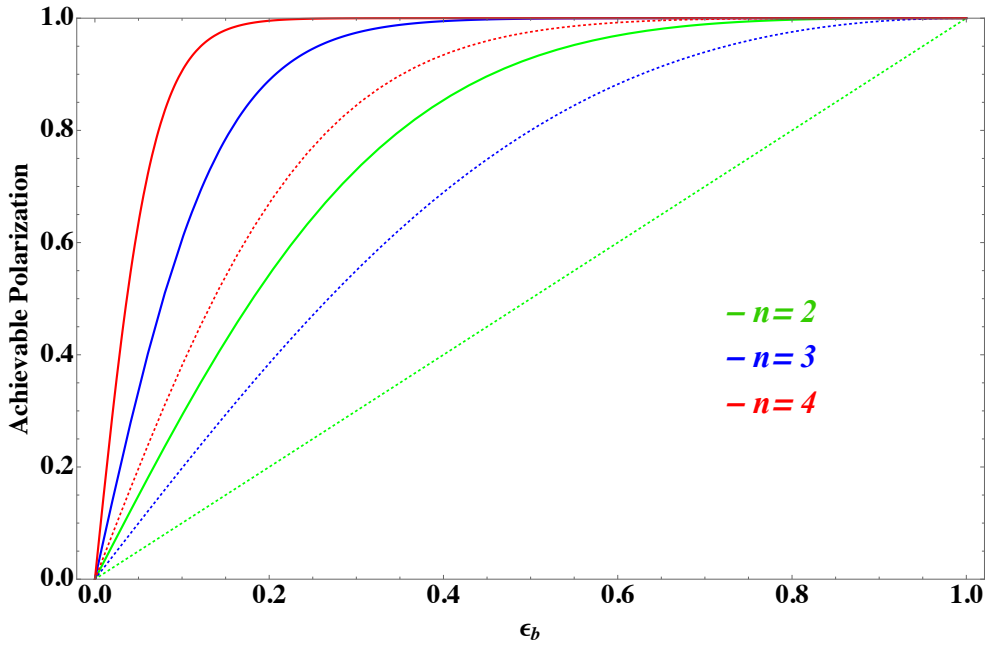

Figure 4.7: Maximum achievable polarization of the SRΓ_n-HBAC and the PPA-HBAC, in solid lines and dotted lines, respectively, as a function of ϵ_b, for different n.

4.7 Conclusion

We have presented a new HBAC technique that achieves a better polarization enhancement than the one obtained by the PPA-HBAC protocol, for any number of qubits. As mentioned in the previous Chapter and in our paper [93], the polarization achieved using the PPA-HBAC should instead be interpreted as a lower bound on the maximum amount of polarization that can be achieved. Its importance is due to the simplicity of the PPA-HBAC when the initial state is totally mixed or in an equilibrium thermal state. In this case, it is possible to get analytical results that describe both the steady state and its polarization, from which we can determine a variety of properties. For example, we can determine how far it is from purity one and explicitly show how many resources are needed. It will be interesting to see if we can generalise the Overhauser effect and determine what advantages it can give as we increase the number of qubits.

Our technique utilizes the coupling to the environment in a way that is not limited to qubit resets, but could also include correlations between the qubits which are reset. The

assumption that entropy can be extracted from the system only via qubit reset (instead of state-reset) was a symmetry which has been implicitly imposed for qubits, but is not generally true. There are other examples of similar imposed symmetries, such as the distinction on subspace and subsystems [58] where the symmetry limits quantum information processing. We have shown a series of algorithms and calculated their resulting polarization for this new method as a function of the number of qubits, n, and as a function of the polarization of the bath, ϵ_b. We have also presented the polarization evolution as a function of the number of iterations of our algorithms and compared between these results and the corresponding ones of the PPA-HBAC. There exist many possibilities for future application of this method. Although originally designed for NMR where measurements are ensemble averages, our technique can be applied in other modalities, e.g. superconducting and ion traps, where we have imperfect projective measurements and initial states. In these modalities it could be implemented by incorporating the qubits in 'leaky' cavities that resonate at twice the fundamental frequency of the qubit, and thus induce the $|11\rangle$ to $|00\rangle$ transition. Our algorithm might be a tool to help NMR or MRI applications to increase the signal to noise ratio or bring these error rates below the threshold for fault tolerance in quantum information applications.

Our results show implicitly that a universal set of unitary gates along with Γ_1 are not universal for open quantum systems with two qubits or more. We conjecture that universality is achieved by including Γ_2 for the two-qubit case and by including all Γ_i for the n-qubit case. This conjecture was proved in a recent paper by C.Perry et al. [85]. Future research should also include a proof of optimality of our algorithms either using only the transitions $|0\rangle^{\otimes n} \longleftrightarrow |1\rangle^{\otimes n}$ ("state reset"), a different m-qubit transition (where $m \leq n$), or a combination of such transitions.

Chapter 5

Initial-correlation Enhanced Algorithmic Cooling

The results presented in this Chapter have been published in Refs. [90, 2].

In this Chapter, I remove another assumption underlying all previous HBAC methods: the assumption that the qubits are not interacting nor initially correlated [29, 73, 98, 26, 99, 28, 55]. I provide explicit methods that extend algorithmic cooling to interacting systems. The physical motivation is that, in practice, the qubits generally possess correlations of both classical and quantum origin, generated thermally and through interaction-induced entanglement respectively. Not taking the correlations into account, when implementing the cooling protocols, could lead to unwanted results which can even reduce the initial purity of the target qubit – an example of this situation is presented in Appendix C2 for the PPA method.

In fact, the correlations among elements of a multipartite quantum system can play a critical role in cooling protocols, leading to fundamental limitations when trying to locally cool down a part of the system. To illustrate this fact, let us consider the case of interacting subsystems whose Hamiltoinian is non-local and that possess non separable low energy global eigenstates states (hence, with entangled ground states). Then, imagine, that we want to cool down a single subsystem of this interacting system. On the one hand, by naively immersing this interacting system in a very cold thermal bath, this would not be sufficient to cool down locally the subsets of the system, since the correlations of non

separable low energy states give locally mixed subsystems. Even when having access to an extremely cold thermal reservoir, the entanglement of the ground state implies that by cooling down the whole system, the target subsystem will remain in a mixed state. Furthermore, by breaking the aforementioned correlations within the system, it will end up with mixed subsystems.

Even more, the correlations between subsystems of a multipartite quantum system can obstruct outgoing energy flows [2] (as detailed in Appendix C1). Indeed, while in ordinary macroscopic systems classical thermodynamics dictates that energy flows from hot to cold; in the microscopic regime, where quantum effects become relevant, this direction of energy flow surprisingly may be blocked or even inverted [2]. Some natural questions arise: How can we characterize a hot system from which it would be impossible to cool down, even by making contact with a colder one? What are the relevant quantum effects that prevent cooling that system? And how can we circumvent these possible cooling limitations in algorithmic cooling protocols?

In this chapter, I present the answers to these questions, in particular for the full characterization of the impossibility of extracting energy *locally* from a bipartite quantum system in the presence of strong coupling and entanglement. Then, I show how to circumvent these limitations by allowing classical communication, by proposing explicit protocols.

Concretely, first, I present the intuition of how quantum effects, such as entanglement, can obstruct outgoing energy flows, via fast local interaction, preventing a hot body to dissipate its energy to a colder one. Later on, in the Appendix C2, I present a full set of necessary and sufficient conditions that fully characterize this thermodynamic feature of impossibility of energy extraction. Then, I show how to circumvent these limitations by allowing classical communication between parts of the interacting system in order to take advantage of pre-existing quantum and classical correlations within the system. This type of setting goes under the name of quantum energy teleportation (QET) [51, 35, 53, 34, 50, 48, 109, 49, 52, 111], which I will describe in more detail in the section 5.2.

Our new proposed HBAC technique shows how correlations present due to the internal interaction provide a resource that can be used to improve cooling. In particular when this interaction is sufficiently strong, the system's quantum correlations can be exploited to achieve cooling beyond the established limits of the previous conventional algorithmic cooling proposals that assume no interaction.

5.1 Preliminaries: Fundamental limitations to local energy extraction in quantum systems

In this section, we focus on the problem of cooling interacting multipartite systems to which only local access to a single subsystem (the target subsystem) is granted. We assume that the most general type of local access is allowed. Namely, any local CPTP map on the target subsystem is allowed, making our results relevant for any physical platform in which the subsystems are spatially separated.

In particular, we examine when it is possible to locally extract energy from a bipartite quantum system in the presence of strong coupling and entanglement, a task which is expected to be restricted by entanglement in the low-energy eigenstates. Concretely, our goal is to fully characterize the necessary and sufficient conditions for such energy extraction to be impossible.

System setup and allowed operations – Let us consider the bipartite quantum system made by the subsystems A and B, with associated Hilbert space $\mathcal{H}_A \otimes \mathcal{H}_B$, and global Hamiltonian H_{AB}. Let the subsystem A be our target subsystem, in which it is allowed to act locally with general local CPTP map $\mathcal{E}_A(\cdot)$.

Given a state ρ_{AB}, the maximum extractable energy under a local map on A is

$$\Delta E_{max} \coloneqq \min_{\mathcal{E}_A} \mathrm{Tr}[H_{AB}(\mathcal{E}_A \otimes \mathcal{I}_B)\rho_{AB}] - \mathrm{Tr}[H_{AB}\rho_{AB}],$$

where $\mathcal{I}_B$ is the identity channel on B, and the optimization is over the whole set of CPTP maps on A. The above optimization can be easily written as a *semidefinite program* (see refs. [10, 115] for introductory references to the subject, and ref. [2] for more details of this example). Then, by using tools from semidefinite programming, it is possible to calculate ΔE_{max} and to solve for the CPTP map which minimizes this energy extraction to zero, since we want to characterize the states from which it is impossible to extract energy for the system even under general local operations. The states we seek motivate the following definition:

Definition 1 (CP-local passivity)**.** *The pair $\{\rho_{AB}, H_{AB}\}$ is defined to be CP-local passive with respect to subsystem A if and only if no general quantum operation applied locally on*

the subsystem A can extract positive energy from the system.

$$\Delta E_{max} = 0. \tag{5.1.1}$$

That is, a system is CP-local passive if the best local strategy for extracting energy (as measured by the global Hamiltonian H_{AB}) is to act trivially on it. The word *passive* is used here in analogy to the commonly known passive states [62], from which energy cannot be extracted under unitary maps.

The intuition behind how these CP-local passive states exist is as follows: During the task of extracting energy locally from the bipartite system, one could expect that if the low-energy eigenstates of the system display entanglement, there are limitations when trying to get closer to them only by means of local maps – since one cannot approach entangled states with local operations. While it could be possible to decrease the energy of the system up to some mixture of those low-energy eigenstates, trying to drive the system to a lower energy state can correspond to increasing the correlations in the system beyond what is possible via local operations alone.

This problem of cooling interacting multipartite systems to which only local access to a single subsystem is granted was first studied in Frey et al. [34], who gave a set of sufficient conditions for the impossibility of energy-yielding via arbitrary local operations. Fret et al. showed that having a non-degenerate ground state with full Schmidt rank is a *sufficient* condition for the system to exhibit this impossibility of local energy extraction, given a large enough population in the ground state. We built on their results in two ways: i) we found *necessary and sufficient conditions* for this energy extraction to be impossible [2] (see Appendix C1) and ii) we strengthened the set of physically-motivated sufficient conditions given in Ref. [34], by finding explicit bounds for the ground state population and critical temperature for which the system displays CP-local passivity.

In this chapter, I show how the cooling limitations given by the CP-local passivity can be circumvented by allowing classical communication between parts of the interacting system to take advantage of the pre-existing correlations within the system. This type of setting goes under the name of quantum energy teleportation. In the next subsection, a summary of the minimal QET technique is provided. Then, I show how this protocol can be adapted and applied on an ensemble of identical systems of two interacting qubits in a fully unitary fashion. This fully unitary version of the minimal QET protocol not only can

break the CP-local passivity of the system but also increase the purity of a target qubit.

5.2 Summary of the Minimal QET

The minimal QET protocol [52] extracts energy locally from a two-qubit system by using information of a distant measurement. Note that, even though this method uses measurements, we will adapt it in the next sections to present a new fully-unitary version of it: a QET-HBAC based protocol. This adaptation is important, since a one of the requirement for HBAC is that it should not rely on measurements. Then, I will show concrete examples of how our method improve the purity beyond previous methods in the strong coupling regime.

5.2.1 System Setup for the Minimal QET

Consider the system of two interacting qubits, A and B, with Hamiltonian

$$H = H_A + H_B + V, \tag{5.2.1}$$

where $H_\nu = h\sigma_z^\nu + f(h,k)\mathbb{1}$, with $\nu = \{\mathrm{A}, \mathrm{B}\}$ and

$$V = 2\left[k\sigma_x^{\mathrm{A}}\sigma_x^{\mathrm{B}} + \frac{k^2}{h^2}f(h,k)\mathbb{1}\right]. \tag{5.2.2}$$

Here, h and k are positive constants and the function $f(h,k) = h^2/\sqrt{h^2+k^2}$ is chosen such that the ground state of the full Hamiltonian has vanishing energy. The choice of the constant term $f(h,k)$ in the Hamiltonian is just for convenience but it is not necessary for the protocol to work. Since the interaction Hamiltonian does not commute with the qubit's free Hamiltonian, the ground state of the system is not separable. Concretely, the system's ground state $|g\rangle$ in terms of eigenstates of $\sigma_z^{\mathrm{A}}, \sigma_z^{\mathrm{B}}$ reads

$$|g\rangle = \frac{1}{\sqrt{2}}\left(F_-|1\rangle_{\mathrm{A}}|1\rangle_{\mathrm{B}} - F_+|0\rangle_{\mathrm{A}}|0\rangle_{\mathrm{B}}\right), \tag{5.2.3}$$

where $F_{\pm} = \sqrt{1 \pm f(h,k)/h}$, $\sigma_z^{\nu}|0\rangle_{\nu} = -|0\rangle_{\nu}$, $\sigma_z^{\nu}|1\rangle_{\nu} = |1\rangle_{\nu}$, with $\nu = \{\mathrm{A}, \mathrm{B}\}$. Note that, given that $|g\rangle$ is an entangled state, even if the system is at zero temperature, the subsystems A and B are not locally pure.

Arguably, the most interesting case of the QET protocol is when it is applied to break the strong local passivity of the ground state $|g\rangle$, since it implies the extraction of the zero-point energy by using local operations and information of the fluctuations of the vacuum.

5.2.2 Steps of the Minimal QET protocol

In the Minimal QET protocol two types of local operations are allowed: a generalized measurement on a qubit A (not necessarily projective), and local unitary operations on the qubit B – which can dependent on the outcomes of the measurement in A. The steps of the Minimal QET are as follows:

Steps of the Minimal QET protocol [52]

The initial state of the system is in the ground state $|g\rangle$.

1) In the first step of the basic QET protocol, Alice carries out a POVM measurement on A with operators that commute with the term of interaction V and the local Hamiltonian of B H_B. The conditions imposed on the POVM are in order to avoid sending energy to B during the measurement.

2) The result of the measurement on A ($\mu = \pm 1$) is announced to Bob through a classical channel. It can be assumed that the information is sent faster than the coupling timescale $1/k$, which means that the non-local dynamics can be considered frozen during that time.

3) Depending on the message, μ, that Bob received, Bob carries out a local unitary operation, $U_B(\mu)$, optimized to extract energy from B without any energy propagating from A to B.

As proved in [52], Bob extracts, on average, energy from the system by acting locally on B without any energy propagating from A to B.

The POVM is demanded to commute with the local Hamiltonian of B, H_B, and the interacting term V. In this case, even though the first step of the protocol –a measurement on A– will have an energy cost $E_{P_A} > 0$, i.e. it pumps energy into the system by acting locally on A, none of this energy goes to the side B at the moment of implementing the step. So, it would be possible to extract energy locally from B, that does not come from the side of A. Note however that the protocol is not concerned about the amount of total energy pay in the measurement.

5.3 QET on the ground state to break its strong local passivity

Implementing the basic QET protocol on the ground state, will have the effect of extracting energy locally from B that does not come from A. Namely, the QET protocol breaks the strong local passivity of the ground state to extract the zero-point energy of B.

Here, we illustrate this case and also show the purify enhancement of the subsystem B, by following the steps of the minimal QET protocol. In particular, we use the unitary $U_B(\mu)$ that optimizes Bob's energy extraction by taking advantage of correlations instead, when we are limited to local operations. By applying the three steps of the protocol (POVM on A, classical communication from A to B, and local unitary in B –see Appendix C3 for the details–), the ground state, eq.(5.2.3), of system AB will evolve on average to

$$\rho_f = \sum_{\mu=\pm 1} U_{\mathrm{B}}(\mu) M_{\mathrm{A}}(\mu) |\psi_0\rangle\langle\psi_0| M_{\mathrm{A}}^{\dagger}(\mu) U_{\mathrm{B}}^{\dagger}(\mu), \tag{5.3.1}$$

where $M_{\mathrm{A}}(\mu) = e^{i\delta_\mu}(m_\mu + e^{i\alpha_\mu} l_\mu \sigma_{\mathrm{A}}^x)$ is the measurement operator that describes the POVM on σ_{A}^x, which commutes with the local Hamiltonian of B H_B and the interaction term of the Hamiltonian V, and μ is the outcome (that can take either value $+1$ or -1). Here, the coefficients m_μ, l_μ, α_μ and δ_μ are real constants satisfying $\sum_\mu (m_\mu^2 + l_\mu^2) = 1$, and $\sum_\mu m_\mu l_\mu \cos\alpha_\mu = 0$. $U_B(\mu)$ is the unitary that maximizes Bob's energy extraction:

$$U_B(\mu) = \cos\Omega_\mu \mathbb{1} + i \sin\Omega_\mu \sigma_y^B, \tag{5.3.2}$$

where, Ω_μ's are real constants that satisfy

$$\cos(2\Omega_\mu) = \frac{(h^2+2k^2)\, p_{\text{A}}(\mu)}{\sqrt{(h^2+2k^2)^2 p_{\text{A}}(\mu)^2 + h^2k^2 q_{\text{A}}(\mu)^2}}, \tag{5.3.3}$$

$$\sin(2\Omega_\mu) = -\frac{hk q_{\text{A}}(\mu)}{\sqrt{(h^2+2k^2)^2 p_{\text{A}}(\mu)^2 + h^2k^2 q_{\text{A}}(\mu)^2}}, \tag{5.3.4}$$

with $p_{\text{A}}(\mu) = m_\mu^2 + l_\mu^2$ and $q_{\text{A}}(\mu) = 2l_\mu m_\mu \cos\alpha_\mu$.

Let us show that the purity on B is boosted while consuming the correlations. From (5.2.3), we can calculate the initial purity of B (defined as $\mathcal{P}_i^{\text{B}} = \text{Tr}\,(\rho_{\text{B}}^2)$ and the initial polarization $\epsilon_i^{\text{B}} = Tr\,(\sigma_z \rho_{\text{B}})$ (for ease of comparison with prior literature):

$$\mathcal{P}_i^{\text{B}} = \frac{2h^2+k^2}{2\,(h^2+k^2)}, \qquad \text{and} \qquad \epsilon_i^{\text{B}} = \frac{h}{\sqrt{h^2+k^2}}. \tag{5.3.5}$$

In the basis that diagonalizes the state of B, the polarization is related to the purity by $\epsilon_i^{\text{B}} = \sqrt{2\mathcal{P}_i^{\text{B}} - 1}$.

After applying the QET-2 [1] protocol, the purity of B is

$$\mathcal{P}_f^{\text{B}} = \frac{2}{(h^2+k^2)}\Bigg(\frac{h^2}{2} + \frac{k^2}{4} - hkl_1m_1 \sin\left[2(\Omega_0-\Omega_1)\right] + \Big[4k^2l_1^2m_1^2 + h^2\Big(l_1^2+m_1^2-1\Big)\Big(l_1^2+m_1^2\Big)\Big]\sin^2(\Omega_0-\Omega_1)\Bigg)$$

and the final polarization is

$$\epsilon_f^{\text{B}} = \frac{1}{\sqrt{h^2+k^2}}(-h\cos 2\Omega_0 + 2kl_1m_1(\sin 2\Omega_0 - \sin 2\Omega_1) + h\left(l_1^2+m_1^2\right)(\cos 2\Omega_0 - \cos 2\Omega_1)). \tag{5.3.6}$$

For simplicity, we assumed $\alpha_\mu = 0$. From this we can see enhancement of the purification in the cases where the energy yield of QET is positive. See Appendices C for details

[1] Let us call this protocol QET-2, since it is using two-qubits, to differentiate it from the other protocols that will be presented later.

about the energy costs of implementing the POVM and the energy extracted locally from B.

In this way, the minimal QET uses the communication of non-local correlations to circumvent the constraints of strong local passivity [34], in this case of the ground state, so that energy can be extracted locally.

In the next section is discussed how the protocol is not just simply applying a POVM on a system and therefore automatically purifying the system, and in fact by having only the POVM without using the optimized unitary on B, it would be impossible to extract energy locally from it in average. This means that after applying the POVM on the system, it is still in a strong local passive state, and only by using the classical communication is possible to extract energy in average.

5.3.1 Impossibility of energy extraction without Alice's announcement of the measurement outcome

Imagine that Bob tries to do a local unitary operation on B after the measurement that Alice performed on A but without knowing anything about the outcome of the measurement μ. It is legitimate to ask whether Bob can extract some energy on average form the process (negative energy cost of its unitary operation).

If Bob does not know about the outcome μ, the action of an arbitrary (μ-independent) local unitary W_B on the post-measurement state would be

$$W_B|\psi_{\mathrm{PM}}\rangle = \frac{1}{\sqrt{p_A(\alpha)}} W_B M_A(\mu)|g\rangle$$

Then, we would get the average state

$$\rho_2 = W_B \rho_1 W_B^\dagger = W_B \left(\sum_{\mu=\pm 1} M_A^\dagger(\mu)|g\rangle\langle g|M_A(\mu) \right) W_B^\dagger.$$

Repeating the calculation of the energy balance computed before (see Appendix C3),

the cost of such a unitary will be given by

$$E_{W_B} = \mathrm{Tr}(\rho_2 H) - \mathrm{Tr}(\rho_1 H) = \mathrm{Tr}(\rho_2 H) - E_{P_A} = \sum_{\mu} \langle g | M_A^\dagger(\mu) W_B^\dagger [H_B + V] W_B M_A(\mu) | g \rangle$$

now since

$$\sum_{\mu} M_A^\dagger(\mu) M_A(\mu) = \mathbb{1}_A$$

we can write

$$E_{W_B} = \mathrm{Tr}(\rho_2 H) - \mathrm{Tr}(\rho_1 H) = \mathrm{Tr}(\rho_2 H) - E_{P_A} = \langle g | W_B^\dagger [H_B + V] W_B | g \rangle$$

Now, given that $H_A W_B = 0$ we know that $\langle g | W_B^\dagger H_A W_B | g \rangle = \langle g | H_A | g \rangle = 0$ and we can write the following equality

$$E_{W_B} = \langle g | W_B^\dagger [H_A + H_B + V] W_B | g \rangle = \langle g | W_B^\dagger H W_B | g \rangle$$

But we know that H is a non-negative operator, therefore this expectation will be always greater or equal than zero.

$$E_{W_B} \geq 0$$

and the Unitary will cost energy on average if Bob has no information about the outcome of the measurement on A.

5.4 QET-2 cooling in Gibbs states

We now show that one can obtain purification enhancement not only for systems in the ground state. In particular, let us focus now on Gibbs states. Consider the two-qubit system whose interaction is described by the Hamiltonian, Eq. (5.2.1), in a Gibbs state of inverse temperature β. The density matrix that describes this state is $\rho_\beta = e^{-\beta H} / \mathrm{tr}\left(e^{-\beta H}\right)$. In Fig. 5.1a we present the initial purity, and final purity after applying the QET-2 protocol as a function of β for different ratios k/h. In the lower part of the figure we also plot the initial purity. The stronger the coupling, the lower the initial purity and the better the amount of purification that the QET method yields.

The POVM that optimizes the purification of B shown in Fig. 5.1a corresponds to the

case when the measurement of A is projective. Remarkably, however, a projection-valued measurement of A is not necessary for high yield purification. We see in Fig.5.1b that for the case of non-projective measurements, one still obtains an improvement in purity above prior algorithmic cooling methods applied to the same system. For the non-projective case plotted in Fig.5.1b, the optimization was limited to POVMs whose measurement operators were at least at a distance of 1/2 in the Frobenius norm from those of the case of projective measurements.

We have compared our results with two other HBAC methods: the PPA-HBAC [78] for two qubits and three qubits (let us call it PPA-2 and PPA-3 respectively) and our new cooling algorithm [89], SRΓ_n-HBAC, based on the Nuclear Overhauser Effect (NOE) (which improves over PPA-HBAC) (presented in previous Chapter).

Note that for the PPA-n (the PPA on n qubits), it is assumed that the reset of qubits is obtained through a full re-thermalization with the bath, breaking quantum and classical correlations in the system, which could lead to more mixed subsystems when the system has strong internal interactions. In particular, as I already mentioned several times, for the two-qubit case, PPA-2 cannot perform better than plain rethermalization with the environment after breakdown of any system correlations. The PPA algorithm is, however, non-trivial in the case of PPA-n with $n > 2$. In further sections, I present a comparison of the PPA-3 with the QET-2.

Concerning resources, the differences between QET-2 and PPA-n can be summarized as follows: PPA-n utilizes non-local n-qubit unitaries to make entropy compression, and the ability to map some of the qubits to an uncorrelated thermal state (modeling re-thermalization with the bath) breaking all correlations in the system. It also assumes that we can repeat the application of the non-local unitary and the reset indefinitely until a fixed point is reached. On the other hand, QET-2 utilizes LOCC: local generalized measurements (POVMs) and local (single-qubit) unitaries without refreshing with a bath. However, we will lift the need for POVMs and classical communication in the next section when we construct the fully unitary version of the protocol that we will call QET-2A.

The second method that we compare to QET-2 in Fig. 5.1b is our new method SRΓ_2-HBAC [89]. In this method, the coupling to the environment is not limited to just re-thermalization, but could also include correlations between the qubits of the system and the bath. This kind of correlations allows to make more efficient "state resets". Con-

cretely, inspired by the Nuclear Overhauser Effect [76], one can use that the state tends to thermalize faster in particular directions in the state space (see previous Chapter for more details). We show in Fig. 5.1b that QET-2 also improves over SRΓ_2-HBACin the strong coupling regime. Let us recall that SRΓ_2-HBAC takes advantage of correlations between the bath and the qubits, whereas QET-2 does not use a thermal bath as a resource and instead utilizes the correlations which are present in the system due to its interaction Hamiltonian.

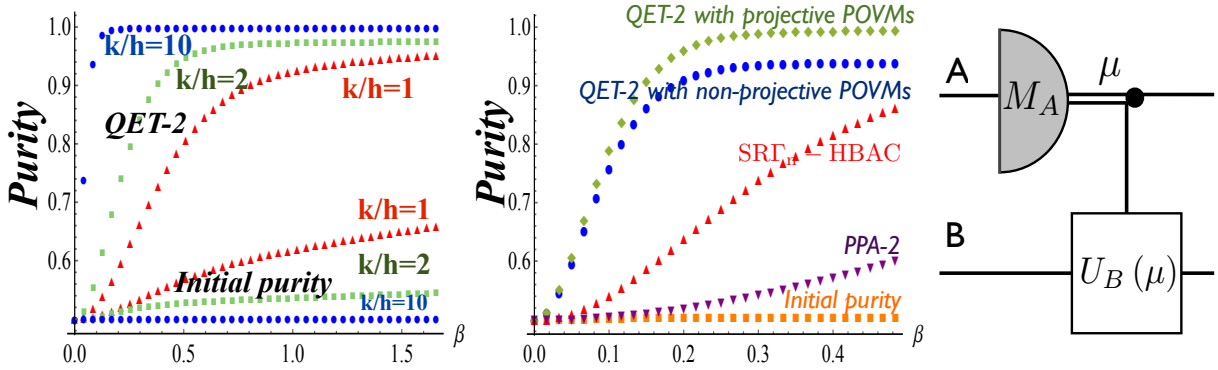

Figure 5.1: (Left) Final purity as a function of $\beta = k_B/T$, obtained by simulation for $k/h \in \{10, 2, 1\}$. Note that the method yields a larger enhancement when increasing the coupling strength. (Centre) Comparison of the final purity as a function of β, for the methods of QET with projective and non projective measurements, the SRΓ_2-HBAC, the PPA-2, and the initial purity. Here $k/h = 5$, for the two-qubit system with Hamiltonian of Eq. (5.2.1). (Right) circuit summarizing the QET-2 protocol.

5.5 Fully unitary QET cooling

We will now use the fact that QET does not need to involve measurements and can be made fully unitary instead. The role of the measurement device is then played by an ancillary quantum system C. In the fist step, Alice applies a joint unitary $U_{\rm A} = \exp(iH^{\rm A}_{\rm probe})$ on qubit A and the ancilla, which is generated by a Hamiltonian $H^{\rm A}_{\rm probe} = \sum_{i,j} \sigma^{\rm A}_i \mathcal{J}^{ij} \sigma^{\rm AN}_j$ (where $\mathcal{J}^{ij}$ is Hermitian) that couples observables of the ancilla to observables of the detector. Through this interaction, the ancilla gains information about Alice's qubit. Instead of

classical communications, the ancilla itself is then sent to Bob. Finally, Bob implements a joint unitary $U_{\rm B} = \exp(iH^{\rm B}_{\rm probe})$ on B and the ancilla, corresponding to the interaction $H^{\rm B}_{\rm probe} = \sum_{i,j} \sigma^{\rm B}_i \mathcal{K}^{ij} \sigma^{\rm AN}_j$ (where $\mathcal{K}^{ij}$ is another Hermitian coupling matrix) to extract work from the system leading to increased purification of Bob. We call this method QET-2A.

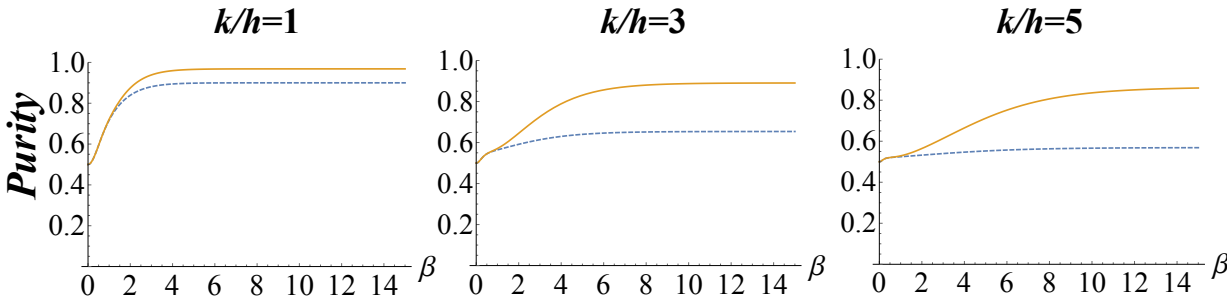

Figure 5.2: Final purity as a function of the inverse of the temperature, β, obtained for the fully unitary picture on the system AB for the example using unitaries $U_A = e^{i\sigma^{\rm A}_y \sigma^{\rm AN}_y}$ and $U_B = e^{i\sigma^{\rm B}_x \sigma^{\rm AN}_z}$, for $k/h = 1, 3$, and $k/h = 5$, from left to the right, respectively. The blue lines represent the initial purity of qubit B, and the yellow lines the final purity of B.

In terms of resources, this method, QET-2A, utilizes local couplings of the ancilla with A and B: first a bipartite unitary generated from the coupling of observables of the ancilla and observables of A, and second a bipartite unitary generated from the coupling of observables of the ancilla with observables of B. We do not require the use of arbitrary bipartite unitaries. It suffices to restrict ourselves to *measurement-like* operations, i.e., the coupling of an observable of the ancilla (which plays the role of the detector indicator) and an observable of the qubits A and B (which plays the role of the measured quantity). (By restricting the ancilla to be a mere quantum detector, we are not yet making full use of the power of three qubits, hence the name QET-2A instead of QET-3.)

As a first illustrative example, we now implement this new method on the two qubit system described by Eqs. (5.2.1)-(5.2.2), and an ancilla with Hamiltonian $H_{\rm AN} = h_{\rm AN}\sigma^{\rm AN}_z$. As a first simple example, consider that the ancilla is coupled to the observable σ_x of the system A, and later is coupled to the observable σ_y of B: $U_A = e^{i\sigma^{\rm A}_y \sigma^{\rm AN}_y}$ and $U_B = e^{i\sigma^{\rm B}_x \sigma^{\rm AN}_z}$.

We obtain for the final purity of the qubit B,

$$P_f^{\mathrm{B}} = \frac{1}{2} + \frac{h_- S_+^2[(h_{\mathrm{A}}+h_{\mathrm{B}})^2 + k^2\sin^4(2)\tanh^2(\beta h_{\mathrm{AN}})]}{2(C_-+C_+)^2 h_- h_+} + \frac{S_-^2[h_+[(h_{\mathrm{A}}-h_{\mathrm{B}})^2 + k^2\sin^4(2)\tanh^2(\beta h_{\mathrm{AN}})] + 2h_{\mathrm{B}}^2 h_r]}{2(C_-+C_+)^2 h_- h_+} - \frac{2h_r S_+ S_-[h_{\mathrm{A}}^2 + k^2\sin^4(2)\tanh^2(\beta h_{\mathrm{AN}})]}{2(C_-+C_+)^2 h_- h_+} \quad (5.5.1)$$

where

$$h_\pm \coloneqq (h_{\mathrm{A}} \pm h_{\mathrm{B}})^2 + k^2, \qquad h_r \coloneqq \sqrt{\frac{1}{2}(h_-^2 + h_+^2) - 8h_{\mathrm{A}}^2 h_{\mathrm{B}}^2}$$
$$S_\pm \coloneqq \sinh\sqrt{h_\pm \beta}, \qquad C_\pm \coloneqq \cosh\sqrt{h_\pm \beta}. \quad (5.5.2)$$

Fig. 5.2 shows three plots with results for different values of the coupling strength between A and B.

After this example, we now optimize the purification of qubit B with respect to the way in which the ancilla couples to the systems A and B. Assuming that this optimization is restricted to coupling of observables of the ancilla with observables of A and B we find optimal values for U_{A} and U_{B} numerically. Our results are presented in Fig. 5.3, in comparison with PPA-3 for $k/h = 1$. Notice that PPA-3 involves the full power of three qubit operations. Also notice that since PPA-3 destroys the system correlations, it fails to cool down the target qubit beyond its initial purity in some regimes. This is because breaking the correlations can be detrimental to the system purity. Remarkably, QET-2A (fully-unitary) can yield the same purification boosting than the POVM based protocol and outperform PPA-3, a protocol which does fully take advantage of three qubit operations but does not use the system's correlations for cooling. Note that for weak interactions, methods like PPA-3 are optimal to cool. However, the stronger the interactions between the components of the subsystems (and therefore the correlations in the system) the more efficient QET-cooling methods become.

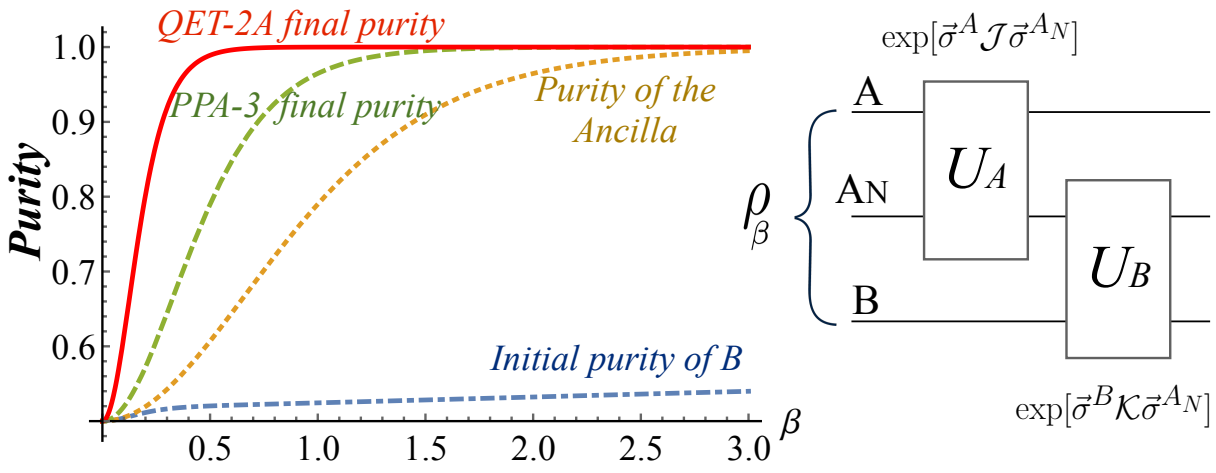

Figure 5.3: (Left) Final purity of QET in the unitary picture (QET-2A) as a function of the inverse of the temperature, β, obtained by simulation for $k/h = 5$, and $h_{\rm A} = h_{\rm B} = h_{\rm AN} = h$. We compare with PPA-3, and the initial purity of the ancilla and the target qubit B. (Right) Circuit summarizing the QET-2A protocol.

Numerical tests show that the protocol is stable under uncertainty in the interaction Hamiltonian. To study this sensitivity quantitatively, we added perturbations in the interaction part of the Hamiltonian, while performing the QET purification protocol that is optimized for the non-perturbed case. In particular, we considered perturbed Hamiltonians of the form $V \propto k\sigma_x^{\rm A}\sigma_x^{\rm B} + \frac{k^2}{h^2} f(h,k)\mathbb{1} + 2\epsilon\sigma_i^{\rm A}\sigma_j^{\rm B}$. We find that, crucially, if the value of the parameter ϵ (quantifying the relative difference between the Hamiltonian assumed to optimize the protocol and the actual Hamiltonian of the system) is small, then the relative impact of the error in the implementation of the protocol is very small (in our case, a relative difference of 10^{-4} in the achievable purity for values of $\epsilon \approx 0.1$)

5.6 Entropy compression on interacting systems

We proved that QET-2A not only can purify beyond the cooling limit of PPA-3, but that it can outperform PPA-3 (i.e., many iterations of entropy compression and qubit reset with a thermal bath) by using much less resources and while only requiring a much more

limited range of operations compared to PPA-3. Furthermore, the fact that QET-2A is not using the full power of applying general joint unitaries on the three qubits (like PPA-3 does) suggests that it is possible to further improve the cooling with the resources that are assumed also for PPA-3.

Let us now compare the power of our unrestricted non-local n-partite unitaries for entropy compression in interacting systems with the analogous entropy compression through PPA-n protocols which break the correlations.

For instance, let us consider the two-qubit system of Eqs. (5.2.1) and (5.2.2), starting in the Gibbs state of inverse temperature β. We optimized the entropy compression numerically for different ratios k/h, and we found, see Fig.5.4, that we can extract more entropy from B to compress in A when the coupling is stronger. This is intuitive, given that a more strongly coupled system will exhibit more correlations in its ground state (due to entanglement) and also in Gibbs states (due to classical thermal correlations).

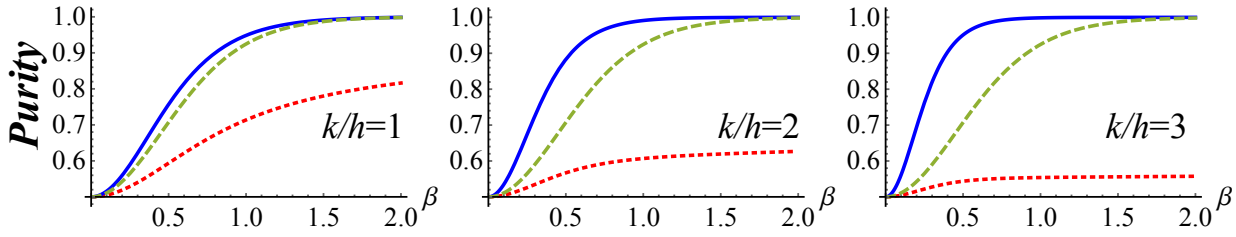

Figure 5.4: Comparison between entropy compression using correlations (blue solid line) and without using correlations (green dashed line), for the 3-qubit case. For reference, initial purity for a Gibbs state of inverse temperature β is shown in red dotted line. The Hamiltonian is $H = h\sigma_z^{\mathrm{A}} + h\sigma_z^{\mathrm{B}} + h\sigma_z^{\mathrm{AN}} + k\sigma_x^{\mathrm{A}}\sigma_x^{\mathrm{B}} + k\sigma_x^{\mathrm{B}}\sigma_x^{\mathrm{AN}}$, we are using A as the target, and compressing the entropy on B and A_N. The stronger the interaction, the more purification can be achieved.

In fact, the unitary that optimizes the entropy compression corresponds to the unitary that diagonalizes the total state and makes a SORT in decreasing order of the elements of the diagonal. Therefore, the unitary drives the system towards a passive state. This indicates deep links between work extraction and purification in non-degenerate interacting systems, and the role of quantum and classical correlations in algorithmic cooling.

5.7 Conclusions

In this chapter, I presented a technique that can be integrated with the HBAC protocols to not only allow the presence of correlations, but also to be able to break the strong local passivity of the system. I showed that by exploiting preexisting interaction-induced correlations, quantum energy teleportation can be used to significantly improve algorithmic cooling in systems with strong interactions. The stronger the interactions, the higher the purification gain. Further increases in the achievable purity should be possible, e.g., by optimizing the ancilla interactions or considering larger interacting systems where there are more correlations in the ground state. QET-cooling may be a good candidate for efficient cooling of strongly interacting systems in, e.g., ultra-strongly coupled superconducting qubits [75, 84, 32]. Another possible setup where this procedure can be thought of is an ensemble of di-atomic molecules where the two atoms in the molecule are modelled by qubits and the two atoms have a non-negligible interaction.

Our new algorithmic cooling protocols show that correlations are important in work extraction and entropy flows in cooling protocols. This is also in agreement with recent works that take advantage of correlations to enhance tasks related to extraction of energy and efficiencies [34, 16, 81, 94, 66, 36].

Chapter 6

n-to-1 distillation of athermality for two-level systems

In this Chapter, we obtain the limit of distillation of athermality – a property whereby a state has a distribution over energy levels that is not thermal [13] – of n identical qubits to one qubit, and relate our result to the maximum purity achievable for one qubit in a string of n identical qubits under thermal operations with no other experimental constraints. In particular, we focus on quasi-classical states, and we ask for their limit on athermality distillation. The systems considered consist of a string of n identical qubits, in a quasi-classical state, starting in a product state. Without loss of generality, we refer to the first qubit of the string as the *target qubit*, i.e. the qubit we are interested in purifying. Furthermore, we connect the optimal entropy compression unitary operations with concepts of resource theory, and provide a different and more simple geometric proof of its optimization using Lorenz curves and majorization, in the context of resource theories. These results connect ideas from resource theory, to be implemented in a useful and simple way to Heat-Bath Algorithmic Cooling (HBAC).

Our study can be understood as an example of heat-bath algorithmic cooling from a perspective of resource theory. In standard HBAC, the target qubit is purified by making suitable redistributions of the entropy among the string of qubits through alternating steps of entropy compression operations and contact with a thermal bath, as it was described in more detail in Chapters 1 and 2. Our first connection, when allowing general reversible

entropy compression operations, is to explain the optimal operations in the framework of resource theories and present a new proof using a geometric representation of the Lorenz curves and majorization. Then, we change the assumptions regarding the allowed type of operations in the cooling protocols: while in HBAC the entropy compression operations used are general global unitaries on the string of qubits, here we explore the case where the allowed operations are the thermal operations – i.e. operations that conserve the energy of the system – in order to connect with the *resource theory of athermality*.

Concretely, we present the analytic expression of the athermal Lorenz curve for n identical qubits. Then, we approximate it for the case of large n. We relate our result with the entropy compression needed for algorithmic cooling, and from them we obtain the maximum achievable purity for a target qubit in a single shot corresponding to two different scenarios. In one scenario we allow thermal operations, while in the other we allow global unitary operations. We present a proof of the best entropy compression under the aforementioned allowed operations by using the Thermo-majorization curves and Lorenz curves, respectively. Our results show that in the framework of resource theories, one can easily get the optimal results for the entropy compression operations and understand them from a more thermodynamic perspective.

In the next subsection, I briefly describe the resource theory of athermality and define the set of allowed operations. This resource theory allows us to study the advantages of possessing a resource state, in this case athermality, in a given quantum information processing protocol, which can be connected to the study of the limits of algorithmic cooling protocols. I then present our results for the maximum achievable entropy compression to purify a qubit in a single shot of reversible entropy compression and similarly for entropy compression with the thermal operations.

6.1 Preliminaries

A resource theory is a mathematical framework developed to study the influence of constraints on the possible evolution of physical systems under a restricted set of physical operations. To define a concrete resource theory, it is required to identify two types of operations: a set of operations that are considered free – i.e. operations that can be used without limit –, and the complementary set of operations which are expensive, which are

treated as resources [41, 18] and may be consumed to perform a given task. Along these lines, there will be also free states, and resources. Furthermore, a resource theory also allow us to understand when two resources are equivalent under a give set of free operations (i.e. when resources can be converted into others with free operations), and give us the conditions in which a given conversion can be accomplished. In a quantum resource theory the allowed operations are limited by the laws of quantum mechanics, with extra constraints that arise from the specification of the particular physical settings, from which it is possible to identify the set of free operations.

The perspective or resource theories rely on understanding and determining the relative usefulness of different sorts of resources in terms of their ability of do certain tasks, for example extracting work. Then, quantum thermodynamics could be seen as a field of studying the accessibility (or inaccessibility) of a physical state to be transformed into another one under certain allowed operations in accordance with the laws of thermodynamics [39, 59]. The set of thermodynamic operations encodes the structure of the thermodynamic arrow of time by telling which states can be reached from a given state [60].

In particular, let's consider the case of having a thermal bath at inverse temperature β, in this scenario a state that is in thermal equilibrium with the bath is considered to be a free state. In fact, such a thermal state at inverse temperature β cannot be a resource, as according to the second law of thermodynamics it cannot be transformed into any other athermal (out-of-equilibrium) state for free. On the other hand, athermal states can be consider as resources since they can be exploited to perform work. Along these lines, a set of free operations with respect to energy, would correspond to the operations that does not change the energy of the system. As free operations, by definition, cannot increase the amount of resources present in a state. This can be formally characterized in the so-called *resource theory of athermality.*

Resource theory of athermality

In the resource theory of athermality, the resources are the quantum states that deviate from the Gibbs form at a given temperature. [13]. This is because such athermal states can be exploited to perform work during the process of equilibration [25, 12], which can also be used to transform another system out of equilibrium. Then, the level of athermality of a quantum system can be understood as the distance of the distribution over its energy

levels from the thermal distribution [13].

Then, the corresponding free processes/operations, also known as *T-thermal operations*, are as follows:

1) Preparing systems in the Gibbs states at the bath temperature (states of the form $e^{-\beta H}/\operatorname{Tr}\left(e^{-\beta H}\right)$).

2) Global unitaries which are energy-preserving, i.e. that commute with the total Hamiltonian of the system and the bath. These type of operations are known as *Thermal Operations* (TO) and are defined with the use of the following general thermodynamic setting: A quantum system of Hamiltonian H, which is brought into thermal contact with a bath described by a Hamiltonian H_B. The joint system-bath evolves unitarly (preserving the energy according the first law of thermodynamics) and after some time the system is decoupled from the bath. With respect to the system alone, the operation is in general a CPTP, mathematically formalized in the following way:

Definition 2. *(Thermal operations) – The set of thermal operations* $\{\mathcal{E}_T\}$ *consists of CPTP maps that act on a system* ρ *in the following way:*

$$\mathcal{E}_T(\rho) = \operatorname{Tr}_B\left[U(\rho \otimes \gamma_B)U^\dagger\right],$$

where U *is a joint unitary commuting with the total Hamiltonian of the system and bath,* $[U, H + H_B] = 0$*, and* γ_B *is a thermal Gibbs state of the bath at some fixed inverse temperature* β*, i.e.* $\gamma_B = e^{-\beta H_B}/\operatorname{Tr}\left(\mathrm{e}^{-\beta \mathrm{H_B}}\right)$.

3) Taking the partial trace over a subsystem.

A general process is *T-thermal* if and only if it has a Stinespring dilation whose ancilla state is the Gibbs state at inverse temperature $\beta = 1/T$ and whose unitary is energy-preserving. On the other hand, the resource processes in resource theory of athermality are the athermal operations, eg. non energy preserving global unitaries.

In particular, quantum resource theory reduces to classical resource theory for quasi-classical states. A classical state is a state which is diagonal in the energy eigenbasis $\{|E_m\rangle\langle E_n|\}$ defined by the eigenstates of its corresponding system Hamiltonian $H = \sum_n \epsilon_n |E_n\rangle\langle E_n|$.

The resource theory of athermality provides a framework for describing many results in quantum thermodynamics, including the limits to work extraction [54, 13, 47, 103], Landauer's solution to the Maxwell demon problem [41], and the status of the second law of thermodynamics [41, 12].

Along those lines, in this chapter, our goal is to use ideas and concepts from resource theory of athermality to describe in a useful and simple way the optimal entropy compression operations of the HBAC protocols. In particular, we describe two different scenarios, first the conventional reversible entropy compression and then the entropy compression under thermal operations. The main difference between the previous studies of heat algorithmic cooling and a resource-theoretical approach lie in the tools used and the questions asked. While in HBAC the explicit steps are specify and are of fundamental importance, in resource theories the question of which particular operations are used to achieve a given resource conversion is typically considered to be of secondary interest.

How can we tell how far a given state is from being a thermal state? Namely, how can we order different quantum states accordingly to their level of athermality? These are basic questions that we will use to characterize later what is the best entropy compression we can achieve by using thermal operations. But before answer these questions, we will start with the simpler question of ordering probability distributions according to their uncertainty, to then connect it with the optimal reversible entropy compression operation, as is presented in the next section.

6.2 Majorization (Lorenz) curves and the optimal reversible entropy compression

A way to order probability distributions according to their uncertainty is given by majorization [9]. Namely, in order to know which of two given probability distributions, $\mathbf{p}$ and $\mathbf{q}$, is less uncertain, we can use a tool based on partial order, known as majorization, which is defined as follows:

Definition 3. *(Majorization) – Given two d-dimensional probability distributions* $\boldsymbol{p}$ *and*

$\boldsymbol{q}$, we say that $\boldsymbol{p}$ majorizes $\boldsymbol{q}$, which is denoted by $\boldsymbol{p} \succ \boldsymbol{q}$, if and only if

$$\sum_{i=1}^{n} p_i^{\downarrow} \leq \sum_{i=1}^{n} q_i^{\downarrow} \quad \forall \quad n = 1, ..., d-1. \tag{6.2.1}$$

where $p_i^{\downarrow}$ corresponds to the ith element of $\boldsymbol{p}^{\downarrow}$ which is $\boldsymbol{p}$ sorted in a non-increasing order.

Then, within majorization theory a probability distribution $\mathbf{p}$ is said to be less uncertain than $\mathbf{q}$, if $\mathbf{p} \succ \mathbf{q}$ [9].

An alternative, more geometrical, definition is easily seen to be equivalent to the previous one is the Majorization (Lorenz) curve:

Definition 4. *(Majorization (Lorenz) curve) – The Majorization (Lorenz) curve $L(\boldsymbol{p})$ is characterized as the linear interpolation of the following points:*

$$\left(\frac{j}{d}, \quad \sum_{i=1}^{j} p_i^{\downarrow} \right), \quad \forall j = 1, ..., d, \tag{6.2.2}$$

and the point $(0, 0)$. We say that the curve $L(\boldsymbol{p})$ majorizes the curve $L(\boldsymbol{q})$, denoted by $L(\boldsymbol{p}) \succ L(\boldsymbol{q})$, if and only if all the points of the curve $L(\boldsymbol{p})$ lie not below $L(\boldsymbol{q})$ and the two curves end at the same height.

The Lorenz curve gives us a simple geometrical way to identify if two probabilities vectors $\mathbf{p}$ and $\mathbf{q}$, satisfy a majorization relationship: namely, $L(\mathbf{p}) \succ L(\mathbf{q})$ if and only if $\mathbf{p} \succ \mathbf{q}$.

In particular, the distribution given by the eigenvalues $\mathbf{p}_\lambda$ of the system's state majorizes the probability distribution given by the diagonal elements $\mathbf{p}$ of system's state. This statement is given and proved by the Schur-Horn theorem, which formally is stated as follows:

Schur-Horn Theorem. – Let $\mathbf{d} = \{d_i\}_{i=1}^{N}$ and $\lambda = \{\lambda_i\}_{i=1}^{N}$ be vectors in $\mathbb{R}^N$ such that their entries are non-increasing order. There is Hermitian matrix with diagonal values $\{d_i\}_{i=1}^{N}$ and eigenvalues $\{\lambda_i\}_{i=1}^{N}$ if and only if

$$\sum_{i=1}^{n} d_i \leq \sum_{i=1}^{n} \lambda_i \quad \text{for} \quad n = 1, 2, ..., N, \quad \text{and} \quad \sum_{i=1}^{N} d_i = \sum_{i=1}^{N} \lambda_i. \tag{6.2.3}$$

Then, since unitaries operations on the system preserve the eigenvalues of the state, the distribution given by these eigenvalues will majorize any distribution given by the diagonal of the system's state under unitary evolution. Namely, for a state ρ with eigenvalues $\mathbf{p}_\lambda$, the following majorization order is satisfied for all unitaries on the system:

$$\mathbf{p}_\lambda \succcurlyeq \mathbf{p} = \text{diag}\left(U\rho U^\dagger\right) \quad \forall U. \tag{6.2.4}$$

This Majorization ordering, in combination with the fact that the Majorization (Lorenz) curves represent equivalence classes of resources under unitary operations, will be relevant to find the optimal reversible entropy compression to purify a target qubit from a system of n qubits. So, let's start by finding the Majorization (Lorenz) curve for our system of interest.

6.2.1 System setup

The system consists of astring of n identical qubits, starting in a product state, each of them in the state $\rho = \begin{pmatrix} p & 0 \\ 0 & 1-p \end{pmatrix}$, with $p \geq 1/2$. Without loss of generality, we can take the first qubit of the string as the *target qubit* (the qubit that we want to purify). We will refer to the rest of the qubits as the *scratch qubits*.

Then, the total state of the system, $\rho_T = \rho^{\otimes n}$, is a diagonal matrix with 2^n elements of the form $p^{n-i}(1-p)^i$ in the diagonal, for $i = 0, 1, ..., n$. More concretely, in the diagonal there are $\binom{n}{i} = \frac{n!}{i!(n-i)!}$ elements with value $p^{n-i}(1-p)^i$, for $i = 0, 1, ..., n$.

6.2.2 Majorization (Lorenz) curve of system setup

The corresponding Majorization Lorenz curve for the system, as presented in Definition 3, is characterized by the curve obtained from the linear interpolation of the following points:

$$\left(\frac{j}{2^n}, \quad S_j\right), \quad \forall j = 0, 1, ..., 2^n, \tag{6.2.5}$$

where S_j is the sum of the j largest components of the diagonal elements of the total state $\rho_T = \rho^{\otimes n}$, for $j = 1, 2, .., 2^n$, and taking $S_0 := 0$ for $j = 0$.

To write explicitly the form of the Majorization Lorenz curve, let's consider the sorting of the different values of the diagonal elements of ρ_T in non-increasing order. For, with $p \geq 1/2$, we have the following order:

$$p^n \geq p^{n-1}(1-p) \geq p^{n-2}(1-p)^2 \geq ... \geq (1-p)^n \tag{6.2.6}$$

i.e. $p^{n-i}\,(1-p)^i \geq p^{n-j}\,(1-p)^j$ for all $i \leq j$.

Then, by partially summing these ordered elements and taking into account the repetition of them in the diagonal, the explicit form of the Lorenz curve will be given by the linear interpolation of the following 2^n points:

$$\begin{aligned} &Q_{k,j} := \left(\frac{1}{2^n}\left[\sum_{i=0}^{k}\binom{n}{i}+j\right],\quad \sum_{i=0}^{k}\binom{n}{i}p^{n-i}\,(1-p)^i + jp^{n-k}\,(1-p)^k\right), \\ &\text{for}\quad j=0,...,\binom{n}{k+1}-1, \qquad \forall k=0,...,n, \end{aligned} \tag{6.2.7}$$

and the point $(0,0)$.

Note that, for a fix k, all the points $Q_{k,j}$, for $j=0,...,\binom{n}{k+1}$, will be in the straight line that connects the points $Q_{k,0}$ and $Q_{k+1,0}$. This is obtained from the linear form on j of the eq.(6.2.7) when k is fix:

$$Q_{k,j} = Q_{k,0} + j\left(2^{-n}, p^{n-k}\,(1-p)^k\right). \tag{6.2.8}$$

From here, we can describe the Lorenz curve by taking only the extreme points of these lines, $Q_{k,0}$, to linear interpolate, while assuring that all the points of eq.(6.2.7) will be within this curve.

Therefore, the Majorization Lorenz curve for our system of n identical qubits is given by the linear interpolation of the points

$$\boxed{\tilde{Q}_k := Q_{k,0} = \left(\frac{1}{2^n}\sum_{i=0}^{k}\binom{n}{i},\quad \sum_{i=0}^{k}\binom{n}{i}p^{n-i}\,(1-p)^i\right),\quad \forall k=0,...,n.} \tag{6.2.9}$$

The second component of the points $\tilde{Q}_k$, corresponds to the cumulative distribution

function of a binomial distribution:

$$F(k,n,1-p) := \sum_{i=0}^{k} \binom{n}{i} p^{n-i} (1-p)^i , \tag{6.2.10}$$

which can also be represented by the regularized incomplete beta function [113], as follows:

$$F(k,n,1-p) = (n-k)\binom{n}{k} \int_0^p t^{n-k-1} (1-t)^k \, dt \tag{6.2.11}$$

Then, eq.(6.2.9) is equivalent to:

$$\tilde{Q}_k = \left(\frac{1}{2^n} \sum_{i=0}^{k} \binom{n}{i}, \quad (n-k)\binom{n}{k} \int_0^p t^{n-k-1} (1-t)^k \, dt \right), \quad \forall k = 0, ..., n. \tag{6.2.12}$$

In the Fig.6.1, it is shown the Lorenz curves, which corresponds to the linear interpolation of the points given by $Q_{k,0}$, for different values of n.

6.2.3 Cooling the target qubit

The maximum achievable probability q_{max} that the target qubit (the first qubit in the string of n qubits) can have, after applying a global unitary operation in the system, will correspond to the value given by the Majorization Lorenz curve of the whole diagonalized system evaluated in 1/2 (i.e. it will be the sum of the 2^{n-1} biggest values of the ρ_T's diagonal).

This can be demonstrated by using the Schur-Horn theorem, which tells us that the Majorization Lorenz curve of the eigenvalues $\mathbf{p}_\lambda$ of the system majorizes all the other Lorenz curves of the system transformed under unitary operations U:

$$\mathbf{p}_\lambda \succcurlyeq \mathbf{p} = \mathrm{diag}\left(U \rho U^\dagger\right) \quad \forall U. \tag{6.2.13}$$

In this case the system has already a diagonal density matrix, but we can conclude that for a general state, the Schur-Horn theorem tell us that the best unitary for entropy compression to purify a target qubit should leave the total system diagonalized (to have

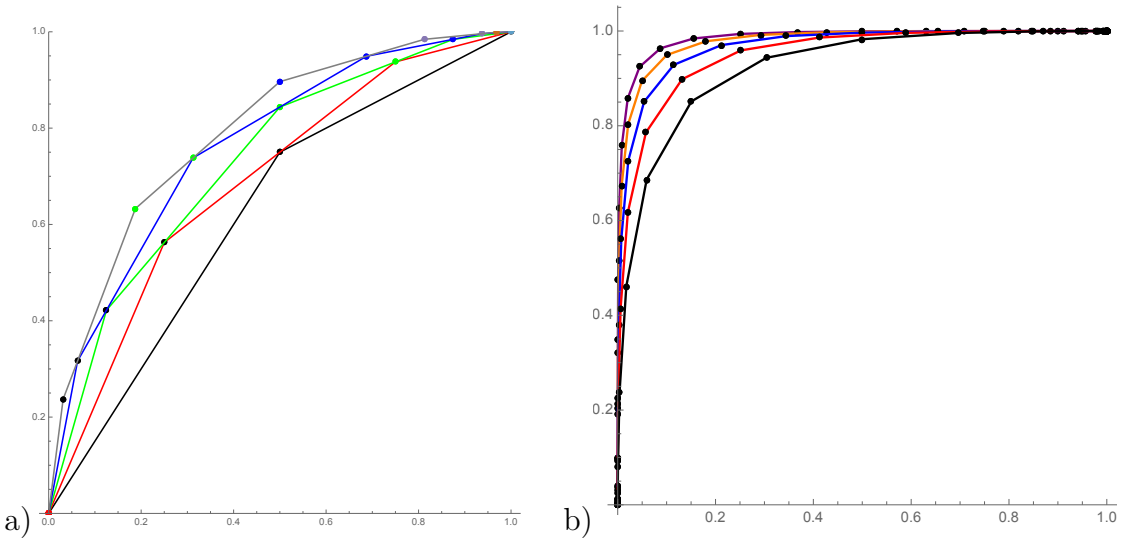

Figure 6.1: **a)** Majorization Lorenz curves for different n ($n = 1, 2, 3, 4, 5$, from lower to higher). The Majorization Lorenz curves allow us to obtain, in a very simple geometrically way, the maximum probability of the target-qubit's ground state after the optimal unitary entropy compression. This aforementioned probability corresponds to the value of the probability given by the middle point of the plot (the point $(\frac{1}{2}, S_{2^n/2})$, namely $S_{2^n/2}$. Note that, this probability $S_{2^n/2}$ is higher when the number n of qubits grows. **b)** Majorization Lorenz curves for different n ($n = 15, 20, 25, 30, 35$, in the thermodynamic limit, the higher Majorizatin Lorenz curves converge to an asymptotic Lorenz curve.

the Majorization lorenz curve that majorizes all the possible ones under unitary operations). Then, the diagonal elements can be permuted, since they are equivalent in the Majorization curve, to favor the first qubit: to increse the propability of the ground state of the target qubit the diagonal elements should be sort in a non-increasing order.

Thus, the middle point of the Majorization lorenz curve gives the maximum probability

of being in the ground state for the first qubit of the system, which is as follows:

$$q_{max} := S_{2^{n-1}}$$

$$q_{max}(p,n) = \begin{cases} \sum_{i=0}^{(n-1)/2} \binom{n}{i} p^{n-i} (1-p)^i, & \text{if } n \text{ is odd} \\ \sum_{i=0}^{n/2} \binom{n}{i} p^{n-i} (1-p)^i - \frac{1}{2}\binom{n}{n/2} p^{n/2} (1-p)^{n/2}, & \text{if } n \text{ is even.} \end{cases} \tag{6.2.14}$$

In the Fig.6.2, q_{max} is illustrated as a function of p for different values of n.

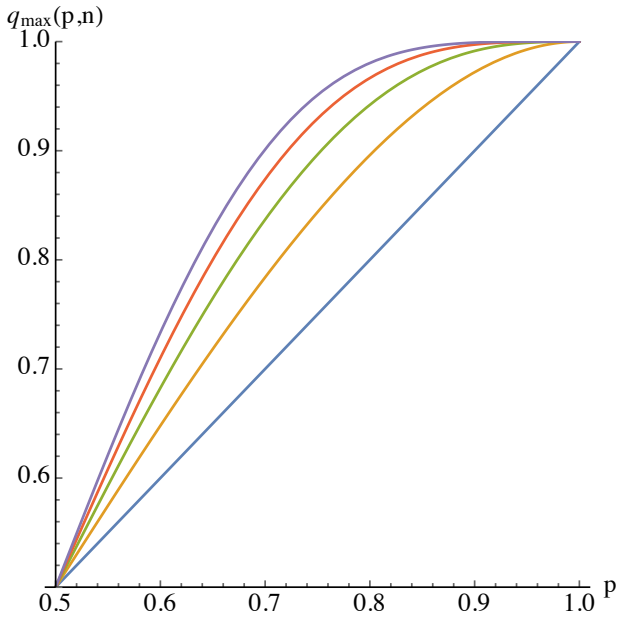

Figure 6.2: Maximum achievable probability for the target qubit, q_{max} as a function of the initial probability p, for different values of n ($n = 2, 4, 6, 8, 10$, from the right to the left. Note: for a n odd, it will give the same q_{max} corresponding to $n + 1$).

Then, from here we can obtain the maximum achievable purity $\mathcal{P} = \mathrm{Tr}(\rho^2_{q_{max}})$ where $\rho_{q_{max}}$ is the diagonal matrix with diagonal elements $(q_{max}, 1 - q_{max})$. Thus, $\mathcal{P} = 2q_{max}(q_{max} - 1) + 1$.

In the PPA-HBAC [93], this entropy operation U is obtained by making a reordering of the diagonal elements in decreasing order, which will be an equivalent final purity as the obtained here. After this entropy compression some qubits can be brought into thermal contact with a bath to be refreshed. This step can be also studied by using the Lorenz curve after the refresh process. We could make an optimization to get the process which gives a final state with a spectrum that majorizes the one of any other refresh process.

We presented a proof, in a simple and clean way by using majorization concepts, that the best entropy compression for a general state, including states with internal correlations, corresponds to diagonalize the state, and make a non-increasing sort on the diagonal elements of the global system.

6.2.4 Lorenz curve for the limit of $n \to \infty$

For a large number of qubits, we can approximate the Majorization Lorenz curve by using the Stirling approximation, and the cumulative distribution function of a normal distribution as an approximation of the binomial one.

The partial sum of the first k binomial coefficients

$$\sum_{i=0}^{k} \binom{n}{i} = \sum_{i=0}^{k} \frac{n!}{i!\,(n-i)!} \leq 2^n \quad \forall k = 0, 1, ..., n, \tag{6.2.15}$$

does not have a close formula for partial sums $k > n$; while for $k = n$, this sum gives 2^n. By applying the the Stirling approximation, which holds for n sufficiently large, we obtain the following approximation:

$$\sum_{i=0}^{k} \binom{n}{i} \sim 1 + \sum_{i=1}^{k} \sqrt{\frac{n}{2\pi i(n-i)}} \frac{n^n}{i^i (n-i)^{n-i}}. \tag{6.2.16}$$

For the Lorenz curve, this expression normalized, then for $n \to \infty$ it will make a division of the interval $[0, 1]$ to infinitesimal parts, when considering all the points given by eq.(6.2.7).

On the other hand, for the second component of the points for the Lorenz curve, eq.(6.2.9), which corresponds to a binomial cumulative distribution function $F(k, n, 1-p)$,

it can be approximated as the normal cumulative distribution function, if n is large enough with p remaining fixed, as a consequence of the Central Limit Theorem. More concretely, the distribution tends towards the normal distribution with mean $n(1-p)$ and variance $np\,(1-p)$ as $n \to \infty$ with p fixed:

$$F(k, n, 1-p) \to \Phi\left(\frac{k-n(1-p)}{\sqrt{np\,(1-p)}}\right) \tag{6.2.17}$$

where $\Phi\,(x) = \frac{1}{2}\left[1 + \text{erf}\left(\frac{x}{\sqrt{2}}\right)\right]$, with $\text{erf}(x) = \frac{2}{\sqrt{\pi}}\int_0^x e^{-t^2}dt$.

Then, the points for the Lorenz curve, for a large n, will be approximated to

$$\tilde{Q}_k \approx \left(\frac{1}{2^n} + \frac{n^{n+1/2}}{\sqrt{2\pi}}\sum_{i=1}^{k}\frac{i^{-i-1/2}}{(n-i)^{n-i+1/2}}, \quad \frac{1}{2}\left[1 + \text{erf}\left(\frac{k-n(1-p)}{\sqrt{2np\,(1-p)}}\right)\right]\right), \quad \forall k = 0, ..., n,$$

which corresponds to the asymptotic Lorenz curve in the thermodynamic limit. The middle point of this curve, gives the maximum achievable probability of the ground sate of the target qubit after a unitary entropy compression operation.

6.3 Thermo-majorization

In thermodynamic considerations instead of comparing which of the two probabilities is more uncertain, we will study which one is closer to the thermal equilibrium distribution. Thus, we will use the ordering with respect to a thermal Gibbs distribution, which is formally defined as follows:

Definition 5. *(Thermal Gibbs distribution γ) – The thermal Gibbs distribution of a system with Hamiltonian $H = \sum_{i=1}^{d} E_i|i\rangle\langle i|$, with non-decreasing set of energies $\{E_1 \leq E_2 \leq ... \leq E_d\}$, at inverse temperature β, is given by*

$$\gamma = \frac{1}{Z}\left(e^{-\beta E_1}, e^{-\beta E_2}, ..., e^{-\beta E_d}\right), \quad \textit{where} \quad Z = \sum_{i=1}^{d} e^{-\beta E_i}. \tag{6.3.1}$$

Note that in the infinite temperature limit, i.e. $\beta \to 0$, the Gibbs state becomes a maximally mixed state: $\gamma \to (1/d, ..., 1/d)$.

In thermodynamics, a way to classify out-of-equilibrium distributions, with respect to a thermal Gibbs distribution γ, is given by the so-called β-ordering [59], which is defined as follows:

Definition 6. *($\beta-$ordering and Gibbs re-scaling) – Given a thermal Gibbs distribution γ, Gibbs re-scaling a probability distribution $\boldsymbol{p}$ is defined by*

$$\boldsymbol{p} \xrightarrow{Gibbs-rescaling} \boldsymbol{p}^{\gamma} = \left(\frac{p_1}{\gamma_1}, \frac{p_2}{\gamma_2}, ..., \frac{p_d}{\gamma_d}\right) = Z\left(p_1 e^{\beta E_1}, p_2 e^{\beta E_2}, ..., p_d e^{\beta E_d}\right). \tag{6.3.2}$$

Then, the $\beta-$ordering of a probability distribution $\boldsymbol{p}$ is defined by a permutation π_p that arranges $\boldsymbol{p}^{\gamma}$ in a non-increasing order, i.e. $\boldsymbol{p}^{\gamma} \xrightarrow{\pi_p} \boldsymbol{p}^{\gamma}_{\pi_p} = (\boldsymbol{p}^{\gamma})^{\downarrow}$, where

$$p_{\pi_p(1)} e^{\beta E_{\pi_p(1)}} \leq p_{\pi_p(2)} e^{\beta E_{\pi_p(2)}} \leq ... \leq p_{\pi_p(d)} e^{\beta E_{\pi_p(d)}}. \tag{6.3.3}$$

Now, the $\beta-$ordered version of a probability vector $\boldsymbol{p}$ is given by $\boldsymbol{p} \xrightarrow{\pi_p^{-1}} \boldsymbol{p}^{\beta}$:

$$\boldsymbol{p}^{\beta} := \boldsymbol{p}_{\pi_p^{-1}} = \left(p_{\pi_p^{-1}(1)}, p_{\pi_p^{-1}(2)}, ..., p_{\pi_p^{-1}(d)}\right). \tag{6.3.4}$$

Then, the thermodynamic ordering is defined with the use of thermo-majorization curves [13], analogous to the Majorization (Lorenz) curves:

Definition 7. *(Thermo-majorization curves) – Given a thermal Gibbs distribution γ and a probability vector $\boldsymbol{p}$, its thermo-majorization curve $f_{\boldsymbol{p}}$ is composed of linear segments connecting the point $(0, 0)$ and the points*

$$\left(\sum_{i=1}^{k} \gamma_i^{\beta}, \quad \sum_{i=1}^{k} p_i^{\beta}\right) = \left(\sum_{i=1}^{k} \gamma_{\pi_p^{-1}(i)}, \quad \sum_{i=1}^{k} p_{\pi_p^{-1}(i)}\right) \tag{6.3.5}$$

for $k \in \{1, 2, ..., d\}$, where π_p is a permutation that β-orders $\boldsymbol{p}$.

Analogous to majorization, a probability distribution $\mathbf{p}$ is said to be further from the thermal equilibrium distribution than $\mathbf{q}$ is if $\mathbf{p}$ *thermo-majorizes* $\mathbf{q}$, which is formally defined as follows:

Definition 8. *(Thermo-majorization) – We say that probability vector* $\boldsymbol{p}$ *thermo-majorizes a probability vector* $\boldsymbol{q}$ *with respect to a thermal Gibbs distribution* γ*, denoting it by* $\boldsymbol{p} \succ_\beta \boldsymbol{q}$*, if the thermo-majorization curve* $f_{\boldsymbol{p}}$ *is above the curve* $f_{\boldsymbol{q}}$ *for all the points, i.e.* $f_{\boldsymbol{p}}(x) \leq f_{\boldsymbol{q}}(x)$ *for all* x*.*

Thermo-majorisation is the notion that characterises how different out of equilibrium distributions can be transformed into each other under thermal-operations.

6.4 Themo-majorization curves for n identical qubits

The density probability $\mathbf{q}$ for our system of n identical qubits, as described before, has 2^n elements, where $\binom{n}{i} = \frac{n!}{i!(n-i)!}$ of them are of the form $p^{n-i}(1-p)^i$, for $i = 0, 1, ..., n$. Assuming that the qubits have only local Hamiltonians $H_L = \omega\sigma_z$, with $\omega > 0$.

It implies that the elements of the corresponding thermal distribution γ, has $\binom{n}{i} = \frac{n!}{i!(n-i)!}$ elements of the form

$$\frac{p^{n-i}(1-p)^i Z}{e^{-\beta\omega(n-2i)}}. \tag{6.4.1}$$

The the non-decreasing order of the elements of γ, when $p \geq 1/2$ and $\omega > 0$ is as follows:

$$\frac{p^n Z}{e^{-\beta\omega(n)}} \geq \frac{p^{n-1}(1-p)Z}{e^{-\beta\omega(n-2)}} \geq \frac{p^{n-2}(1-p)^2 Z}{e^{-\beta\omega(n-4)}} \geq ... \geq \frac{(1-p)^n Z}{e^{\beta\omega(n)}}. \tag{6.4.2}$$

Then, by partially summing in the corresponding order the elements of γ, and q, we can obtain the explicit form of the thermo-majorization Lorenz curve that thermo-majorizes all possible combinations states of the system, which will be linear interpolation of the following 2^n points:

$$\boxed{\left(\frac{1}{Z}\sum_{i=0}^{k}\binom{n}{i}e^{-\beta\omega(n-2i)}, \quad \sum_{i=0}^{k}\binom{n}{i}p^{n-i}\left(1-p\right)^i\right), \quad \forall k = 0, ..., n.} \tag{6.4.3}$$

where $Z = \sum_{i=0}^{n}\binom{n}{i}e^{-\beta\omega(n-2i)}$. In the Fig. 6.3, it is shown the thermo-majorization Lorenz curve for different values of n, with $\beta = 0.001$ and $\omega = 1$.

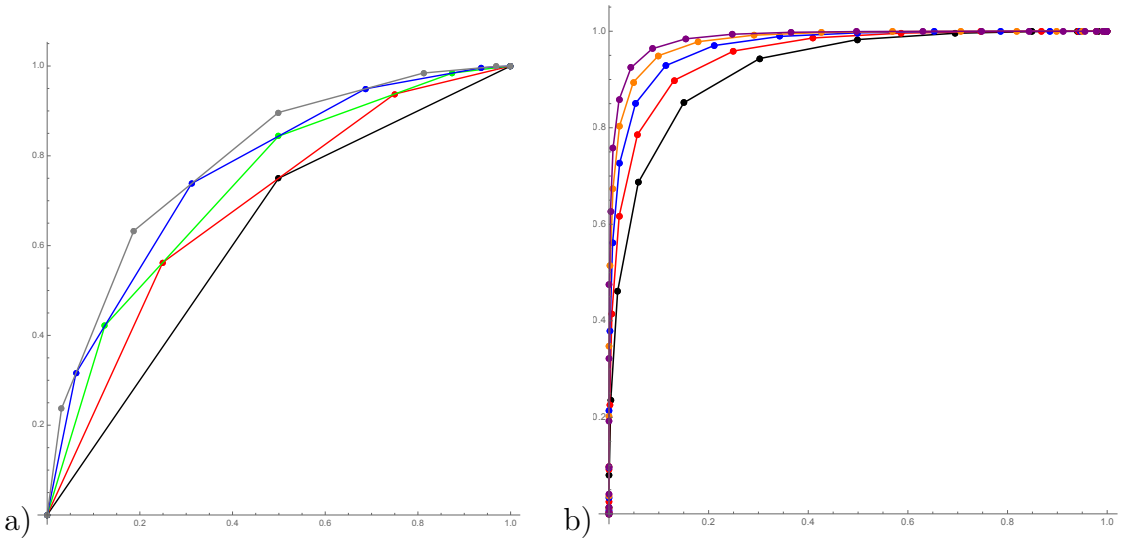

Figure 6.3: **a)** Thermo-majorization Lorenz curves for different n ($n = 1, 2, 3, 4, 5$, from lower to higher). Analogous to the Majorization-Lorenz curves of Fig. 6.1, the Thermo-majorization Lorenz curves allow us to obtain, in a very simple geometrically way, the maximum probability of the target-qubit's ground state but in this case after thermal operations (instead of an optimal unitary for the entropy compression as in Fig. 6.1). The corresponding maximum probability is given by the value of the probability of the middle point from the plot. Note that, the probability of this middle point is higher when the number n of qubits grows. **b)** Thermo-majorization Lorenz curves for different n ($n = 15, 20, 25, 30, 35$, in the thermodynamic limit, the higher Thermo-majorizatin Lorenz curves converge to an asymptotic curve.; both with $\beta = 0.001$ and $\omega = 1$

We are interested in a particularly important β-permutation. $\beta-$permutations have a simple geometrical description in terms of thermomajorization curves. In this context, we want to maximize the population of of the ground state of the target qubit subject to the thermo-majorization constraints. Namely, we are looking for the maximization of the partial sum of the first half elements of the diagonal elements, among all thermal operations. Then, similar to the Majorization (lorenz) curves, the best entropy compression to the purity a target qubit, under thermal operations, corresponds to the one that distills the most athermally from the rest of the qubits.

6.5 Conclusions

We showed how by using ideas and concepts from resource theory it is possible to find the optimal entropy compression (single shot) required for HBAC. In particular, two different scenarios were studied, with the first one corresponding to the case where the allowed operations are reversible entropy compressions, which are given by global unitaries. The second scenario, when the set of operations are restricted to thermal operations. We presented the analytic expression of the majorization (Lorenz) curve and the Thermo-Majorization curve for n identical qubits. Then, we approximated it for the case of large n. We related our result with the entropy compression needed for algorithmic cooling. Concretely, we obtained the maximum achievable purity for a target qubit in a single shot corresponding to the two aforementioned scenarios. We present a proof of the best entropy compression by using the Thermo-majorization curves and Lorenz curves together with the Schur-Horn theorem. Our results show that in the framework of resource theories, one can easily get the optimal results for the entropy compression operations and understand the results from a more geometric and thermodynamic perspective. Other questions that we would like to explore for future work are: How can one generalize our results beyond two-level systems? Can we use Majorization Lorenz curves for n qubits to get insight into other resource theory problems involving asymptotics?

Chapter 7

Conclusions

Quantum information processing brings ways for cooling physical systems by manipulating entropy in an algorithmic way. Understanding these processes and their cooling limits can elucidate fundamental theoretical properties of quantum thermodynamics and lead to new experimental possibilities. In particular, heat-bath algorithmic cooling (HBAC) methods have important applications in quantum computing as they provide a potential solution to prepare quantum systems with sufficient purity.

In this thesis, more refined algorithmic cooling protocols were created that can lead to a lower achievable temperature than standard HBAC. In our first model, we presented a more general control on the interaction with the thermal bath, in particular by considering relaxation processes where the bath only couples to certain energy transitions of the ancilla, a crucial step that has not been taken into account in previous protocols. In our second model, we circumvented the previous limits by taking advantage of correlations present in the initial state induced by the internal interactions of the system. This second model contrasts with all previous algorithmic cooling methods, since it has been assumed that the system's initial state is in a product state and that the interaction with the bath breaks correlations. These two models of algorithms show how correlations can be used to improve cooling. Furthermore, we study how to optimize the entropy compression using tools from resource theories, closing the bridge between these two frameworks. In particular, we found how to obtain the optimal reversible entropy compression in the context of distillation of athermality, finding that the results are deeply related to the N-to-1 distillation of

athermality from two level systems.

Concretely, the main results of this thesis are presented as follows:

HBAC with cross relaxation processes.

We showed that the HBAC protocols can be further optimised by designing a novel reset step that generalizes the control on the interaction with the thermal bath. This enhancement is physically motivated by cross relaxation processes. In particular, we considered relaxation processes where the bath only couples to certain energy transitions of the ancilla. The engineered relaxations required for our new reset step utilize the coupling to the environment in a way that is not limited to individual qubit-resets, but could also include correlations between the qubits as they are in contact with the environment. The assumption that entropy can be extracted from the system only via qubit reset (instead of state-reset) is a symmetry that was implicitly imposed for qubits but is not generally true. There are other examples of similar imposed symmetries, such as the distinction on subspace and subsystems [58] where the symmetry limits quantum information processing.

We presented explicit algorithmic cooling protocols that provide new fundamental limits on HBAC by engineering the aforementioned thermalisation processes. Concretely, we have shown a series of algorithms and calculated their resulting polarization for this new method as a function of the number of qubits, n, and as a function of the polarization of the bath, ϵ_b. We have also presented the polarization evolution as a function of the number of iterations of our algorithms and compared between these results and the corresponding ones of the PPA.

There exist many possibilities for future application of this method. Although originally designed for NMR where measurements are ensemble averages, we believe that our technique can be applied in other modalities, e.g. superconducting and ion traps, where we have imperfect projective measurements and initial states. In these modalities it could be implemented by incorporating the qubits in 'leaky' cavities that resonate at twice the fundamental frequency of the qubit, and thus induce the $|11\rangle$ to $|00\rangle$ transition. Our algorithm might be a tool to help in NMR or MRI applications to increase signal to noise ratio or bring these error rates below the threshold for fault tolerance in quantum information applications.

We expect that our state-reset operation could be implemented on devices with sufficient control of the thermal bath such as in Ref. [87], for example. Also, we have been exploring the scenario of implementing our algorithm in superconducting qubits where Γ_2, the fully correlated relaxation process of two qubits, would be implemented through a cavity at twice the resonance of the fundamental mode with interaction of the form $H_{int} = \sigma_1^+ \sigma_2^+ a^\dagger + cc.$ where σ_i^+ create a qubit i excitation and $a^\dagger$ absorb the double excitation. We are still in the early stages of this work and have been designing the required Hamiltonian that can be created experimentally. On the other hand, we have preliminary experimental results in NMR showing that the effect of the Γ_2 process can be observed.

Our results show implicitly that a universal set of unitary gates along with Γ_1 are not universal for open quantum systems with two qubits or more. We conjectured that universality is achieved by including Γ_2 for the two-qubit case and by including all Γ_i for the n-qubit case. This was proved in a recent paper of C.Perry et al. [85].

Furthermore, our work shows that exploiting non-Markovian effects can lead to enhanced cooling protocols. Our protocol has also inspired other recent cooling methods. One example of this is the work of Alhambra, Lostaglio, and Perry, who pushed our idea to its limits by finding optimal strategies for HBAC under general engineered thermalisation processes, leading to ground state cooling with an exponential convergence with the number of steps [1]. Another example is the work of XinHua Peng et al. [114], who created a new two-qubit reset sequence together with a decoherence-free subspace and present a new algorithmic cooling technique based on our cross relaxation reset-step.

Correlation-Enhanced Algorithmic cooling due internal correlations

In our second model, we combined techniques from quantum field theory, such as quantum energy teleportation (QET) protocols, to exploit internal correlations of the system in order to enhance cooling. We showed that by exploiting these correlations it is possible to extract more entropy from qubits than with methods that do not take these interactions into account. In particular, our new model removes two implicit assumptions underlying all previous cooling protocols: the assumption that the initial state of the system should be in a product state, and the assumption that the optimal contact with the thermal bath is the one that fully thermalizes the reset qubits while destroying the internal correlations between these reset qubits and the other qubits of the system. Instead, our model uses the

internal correlations to fuel the extraction of energy from the target qubit.

Concretely, we used QET protocols to show how, by exploiting preexisting interaction-induced correlations, it is possible to significantly improve algorithmic cooling in systems with interactions, especially in the strong coupling regime. Further increases in the achievable purity should be possible, e.g., by optimizing the ancilla interactions or considering larger interacting systems where there are more correlations in the ground state.

Our new approach opens the door to further efficiency gains in algorithmic cooling, e.g., by optimizing the quantum interactions with ancillas that replace the classical measurements in the QET part of the protocol. QET-cooling may be a good candidate for efficient cooling of strongly interacting systems in, e.g., ultra-strongly coupled superconducting qubits [75, 84, 32].

N-to-1 distillation of athermality and entropy compression

Finally, we showed how by using ideas and concepts from resource theory it is possible to find the optimal entropy compression required for HBAC by studying the N-to-1 distillation of athermality of two level systems. We present the analytic expression of the athermal Lorenz curve for N identical qubits. Then, we approximate it for the case of large N. We relate our result with the entropy compression needed for algorithmic cooling, and from them we obtained the maximum achievable purity for a target qubit in a single shot corresponding to two different scenarios that allow the following operations: in one scenario the thermal operations, and in the other global unitary operations. We present a proof of the best entropy compression under the aforementioned allowed operations by using the Thermo-majorization curves and Lorenz curves, respectively. Our results show that in the framework of resource theories, one can easily get the optimal results for the entropy compression operations and understand the results from a more thermodynamic perspective.

Appendix A: Achievable Cooling for the PPA

In this appendix, it is explained in detail how to obtain the principal results of the Chapter 3. First, we give the conditions of the cooling limit and the requirements to have a steady state. Then, we show that these conditions can be reached asymptotically when we start from the maximally mixed state. We derive the maximum polarization achievable when the initial state is totally mixed, and the corresponding temperature. Furthermore, we explain how to get the number of steps needed to have a certain polarization $\epsilon_{\mathbb{1}}^{\infty} - \delta$ (we give the exact solution for $n = 3$, and an upper bound for $n > 3$).

A1. Cooling limit

In the cooling limit it is not possible to continue extracting entropy from the computational qubits. Thus, the corresponding state, ρ_{com}, will not change by applying the compression and refresh steps of HBAC.

The method to find this steady state is to consider the general form of ρ_{com}, and apply the two steps of the HBAC method to get ρ''_{com}. The conditions for the steady state are given by the equality of these states.

Assume that we start with a system in the totally mixed state. By applying compression and refresh operations, the state remains diagonal. Thus, the state of the whole qubit

system, ρ, can be completely described by its diagonal elements,

$$diag(\rho) = \begin{bmatrix} p_1 \\ p_2 \\ . \\ . \\ . \\ p_D \end{bmatrix}, \tag{7.0.1}$$

where $diag(\rho)$ is the vector of the diagonal elements of ρ, and D is the dimension of the Hilbert space of the whole string of qubits ($D = 2d2^m$).

Applying HBAC, the state evolves through the following two steps:

Entropy Compression Step: $\rho \xrightarrow{Compress} \rho' = U\rho U^\dagger$**.** In the PPA, U sorts the diagonal elements of ρ in decreasing order, giving a ρ' with diagonal elements

$$p'_1 \geq p'_2 \geq ... \geq p'_{D-1} \geq p'_D. \tag{7.0.2}$$

The state of the computational qubits, ρ'_{com}, is given by

$$diag(\rho'_{com}) = diag(\mathrm{Tr}_m(\rho')) := \begin{bmatrix} A_1 \\ A_2 \\ . \\ . \\ . \\ A_{2d} \end{bmatrix}, \tag{7.0.3}$$

where $\mathrm{Tr}_m()$ is the partial trace operation over the m reset qubits, and $A_k = \sum_{j=j_{k_0}}^{j_k} p'_j$, with $j_{k_0} = (k-1)2^m + 1$ and $j_k = k2^m$. This, with eq. (7.0.2), implies that

$$A_1 \geq A_2 \geq ... \geq A_{2d-1} \geq A_{2d}. \tag{7.0.4}$$

Refresh Step: $\rho' \xrightarrow{Refresh} \rho'' = \mathrm{Tr}_m(\rho') \otimes \rho_{\epsilon_b}^{\otimes m}$**,** where $\rho_{\epsilon_b} = \frac{1}{2}\begin{pmatrix} 1+\epsilon_b & 0 \\ 0 & 1-\epsilon_b \end{pmatrix}$ is the

state of a qubit with heat-bath polarization ϵ_b.

After these compression and refresh steps, the state of the total qubit system, ρ'', will be described by

$$diag\left(\rho''\right) = \begin{bmatrix} A_1 \\ A_2 \\ . \\ . \\ . \\ A_{2d-1} \\ A_{2d} \end{bmatrix} \otimes \frac{1}{2^m} \begin{pmatrix} 1+\epsilon_b \\ 1-\epsilon_b \end{pmatrix}^{\otimes m}. \tag{7.0.5}$$

In the cooling limit there is no operation that can compress any further the entropy of the computational qubits, or equivalently, the diagonal elements of ρ'' are already sorted in decreasing order.

Starting with the simplest case, m=1 (using only one reset qubit), the $diag(\rho'')$ is as follows (from eq.(7.0.5)):

$$diag\left(\rho''\right) = \frac{1}{2} \begin{bmatrix} A_1\left(1+\epsilon_b\right) \\ A_1\left(1-\epsilon_b\right) \\ A_2\left(1+\epsilon_b\right) \\ A_2\left(1-\epsilon_b\right) \\ . \\ . \\ . \\ A_{2d}\left(1+\epsilon_b\right) \\ A_{2d}\left(1-\epsilon_b\right) \end{bmatrix}. \tag{7.0.6}$$

If the elements of ρ'' are already sorted, it implies that

$$A_i(1-\epsilon_b) \geq A_{i+1}(1+\epsilon_b), \tag{7.0.7}$$

for all $i = 1, 2, ..., 2d-1$, which is a condition required for a steady state under the PPA-HBAC. Note that there are many solutions to this set of equations, and, not surprisingly, many steady states of HBAC.

Now, we will show that we can reach a steady state if we start from the totally mixed

state.

Let A_i^t be the evolution of A_i after t iterations of the PPA-HBAC, with $A_i^0 = \frac{1}{2d}$ when the initial state is totally mixed. Interestingly, we have

$$A_i^0(1-\epsilon_b) \leq A_{i+1}^0(1+\epsilon_b), \tag{7.0.8}$$

for all $i = 1, 2, ..., 2d-1$. Note that it is a less than equal sign in distinction from (7.0.7). We will show that if (7.0.8) is true at $t = 0$, it will be true for all future steps t. Moreover, we will also show that if (7.0.8) is obeyed, the rounds of HBAC keep cooling the computational qubits. Thus, the state of the system reaches asymptotically the condition of (7.0.7) with the equality.

We will prove that if we have $\frac{A_i^t}{A_{i+1}^t} \leq \frac{1+\epsilon_b}{1-\epsilon_b}$ for all $i = 1, 2, ..., 2d-1$ at a given moment t, then after an iteration of HBAC we will have $\frac{A_i^{t+1}}{A_{i+1}^{t+1}} \leq \frac{1+\epsilon_b}{1-\epsilon_b}$.

Let ρ_{com}^t be the state of the computational qubits after t iterations. Then, the density matrix of the total qubit system state will be given by $\rho^t = \rho_{com}^t \otimes \rho_{\epsilon_b}$, just after a refresh step. Thus, the total state is as follows:

$$diag(\rho^t) = \begin{bmatrix} p_1^t \\ p_2^t \\ p_3^t \\ p_4^t \\ p_5^t \\ p_6^t \\ . \\ . \\ . \\ p_{2(2d)-1}^t \\ p_{2(2d)}^t \end{bmatrix} = \frac{1}{2} \begin{bmatrix} A_1^t\,(1+\epsilon_b) \\ A_1^t\,(1-\epsilon_b) \\ A_2^t\,(1+\epsilon_b) \\ A_2^t\,(1-\epsilon_b) \\ A_3^t\,(1+\epsilon_b) \\ A_3^t\,(1-\epsilon_b) \\ . \\ . \\ . \\ A_{2d}^t\,(1+\epsilon_b) \\ A_{2d}^t\,(1-\epsilon_b) \end{bmatrix}. \tag{7.0.9}$$

The elements of ρ^t can be written as

$$p^t_{2i-1} = A^t_i(1+\epsilon_b)/2, \text{and} \tag{7.0.10}$$
$$p^t_{2i} = A^t_i(1-\epsilon_b)/2, \tag{7.0.11}$$

for $i = 1, 2, ..., 2d$.

For the next step, we have to compress ρ^t to get ρ^{t+1}, i.e. we have to sort the diagonal elements of ρ^t in decreasing order.

Observe that the elements with factor $(1+\epsilon_b)$ (the blue elements in (7.0.9)) are already in descending order, since $A^t_1 \geq A^t_2 \geq ... \geq A^t_{2d}$. Therefore, during the compression step, these elements can be moved to different entries of the diagonal matrix from the initial ones, but they will have the same order among them (because they are already sorted). It is similar for the elements with factor $(1-\epsilon_b)$ (the red elements).

Assuming $\frac{A^t_i}{A^t_{i+1}} \leq \frac{1+\epsilon_b}{1-\epsilon_b}$, as we have in the initial state, implies that the blue elements are going to go up at least one row, except for $A^t_1(1+\epsilon_b)$ which stays in the same position. Similarly, the red elements are going to go down at least one row, except for $A^t_{2d}(1-\epsilon_b)$ which stays in the same position.

Considering this element movement, we can conclude that the elements of ρ^{t+1} will satisfy the following inequalities:

$$A^t_{i-1}(1-\epsilon_b)/2 \leq p^{(t+1)}_{2i-1} \leq A^t_i(1+\epsilon_b)/2, \text{and} \tag{7.0.12}$$
$$A^t_i(1-\epsilon_b)/2 \leq p^{(t+1)}_{2i} \leq A^t_{i+1}(1+\epsilon_b)/2, \tag{7.0.13}$$

for $i = 2, 3, ..., 2d-1$.

The new computational state, $\rho^{t+1}_{com} = \text{Tr}_m(\rho^{t+1})$, will have diagonal elements $A^{t+1}_i = p^{(t+1)}_{2i-1} + p^{(t+1)}_{2i}$. From this and (7.0.12)-(7.0.13), we have

$$(A^t_{i-1} + A^t_i)(1-\epsilon_b)/2 \leq A^{(t+1)}_i \leq (A^t_i + A^t_{i+1})(1+\epsilon_b)/2, \tag{7.0.14}$$

for $i = 2, 3, ..., 2d-1$. For the first and last diagonal elements of ρ_{com} ($i = 1$ and $i = 2d$),

we know exactly their corresponding values,

$$A_1^{t+1} = (A_1^t + A_2^t)(1+\epsilon_b)/2, \text{and} \tag{7.0.15}$$
$$A_{2d}^{t+1} = (A_{2d-1}^t + A_{2d}^t)(1-\epsilon_b)/2. \tag{7.0.16}$$

These last three equations imply that $\frac{A_i^{t+1}}{A_{i+1}^{t+1}}$ satisfy the following inequality:

$$\frac{A_i^{t+1}}{A_{i+1}^{t+1}} \leq \frac{A_i^t(1+\epsilon_b) + A_{i+1}^t(1+\epsilon_b)}{A_i^t(1-\epsilon_b) + A_{i+1}^t(1-\epsilon_b)} = \frac{1+\epsilon_b}{1-\epsilon_b}, \tag{7.0.17}$$

for all $i = 1, 2, ..., 2d-1$, as we claimed.

A1.1. Increasing purity

We now show that starting in the totally mixed state and applying steps of HBAC, the system will asymptotically go to a state that satisfies the equality in (7.0.7). To show this, we will prove that the target qubit (the spin$-1/2$) is cooled after each iteration of HBAC, and the reset qubit keeps extracting entropy from the system (cooling the system) after each iteration. All this drives asymptotically the initial state to the steady state.

Consider the state of the system after t iterations, (state of the eq. (7.0.9)). Then, the reduced density matrix for the target qubit is

$$diag(\rho_{target}^t) = \begin{bmatrix} \rho_{00_{target}}^t \\ \rho_{11_{target}}^t \end{bmatrix}, \tag{7.0.18}$$

where $\rho_{00_{target}}^t = \sum_{i=1}^{2d} p_i^t = \sum_{i=1}^{d} A_i^t$, and $\rho_{11_{target}}^t = 1 - \rho_{00_{target}}^t$.

Since the compression step reorders the diagonal elements of ρ^t in decreasing order, it is clear that the first $2d$ elements of the new state, ρ^{t+1}, will satisfy $\sum_{i=1}^{2d} p_i^{t+1} \geq \sum_{i=1}^{2d} p_i^t$,

$$\implies \rho_{00_{target}}^{t+1} \geq \rho_{00_{target}}^t. \tag{7.0.19}$$

Therefore, the target qubit is always colder (or remains same) after each iteration of HBAC.

On the other hand, the reset qubit, which has reduced density matrix ρ_r^t when the total system has state ρ^t, will be

$$diag(\rho_r^{t+1}) = \begin{bmatrix} \rho_{00_r}^{t+1} \\ \rho_{11_r}^{t+1} \end{bmatrix}, \tag{7.0.20}$$

where $\rho_{00_r}^{t+1} = \sum_{i=1}^{2d} p_{2i-1}^{t+1}$. This equation, with (7.0.12) and (7.0.10), gives

$$\rho_{00_r}^{t+1} = \sum_{i=1}^{2d} p_{2i-1}^{t+1} \quad \leq \quad \sum_{i=1}^{2d} A_i^t(1+\epsilon_b)/2 = (1+\epsilon_b)/2. \tag{7.0.21}$$

Therefore, the reset qubit will always be hotter than the bath after the compression step of HBAC as long as we do not reach the equality. This implies that the reset qubit always extracts entropy from the total system when it is brought into contact with the heat-bath. The system is cooled in every iteration of the refresh step, with a smaller and smaller amount of entropy extracted, going asymptotically the cooling limit.

The two elements above show that, starting from the totally mixed state, we will converge to the equality of (7.0.7). At this limit, the steady state of the computational qubits should have elements which satisfy

$$\frac{A_{i+1}^{\infty}}{A_i^{\infty}} = \frac{1-\epsilon_b}{1+\epsilon_b} \equiv Q. \tag{7.0.22}$$

Using (7.0.22) and $Tr(\rho_{com}) = 1$, it is possible to find the exact solution of each A_i^{∞}:

$$A_i^{\infty} = \frac{1-Q}{1-Q^{2d}} Q^{i-1}, \tag{7.0.23}$$

and therefore the analytical solution of the steady state of the computational qubits will

be

$$diag\left(\rho_{com}^{\infty}\right) = A_1^{\infty} \begin{bmatrix} 1 \\ Q \\ Q^2 \\ . \\ . \\ . \\ Q^{2d-1} \end{bmatrix}. \tag{7.0.24}$$

A1.2 Asymptotic Polarization of the target qubit for one and multiple reset qubits

Using eq.(7.0.24), the reduced density matrix of the target qubit in the cooling limit is given by

$$diag(\rho_{target}^{\infty}) = A_1^{\infty} \sum_{i=0}^{d-1} Q^i \begin{bmatrix} 1 \\ Q^d \end{bmatrix} = \frac{1}{2} \begin{bmatrix} 1+\epsilon_{\mathbb{1}}^{\infty} \\ 1-\epsilon_{\mathbb{1}}^{\infty} \end{bmatrix}, \tag{7.0.25}$$

where $\epsilon_{\mathbb{1}}^{\infty}$ is the asymptotic polarization of the target qubit when we start with the maximally mixed state.

From this equation we can derive:

$$\epsilon_{\mathbb{1}}^{\infty} = \frac{(1+\epsilon_b)^d - (1-\epsilon_b)^d}{(1+\epsilon_b)^d + (1-\epsilon_b)^d}, \tag{7.0.26}$$

where d is the dimension of the Hilbert space of the scratch qudit ($d = 2l+1$ if we use a spin$-l$, or $d = 2^{n'}$ if we use a string of n' qubits).

Now, if we generalize to the case $m > 1$, we have that the state of the m reset qubits is given by

$$diag(\rho_{\epsilon_b}^{\otimes m}) = \begin{pmatrix} 1+\epsilon \\ 1-\epsilon \end{pmatrix}^{\otimes m} = \begin{pmatrix} (1+\epsilon)^m \\ . \\ . \\ . \\ (1-\epsilon)^m \end{pmatrix}, \tag{7.0.27}$$

where $(1+\epsilon_b)^m$ is the biggest element, and $(1-\epsilon_b)^m$ the smallest one, which correspond to the first entry and the last entry, respectively. Observe that in general the diagonal elements of $\rho_{\epsilon_b}^{\otimes m}$ are not in decreasing order.

From eq. (7.0.5), ρ'' is as follows:

(here I skipped a matrix, that maybe I will not keep as part of the new thesis)

First, notice that any swap between two elements within the same box (which has the same factor A_i) will not improve the entropy compression on the computational qubits state. The reason is once the reset qubits are traced out, the permutation inside the same box contributes to the sum of the probabilities corresponding to same basis state of the computational qubits that they contributed before the compression.

Then, we are just interested in permuting elements to a different box from where they were previously, in particular the biggest element or smallest element of each box (to have the maximum entropy compression). At the cooling limit, there is no operation that can improve the compression, or equivalently, the elements (just taking the largest and smallest of each box) are already sorted.

Following the same reasoning to the case when $m = 1$, the steady state should have elements which hold:

$$A_i^{\infty}(1-\epsilon_b)^m \geq A_{i+1}^{\infty}(1+\epsilon_b)^m. \tag{7.0.28}$$

Moreover, similarly to the case of $m = 1$, the inequality $\frac{A_i}{A_{i+1}} \leq \frac{(1+\epsilon_b)^m}{(1-\epsilon_b)^m}$ cannot be inverted by applying the steps of HBAC. Therefore, if we start with a totally mixed state (which holds the last inequality mentioned), the steady state should have elements which hold

$$A_i^{\infty}(1-\epsilon_b)^m = A_{i+1}^{\infty}(1+\epsilon_b)^m. \tag{7.0.29}$$

Then, the analytical solution of the steady state of the computational qubits will be

$$diag\left(\rho_{com}^{\infty}\right) = A_1^{\infty} \begin{bmatrix} 1 \\ Q^m \\ Q^{2m} \\ . \\ . \\ . \\ Q^{(2d-1)m} \end{bmatrix}. \tag{7.0.30}$$

Similarly, the maximum achievable polarization using m reset qubits will be

$$\epsilon_{\mathbb{1}}^{\infty} = \frac{(1+\epsilon_b)^{md} - (1-\epsilon_b)^{md}}{(1+\epsilon_b)^{md} + (1-\epsilon_b)^{md}}. \tag{7.0.31}$$

Note that a similar polarization would be obtained if we start with a different initial state but which obeys eq.(7.0.8). Numerical simulation indicate that this could also happens with some initial states not obeying eq.(7.0.8). Finally, we can give explicit examples of initial states that lead to an asymptotic polarization higher than eq.(7.0.26).

A1.3. Temperature in the cooling limit

The state of the heat-bath in thermal equilibrium, temperature T_b, is given by $\rho_b = \frac{1}{e^{\Delta E_b/2kT_b} + e^{-\Delta E_b/2kT_b}} \begin{pmatrix} e^{\Delta E_b/2kT_b} & 0 \\ 0 & e^{-\Delta E_b/2kT_b} \end{pmatrix}$, where ΔE_b is the energy gap between the two energy levels of a qubit from the bath.

Then, the heat-bath polarization corresponds to $\epsilon_b = \tanh\left(\frac{\Delta E_b}{2kT_b}\right)$, or equivalently,

$$\frac{\Delta E_b}{2kT_b} = \frac{1}{2}\log\left[\frac{1+\epsilon_b}{1-\epsilon_b}\right]. \tag{7.0.32}$$

Similarly for the target qubit in the steady state at temperature T_{steady}, we will have $\frac{\Delta E_t}{2kT_{steady}} = \frac{1}{2}\log\left[\frac{1+\epsilon_{\mathbb{1}}^{\infty}}{1-\epsilon_{\mathbb{1}}^{\infty}}\right]$, where ΔE_t is the energy gap of the two energy levels of the

target qubit. From this and eq.(7.0.26), we can obtain the temperature in the cooling limit,

$$T_{steady} = \left(\frac{1}{md}\right) T_b \left(\frac{\Delta E_t}{\Delta E_b}\right), \tag{7.0.33}$$

$d = 2^{n'}$ when the scratch qudit is a string of n' qubits ($n'+1$ computational qubits).

The PPA-HBAC method is in line with the third law of thermodynamics, which says that "it is impossible by any procedure, no matter how idealized, to reduce any assembly to absolute zero temperature in a finite number of operations" [64, 68]. Indeed, the evolution of the state of the system goes asymptotically to a steady state, which has non zero temperature for a finite number of qubits. The limit when the temperature is exactly zero corresponds to the case of having an infinite number of qubits. Since the number of gates needed grows with the number of qubits, the operations required to achieve temperature zero will be infinite.

Although the algorithm keeps cooling the target qubit at each time, it does so with a smaller and smaller amount of entropy extracted, asymptotically reaching the steady state of non-zero temperature. This is in agreement with the third law of thermodynamics.

A1.4. Polarization of different computational qubits

Consider the case of having a string of n' qubits as the scratch qudit. The polarization of each qubit can be obtained from the steady state (7.0.24). We already showed how to get the polarization of the target qubit. If we trace out the target qubit from the computational qubits, we can repeat the same calculations to get the polarization of the neighbor qubit in the string (which is labeled as qubit n') since this qubit will be now the first from the left.

The state of the computational qubits without the target qubit is

$$diag(\rho^{\infty}_{target}) = \mathrm{Tr}_{target}(\rho^{\infty}_{com}) = \begin{bmatrix} A^{\infty}_1 + A^{\infty}_{d+1} \\ A^{\infty}_2 + A^{\infty}_{d+2} \\ \cdot \\ \cdot \\ \cdot \\ A^{\infty}_d + A^{\infty}_{2d} \end{bmatrix}. \tag{7.0.34}$$

Let B_i be the ith element of the $diag(\rho^{\infty}_{target})$, i.e. $B_i = A^{\infty}_i + A^{\infty}_{d+i}$. From eq. (7.0.23), $B_i = A^{\infty}_1 Q^{i-1} + A^{\infty}_1 Q^{d+i-1} = A^{\infty}_1 (1+Q^d) Q^{i-1}$. Thus, $B_i = kQ^{i-1}$, where $k = A^{\infty}_1 (1+Q^d)$. Comparing B_i with eq(7.0.23), we see that this state has the same form of the state eq. (7.0.24), but with Hilbert space dimension $d/2$. Thus, the asymptotic polarization of the $n'th$ qubit is

$$\epsilon^{n'}_{max} = \frac{(1+\epsilon_b)^{md/2} - (1-\epsilon_b)^{md/2}}{(1+\epsilon_b)^{md/2} + (1-\epsilon_b)^{md/2}} \tag{7.0.35}$$

where $d = 2^{n'}$.

Similarly, we can get the polarization of the $(n'-1)^{th}$ qubit, and so on. Then, the polarization of the j^{th} qubit will be

$$\epsilon^{(j)}_{max} = \frac{(1+\epsilon_b)^{m2^{j-1}} - (1-\epsilon_b)^{m2^{j-1}}}{(1+\epsilon_b)^{m2^{j-1}} + (1-\epsilon_b)^{m2^{j-1}}}. \tag{7.0.36}$$

A2. Number of steps needed to get $\epsilon = \epsilon^{\infty}_{\mathbb{1}} - \delta$

A2.1. Analytical result for a string of three qubits (m=1, d=2).

The quantum circuit required to perform the PPA-HBAC on three qubits initially in the total mixed state is showed in Fig.2.8. This circuit shows the operations required for the first five iterations (each iteration consists of a refresh step and an entropy compression step). Subsequent iterations gates are the alternate repetition of the second and third iterations gates in Fig.2.8. The application of those two iterations will be referred as a

3qubit-round.

In order to know the effect of one 3qubit-round on the system, consider the state of the computational qubits at a given moment,

$$diag(\rho_{com}^{t}) = \begin{bmatrix} A_1^t \\ A_2^t \\ A_3^t \\ A_4^t \end{bmatrix}, \tag{7.0.37}$$

and the total system as $\rho^t = \rho_{com}^t \otimes \rho_{\epsilon_b}$. The polarization of the target qubit, ϵ^t, can be obtained from its reduced density matrix, $diag(\rho_{target}^t) = \begin{bmatrix} A_1^t + A_2^t \\ A_3^t + A_4^t \end{bmatrix} = \frac{1}{2}\begin{bmatrix} 1+\epsilon^t \\ 1-\epsilon^t \end{bmatrix}$

$$\implies \epsilon^t = 2(A_1^t + A_2^t) - 1. \tag{7.0.38}$$

In the first iteration of the 3qubit-round, the compression gate swaps the scratch qubit and the reset qubit. This swap can be performed by applying the unitary matrix shown in Fig.2.7, thus

$$diag(\rho^t) = \frac{1}{2}\begin{bmatrix} A_1^t(1+\epsilon_b) \\ A_1^t(1-\epsilon_b) \\ A_2^t(1+\epsilon_b) \\ A_2^t(1-\epsilon_b) \\ A_3^t(1+\epsilon_b) \\ A_3^t(1-\epsilon_b) \\ A_4^t(1+\epsilon_b) \\ A_4^t(1-\epsilon_b) \end{bmatrix} \implies \frac{1}{2}\begin{bmatrix} A_1^t(1+\epsilon_b) \\ A_2^t(1+\epsilon_b) \\ A_1^t(1-\epsilon_b) \\ A_2^t(1-\epsilon_b) \\ A_3^t(1+\epsilon_b) \\ A_4^t(1+\epsilon_b) \\ A_3^t(1-\epsilon_b) \\ A_4^t(1-\epsilon_b) \end{bmatrix}. \tag{7.0.39}$$

Then, the density matrix of the computational qubits after the first iteration of the 3qubit-round is

$$diag(\rho_{com}^{t+1}) = \frac{1}{2}\begin{bmatrix} (A_1^t + A_2^t)(1+\epsilon_b) \\ (A_1^t + A_2^t)(1-\epsilon_b) \\ (A_3^t + A_4^t)(1+\epsilon_b) \\ (A_3^t + A_4^t)(1-\epsilon_b) \end{bmatrix}. \tag{7.0.40}$$

In the second iteration of the 3qubit-round, the compression step is performed by applying the unitary matrix shown in Fig.2.4. In this step we obtain ρ^{t+2},

$$diag(\rho^{t+2}) = \frac{1}{4}\begin{bmatrix} (A_1^t + A_2^t)(1+\epsilon_b)^2 \\ (A_1^t + A_2^t)(1+\epsilon_b)(1-\epsilon_b) \\ (A_1^t + A_2^t)(1-\epsilon_b)(1+\epsilon_b) \\ (A_3^t + A_4^t)(1+\epsilon_b)^2 \\ (A_1^t + A_2^t)(1-\epsilon_b)^2 \\ (A_3^t + A_4^t)(1+\epsilon_b)(1-\epsilon_b) \\ (A_3^t + A_4^t)(1-\epsilon_b)(1+\epsilon_b) \\ (A_3^t + A_4^t)(1-\epsilon_b)^2 \end{bmatrix}. \tag{7.0.41}$$

From this state, with the normalization property of the density matrix and (7.0.38), we can obtain the new polarization of the target qubit,

$$\epsilon^{t+2} = 2ab\epsilon^t + \epsilon_b, \tag{7.0.42}$$

where $a = \frac{1+\epsilon_b}{2}$ and $b = \frac{1-\epsilon_b}{2}$.

Let $t = 0$ (just after the iteration 0 which swaps the target qubit and the reset qubit, Fig.2.8), then the polarization of the target qubit at that moment will be $\epsilon^0 = \epsilon_b$. From eq.(7.0.42), we can get the exact polarization after each 3qubit-round, i.e. every two iterations,

$$\epsilon^{t=2j} = \frac{2\epsilon_b}{1+\epsilon_b^2} - q^j\left(\frac{2\epsilon_b}{1+\epsilon_b^2} - \epsilon_0\right), \tag{7.0.43}$$

where $q = \frac{1-\epsilon_b^2}{2}$. From (7.0.26), the asymptotic polarization for this case is $\epsilon_{\mathbb{1}}^{\infty} = \frac{2\epsilon_b}{1+\epsilon_b^2}$, thus eq.(7.0.43) can be written as

$$\epsilon^{t=2j} = \epsilon_{\mathbb{1}}^{\infty} - q^j\left(\epsilon_{\mathbb{1}}^{\infty} - \epsilon_b\right). \tag{7.0.44}$$

Since $q < 1$, $\epsilon^t \to \epsilon_{\mathbb{1}}^{\infty}$ when we increase j.

We can use (7.0.44) to know the number of rounds t needed to achieve polarization $\epsilon_{\mathbb{1}}^{\infty} - \delta$. From Eq. (7.0.44), we have $\delta = q^j\left(\epsilon_{\mathbb{1}}^{\infty} - \epsilon_b\right)$, then the number of rounds required

will be

$$N(\delta, \epsilon_b) := t = 2\frac{\log\left(\frac{\delta}{\epsilon_{\mathbb{1}}^{\infty} - \epsilon_b}\right)}{\log q}, \tag{7.0.45}$$

to get polarization

$$\epsilon_\delta(\epsilon_b, \delta) := \epsilon_{\mathbb{1}}^{\infty} - \delta = \frac{2\epsilon_b}{1+\epsilon_b^2} - \delta. \tag{7.0.46}$$

A2.2. Numerical results

Let $\delta_{rel} = \frac{\epsilon_{\mathbb{1}}^{\infty} - \epsilon}{\epsilon_{\mathbb{1}}^{\infty}} = \delta/\epsilon_{\mathbb{1}}^{\infty}$. Fig.3.3 shows simulations of the number of refresh steps needed to achieve a polarization $\epsilon = \epsilon_{\mathbb{1}}^{\infty}(1 - \delta_{rel})$ as function of δ_{rel} for different values of d. The exact solution of number of steps needed for the 3 qubit case is consistent with the results from the simulations.

A2.3 Upper bound of the number of steps to get a certain polarization, for n qubits

Consider a string of $n' + 1$ computational qubits, enumerated from left to right, and one reset qubit, all starting in totally mixed state. Applying the compression for three qubits, using the reset qubit and qubit 1 to cool qubit 2, we can increase the polarization of qubit 2 to $\epsilon_1 = \epsilon_\delta(\epsilon_b, \delta)$ in $N_1 = N(\delta, \epsilon_b)$ steps, from (7.0.45) and (7.0.46).

After this preparation of qubit 2, we can swap it with qubit 3, and then prepare again qubit 2. We can apply again the compression for three qubits, but now using qubits 2 and 3 to cool qubit 4. In this case, we will need $N_2 = N(\delta, \epsilon_1) \cdot N_1$ number of steps to get polarization $\epsilon_2 = \epsilon_\delta(\epsilon_1, \delta)$ on qubit 4.

We can iterate this idea to use qubit 4 and qubit 5 to cool qubit 6, getting that we need $N_3 = N(\delta, \epsilon_2) \cdot N_2$ number of steps to achieve polarization $\epsilon_3 = \epsilon_\delta(\epsilon_2, \delta)$, and so on.

Since this is not the optimal compression (in terms of entropy extraction, under the assumption that the refresh step re-thermalizes the reset qubits to the heat-bath temperature), this number of iterations gives an upper bound of the optimal number given by PPA. The upper bound is $N_{upper-bound} = \prod_{k=1}^{k=[n'/2]} N(\delta, \epsilon_k)$, to achieve polarization $\epsilon < \epsilon_{max}$

on the target qubit, where $\epsilon_{max} = \epsilon_{\mathbb{1}}^{\infty} = \frac{(1+\epsilon_b)^{d/2}-(1-\epsilon_b)^{d/2}}{(1+\epsilon_b)^{d/2}+(1-\epsilon_b)^{d/2}}$, and $\epsilon = \epsilon_\delta(\epsilon_{h-1}, \delta)$ with $\epsilon_0 = \epsilon_b$, and $h = [n'/2]$ (the integer part of $n'/2$).

Appendix B: HBAC with correlated qubit-environment interactions

B1: Precise calculation for NOE on two qubits

We generalize our calculation of the maximum polarization for the NOE algorithm to any bath-polarization, $|\epsilon_b| \leq 1$, following the circuit of Fig. 4.2. The operation Γ_2, applied to an initial diagonal density-matrix of a 2-qubit-system, produces

$$\begin{aligned} &\mathrm{diag}\,(\rho) = (N_0, N_1, N_2, N_3) \\ &\xrightarrow{\Gamma_2} [(N_0+N_3)p_2, N_1, N_2, (N_0+N_3)(1-p_2)], \end{aligned} \tag{7.0.47}$$

where $p_2 = \frac{e^{2\xi}}{2\cosh 2\xi}$ (with $\epsilon_b = \tanh(\xi)$)is the population of the state $|00\rangle$ at thermal equilibrium with the heat-bath, normalized by the sum of thermal populations of both states $|00\rangle$ and $|11\rangle$ (i.e. $p_2 = e^{2\xi}/N$, where $N = e^{2\xi} + e^{2\xi} = 2\cosh 2\xi$); and so $1-p_2$ is the complementary population of $|11\rangle$ at thermal equilibrium.

In the cooling limit, the polarization of the target qubit ϵ^{∞}_{NOE} is a fix point of the algorithm, thus after applying an iteration it will remain the same, i.e.

$$\begin{aligned} &\frac{1}{2}\left(1+\epsilon^{\infty}_{NOE}, 1-\epsilon^{\infty}_{NOE}\right) \otimes \frac{1}{2}\left(1,1\right) \\ &\xrightarrow{\Gamma_2} \frac{1}{4}\left(2p_2, 1+\epsilon^{\infty}_{NOE}, 1-\epsilon^{\infty}_{NOE}, 2(1-p_2)\right) \\ &\xrightarrow{CMS} \frac{1}{2}\left(\frac{1+2p_2+\epsilon^{\infty}_{NOE}}{2}, \frac{3-2p_2-\epsilon^{\infty}_{NOE}}{2}\right) \otimes \frac{1}{2}\left(1,1\right). \end{aligned} \tag{7.0.48}$$

The asymptotic polarization should hence obey

$$\begin{aligned} 2p_2 &= \tfrac{1+2p_2+\epsilon_{NOE}^{\infty}}{2} \\ \Rightarrow \epsilon_{NOE}^{\infty} &= 2p_2 - 1 = \tanh 2\xi \end{aligned} \tag{7.0.49}$$

B2. NOE with multiple reset qubits

We generalize our description of NOE to a system of n qubits. The description consists of the iteration of two steps. In the first step, we saturate (totally mix) all the qubits with the exception of the first qubit. In the second step, we apply the state-reset Γ_n. Under this process, the polarization evolution of the first qubit will increase asymptotically to a maximum value. To find the cooling limit, which corresponds to the fixed point of the algorithm, we assume that it has a final polarization ϵ_f, and we use the condition that if we reapply the two steps of the algorithm that polarization will stay the same. Then, by applying the two steps we have the following: after the saturation, the diagonal of the state of the system is

$$\begin{aligned} &\xrightarrow{CMS} \frac{1}{2}\left(1+\epsilon_f, 1-\epsilon_f\right) \otimes \left[\frac{1}{2}\left(1,1\right)\right]^{\otimes(n-1)} \\ &= \frac{1}{2^n}\left(1+\epsilon_f, 1+\epsilon_f, ..., 1-\epsilon_f, 1-\epsilon_f\right), \end{aligned} \tag{7.0.50}$$

this is a vector with the first 2^{n-1} elements equal to $\frac{1}{2^n}\left(1+\epsilon_f\right)$ and the last 2^{n-1} elements equal to $\frac{1}{2^n}\left(1-\epsilon_f\right)$. Then, under the operation Γ_n, for low polarization, the system will evolve to

$$\frac{1}{2^n}\left(1+n\epsilon_b, 1+\epsilon_f, ..., 1-\epsilon_f, 1-n\epsilon_b\right), \tag{7.0.51}$$

changing the first and last element to $\frac{1}{2^n}\left(1+n\epsilon_b\right)$ and $\frac{1}{2^n}\left(1-n\epsilon_f\right)$, respectively. This results in a polarization $\left[n\epsilon_b + \left(2^{n-1}-1\right)\epsilon_f\right]/2^{n-1}$, which should be equal to the final polarization ϵ_f, thus $\epsilon_f = n\epsilon_b$. This generalized NOE, taken on its own, does not always give better results than the PPA (see section IV-C, where we present the SRΓ_n-HBAC method: a different way to exploit Γ_n to increase the polarization beyond the PPA class of algorithms, in a smaller number of iterations).

B3. State-Reset HBAC protocols

B3.1. Maximum achievable polarization of the SRΓ_2-HBAC

Let's start with two qubits at thermal equilibrium, with polarizations ϵ_b, i.e. with state

$$\rho_0^{n=2} = \rho_{\epsilon_b}^{\otimes 2} = \left[\frac{1}{2}\begin{pmatrix} 1+\epsilon_b & 0 \\ 0 & 1-\epsilon_b \end{pmatrix}\right]^{\otimes 2} = \left[\frac{1}{2\cosh\xi_b}\begin{pmatrix} e^{\xi_b} & 0 \\ 0 & e^{-\xi_b} \end{pmatrix}\right]^{\otimes 2}, \tag{7.0.52}$$

where ξ_b is related to the bath polarization by $\epsilon_b = \tanh(\xi_b)$. This state can be expressed as a vector of its diagonal elements as $\mathrm{diag}\left(\rho_0^{n=2}\right) = \frac{1}{4\cosh^2\xi_b}\left(e^{2\xi_b}, 1, 1, e^{-2\xi_b}\right)$.

For a general polarization, the state-evolution during the first round of the algorithm will be as follows:

$$\begin{aligned}
&\mathrm{diag}\left(\rho_0^{n=2}\right) = \frac{1}{4\cosh^2\xi_b}\left(e^{2\xi_b}, 1, 1, e^{-2\xi_b}\right) \\
&\xrightarrow{X} \frac{1}{4\cosh^2\xi_b}\left(1, e^{2\xi_b}, e^{-2\xi_b}, 1\right) \\
&\xrightarrow{\Gamma_2} \frac{1}{4\cosh^2\xi_b}\left(2p_2, e^{2\xi_b}, e^{-2\xi_b}, 2\left(1-p_2\right)\right) \\
&= \frac{1}{4\cosh^2\xi_b}\left(\frac{e^{2\xi_b}}{\cosh 2\xi_b}, e^{2\xi_b}, e^{-2\xi_b}, \frac{e^{-2\xi_b}}{\cosh 2\xi_b}\right) \\
&\xrightarrow{\Gamma_1} \frac{1}{2\cosh 2\xi_b}\left(e^{2\xi_b}, e^{-2\xi_b}\right) \otimes \frac{1}{2}\left(p_1, 1-p_1\right) \\
&= \frac{1}{2\cosh 2\xi_b}\left(e^{2\xi_b}, e^{-2\xi_b}\right) \otimes \frac{1}{2\cosh\xi_b}\left(e^{\xi_b}, e^{-\xi_b}\right).
\end{aligned} \tag{7.0.53}$$

After the first round, the polarization of the first qubit will increase to $\tanh 2\xi_b$ ($\approx 2\epsilon_b$ for low polarization). Assume that after k rounds of the algorithm, the polarization of the first qubit is $\epsilon_k^{(n=2)} = \tanh\xi_k$. Note that after the operation Γ_1, the system will be in a product state, with the second qubit with polarization $\epsilon_b = \tanh\xi_b$. Then, we apply one

more round to obtain $\epsilon_{k+1}^{(n=2)}$, as follows:

$$\begin{aligned}
&\frac{1}{2\cosh\xi_k}\left(e^{\xi_k},e^{-\xi_k}\right)\otimes\frac{1}{2\cosh\xi_b}\left(e^{\xi_b},e^{-\xi_b}\right)=\\
&\frac{1}{4}\left(1+\tanh\xi_k,1-\tanh\xi_k\right)\otimes\left(1+\tanh\xi_b,1-\tanh\xi_b\right)\\
&\xrightarrow{X}\frac{1}{4}\left(1+\tanh\xi_k,1-\tanh\xi_k\right)\otimes\left(1-\tanh\xi_b,1+\tanh\xi_b\right)\\
&\xrightarrow{\Gamma_2}\frac{1}{4}((2-2\tanh\xi_k\tanh\xi_b)\,p_2,(1+\tanh\xi_k)\left(1+\tanh\xi_b\right),\\
&\qquad\left(1-\tanh\xi_k\right)\left(1-\tanh\xi_b\right),(2-2\tanh\xi_k\tanh\xi_b)\left(1-p_2\right))\\
&=\quad\frac{1}{4}((1-\tanh\xi_k\tanh\xi_b)\left[1+\tanh(2\xi_b)\right],(1+\tanh\xi_k)\left(1+\tanh\xi_b\right),\\
&\qquad\left(1-\tanh\xi_k\right)\left(1-\tanh\xi_b\right),(1-\tanh\xi_k\tanh\xi_b)\left[1-\tanh(2\xi_b)\right])\\
&\xrightarrow{\Gamma_1}\frac{1}{2}(1+\frac{1}{2}\mathrm{sech}(2\xi_b)\left[\sinh(3\xi_b)\mathrm{sech}\xi_b+\tanh\xi_k\right],\\
&\qquad1-\frac{1}{2}\mathrm{sech}(2\xi_b)\left[\sinh(3\xi_b)\mathrm{sech}\xi_b+\tanh\xi_k\right])\otimes\frac{1}{2}\left(1+\tanh\xi_b,1-\tanh\xi_b\right).
\end{aligned}\tag{7.0.54}$$

From here, the polarization increases from ϵ_k to $\epsilon_{k+1}=\frac{1}{2}\mathrm{sech}(2\xi_b)\left[\sinh(3\xi_b)\mathrm{sech}\xi_b+\tanh\xi_k\right]$. With initial polarization $\epsilon_0=\epsilon_b\,(=\tanh\xi_b)$, we find that $\epsilon_k\leq\epsilon_{k+1}$, for all k. In the cooling limit, $\epsilon_\infty=\epsilon_{\infty+1}$, i.e.

$$\tanh\xi_\infty=\frac{1}{2}\mathrm{sech}(2\xi_b)\left[\sinh(3\xi_b)\mathrm{sech}\xi_b+\tanh\xi_\infty\right].\tag{7.0.55}$$

From here, the maximum polarization achievable, in the two-qubit case, will be

$$\boxed{\epsilon_\infty^{(n=2)}=\tanh 3\xi_b}$$

leading to a significant improvement abpve PPA.

B3.2. Maximum achievable cooling of the SRΓ_3 HBAC

In general for any ϵ_b, to calculate the polarization's evolution as a function of the number of rounds, let $\epsilon_k^{(n=3)}$ be the polarization of the first qubit after k rounds. Then,

let's apply one more round on the system to obtain $\epsilon_{k+1}^{(n=3)}$. After applying $\text{Alg}_{\text{n=2}}$ in round $k+1$, the state will be $\frac{1}{2}(1+\epsilon_k, 1-\epsilon_k) \otimes \frac{1}{2}(1+\tanh 3\xi_b, 1-\tanh 3\xi_b) \otimes \frac{1}{2}(1+\epsilon_b, 1-\epsilon_b)$. Then, by flipping the second and third qubit, the state will evolve to $\frac{1}{2}(1+\epsilon_k, 1-\epsilon_k) \otimes \frac{1}{2}(1-\tanh 3\xi_b, 1+\tanh 3\xi_b) \otimes \frac{1}{2}(1-\epsilon_b, 1+\epsilon_b)$. At this point, the first and last elements of the diagonal density matrix are $\alpha_1 := 1/8(1+\epsilon_k)(1-\tanh 3\xi_b)(1-\epsilon_b)$ and $\alpha_2 := 1/8(1-\epsilon_k)(1+\tanh 3\xi_b)(1+\epsilon_b)$, respectively. The sum of these two elements is $A := \alpha_1 + \alpha_2 = 1/4(1-\epsilon_k \tanh 3\xi_b + \tanh 3\xi_b \epsilon_b - \epsilon_k \epsilon_b)$, thus the state-reset Γ_3 will change these elements to Ap_3 and to $A(1-p_3)$, respectively. Thus, the new polarization of the first qubit will be $\epsilon_{k+1} = \epsilon_k + 2(Ap_3 - \alpha_1)$. Substituting α_1, A, $p_3 = (1+\tanh 3\xi_b)/2$, and $\epsilon_b = \tanh \xi_b$ in ϵ_{k+1}, we obtain

$$\epsilon_{k+1}^{(n=3)} = \frac{\epsilon_k^{(n=3)}(2\cosh \xi_b + \cosh 5\xi_b) + \sinh 7\xi_b}{2\cosh \xi_b + \cosh 5\xi_b + \cosh 7\xi_b}. \tag{7.0.56}$$

From here, starting with polarization $\epsilon_0 = \epsilon_b$ $(= \tanh \xi_b)$, each round gives an improvement, $\epsilon_k \leq \epsilon_{k+1}$, for all k.

In the cooling limit it is not possible to keep increasing this purity, i.e. $\epsilon_\infty^{(n=3)} = \epsilon_{\infty+1}^{n=3}$, then, from eq.(7.0.56), the maximum polarization achievable with our algorithm for the three qubit case is

$$\boxed{\epsilon_\infty^{(n=3)} = \tanh 7\xi_b}$$

leading to an improvement on both the NOE and the PPA.

B4. NOE-based HBAC

In this appendix, we present a more practical algorithm based on regular NOE. In this case, the algorithm is limited to use only Γ_2 to implement regular NOE within a subroutine, in addition to entropy compressions, and qubit-resets. Note that this method is less general than our SRΓ_n-HBAC, presented in this paper, but still gets better polarization than the PPA.

i. The two-qubit case

When NOE is complemented with a final step of qubit-reset on the non-target qubit, the entire system will be cooled (the target qubit will increase its polarization to tanh2ξ, and the second qubit will be returned to the equilibrium after being saturated). We name this simple algorithm "2-NOE-based HBAC", and it will be used as a subroutine in this appendix, when cooling a string of more qubits.

The obtained probabilities to be in state $|0\rangle$ for each qubit, after applying the "2-NOE-based HBAC", are $(1+2\epsilon_b)/2$, and $(1+\epsilon_b)/2$, respectively, in the low polarization case. We can denote this probabilities in a more simply way, using the shifted-and-scaled diagonal terms $\{2,1\}$ in units of ϵ_b.

ii. The 3 qubit case

Here, we show how to use the subroutine "2-NOE-based HBAC" in the three-qubit case, to get probabilities $\{3,2,1\}$ written in the shifted-and-scaled diagonal form in units of ϵ_b, for low polarization.

Let's start from thermal equilibrium, i.e. with $\{1,1,1\}$ in the shifted-and-scaled diagonal form. First, we apply the subroutine "2-NOE-based HBAC" on the second and third qubits, to obtain $\{1,2,1\}$. Then, we cool the target qubit to 2 using a SORT step (known as 3-bit-compression in the three-qubit case), to get $\{2,1,1\}$. Applying again a subroutine "2-NOE-based HBAC", we obtain $\{2,2,1\}$). We can repeat these steps, to achieve $\{2.5,2,1\}$). In the same way, another repetition yields $\{2.75,2,1\}$).

The polarization enhancement of the target qubit grows asymptotically to a fixed point, corresponding to polarization ϵ^∞. After one iteration, in the cooling limit, $\epsilon^\infty \to (3\epsilon_b + \epsilon^\infty)/2$ implies that $\epsilon^\infty = 3\epsilon_b$, yielding the final string polarization $\{3,2,1\}$.

iii. The n-qubit case

Using the same process as above, in combination with 3-bit-compressions, it is easy to obtain a Fibonacci-like series $\{...,13,8,5,3,2,1\}$, for low polarization; note the only advantage over the SMW-Fibonacci is that the above is better than $\{...,8,5,3,2,1,1\}$ with

the same number of qubits.

Moreover, by using entropy compressions, SORT, rather than 3-bit-compression, as in the original PPA, we obtain polarizations $\{...24, 12, 6, 3, 2, 1\}$, improving over the original PPA, namely $\{...16, 8, 4, 2, 1, 1\}$.

Appendix C: Initial-Correlation Enhanced Algorithmic Cooling

C1. CP-local passivity: Fundamental limitations to Local Energy Extraction in Quantum Systems

Leave a hot mug of coffee on your desk and it will cool down; but in the quantum world, could it heat up? In ordinary macroscopic systems, classical thermodynamics dictates that energy flows from hot to cold; however in the microscopic regime, where quantum effects become relevant, this direction of energy flow surprisingly may be blocked or even inverted [2]. Some natural questions arise: When would it be impossible to extract energy to cool down a hot body, even by making contact with a colder one? What are the relevant quantum effects that prevent that? How can we circumvent these possible cooling limitations?

In this Appendix, a partial answer to these questions is presented, in particular for the impossibility of extracting energy *locally* from a bipartite quantum system in the presence of strong coupling and entanglement. Here it is shown how quantum effects, such as entanglement, can obstruct outgoing energy flows, via fast local interaction, preventing a hot body to dissipate its energy to a colder one. I will present a full set of necessary and sufficient conditions that fully characterize this type of passivity, which we called CP-Local passivity.

System setup and allowed operations – We focus on the problem of cooling interacting multipartite systems to which only local access to a single subsystem is granted.

We explore the most general type of local access to quantum systems, which is given by the CPTP maps, making our results relevant for any physical platform in which the subsystems are spatially separated.

Let us consider the bipartite quantum system made by the subsystems A and B, with associated Hilbert space $\mathcal{H}_A \otimes \mathcal{H}_B$, and global Hamiltonian H_{AB}.

Given a state ρ_{AB}, the maximum extractable energy under a local map on A is

$$\begin{aligned} \Delta E_{(A)B} &= \min_{\mathcal{E}_A} \Delta E^{\mathcal{E}_A}_{(A)B} \\ &:= \min_{\mathcal{E}_A} \mathrm{Tr}[H_{AB}(\mathcal{E}_A \otimes \mathcal{I}_B)\rho_{AB}] - \mathrm{Tr}[H_{AB}\rho_{AB}], \end{aligned} \tag{7.0.57}$$

where $\mathcal{I}_B$ is the identity channel on B, and the optimization is over the whole set of CPTP maps on A. The above optimization can be easily written as a *semidefinite program* (see [10, 115] for introductory references to the subject). Therefore, it is very practical to calculate $\Delta E_{(A)B}$ and to find the CPTP map which minimizes the energy. Moreover, we see that energy cannot be extracted when this quantity is zero, which motivates the following definition.

Definition 9. *[CP-local passivity] The pair $\{\rho_{AB}, H_{AB}\}$ is CP-local passive with respect to subsystem A if and only if*

$$\Delta E_{(A)B} = \Delta E^{\mathcal{I}_A}_{(A)B} = 0. \tag{7.0.58}$$

That is, a system is CP-local passive if the best local strategy for extracting energy (as measured by the global Hamiltonian H_{AB}) is to act trivially on it. The word *passive* is used here in analogy to the commonly known passive states [62], from which energy cannot be extracted under unitary maps. Throughout, we assume that the time evolution given by the Hamiltonian H_{AB} does not play a role. This means that this setting applies to situations in which the local actions happen quickly, in the same spirit as that of fast local quenches or pulses in other quantum thermodynamic settings [37, 82].

Let us now outline how this might be possible. First, let us rewrite the term corresponding to the average energy of the system after applying a local map, as follows:

$$\mathrm{Tr}[H_{AB}(\mathcal{E}_A \otimes \mathcal{I}_B)\rho_{AB}] = \mathrm{Tr}[C_{AA'}E_{AA'}]. \tag{7.0.59}$$

where $E_{AA'}$ is the Choi-Jamiołkowski operator for an arbitrary channel $\mathcal{E}_A : A \to A'$, and

$C_{AA'} \in \mathcal{H}_A \otimes \mathcal{H}_{A'}$ the Hermitian operator $C_{AA'} \equiv \mathrm{Tr}_B[\rho_{AB}^{\Gamma_A} H_{A'B}]$, with $\rho_{AB}^{\Gamma_A}$ the partial transpose on A [1].

Let us now assume that CP-local passivity holds, such that for all $E_{AA'}$ the energy of the system does not decrease after the local action:

$$\mathrm{Tr}[C_{AA'} E_{AA'}] \geq \mathrm{Tr}[H_{AB}\rho_{AB}], \tag{7.0.60}$$

We can rewrite the right hand side, using the fact that $E_{AA'}$ satisfies $\mathrm{Tr}_{A'}[E_{AA'}] = \mathbb{I}_A$, and defining $d_A|\Phi\rangle\langle\Phi|$ as the Choi-Jamiołkowski operator for the identity channel, as

$$\begin{aligned} \mathrm{Tr}[H_{AB}\rho_{AB}] &= \mathrm{Tr}\left[d_A|\Phi\rangle\langle\Phi|C_{AA'}\right] \\ &= \mathrm{Tr}_A\left[\mathrm{Tr}_{A'}[d_A|\Phi\rangle\langle\Phi|C_{AA'}]\mathrm{Tr}_{A'}[E_{AA'}]\right] \\ &= \mathrm{Tr}[(\mathrm{Tr}_{A'}[d_A|\Phi\rangle\langle\Phi|C_{AA'}] \otimes \mathbb{I}_{A'})E_{AA'}]. \end{aligned} \tag{7.0.61}$$

Since this holds for all $E_{AA'}$, this suggests that CP-local passivity will hold whenever the following operator inequality is true

$$C_{AA'} \geq \mathrm{Tr}_{A'}[d_A|\Phi\rangle\langle\Phi|C_{AA'}] \otimes \mathbb{I}_{A'}.$$

Complete conditions – The previous inequality in fact gives the necessary and sufficient condition. This constitutes our first main result:

Theorem 1. – The pair $\{\rho_{AB}, H_{AB}\}$ is CP-local passive with respect to subsystem A if and only if $\mathrm{Tr}_{A'}[d_A|\Phi\rangle\langle\Phi|C_{AA'}]$ is Hermitian and

$$C_{AA'} - \mathrm{Tr}_{A'}[d_A|\Phi\rangle\langle\Phi|C_{AA'}] \otimes \mathbb{I}_{A'} \geq 0, \tag{7.0.62}$$

where $\mathcal{H}_{A'}$ is a copy of the Hilbert space $\mathcal{H}_A$, $C_{AA'} \in \mathcal{H}_A \otimes \mathcal{H}_{A'}$ is a Hermitian operator defined as $C_{AA'} \equiv \mathrm{Tr}_B[\rho_{AB}^{\Gamma_A} H_{A'B}]$, with $\rho_{AB}^{\Gamma_A}$ the partial transpose on A, and $d_A|\Phi\rangle\langle\Phi|$ the (maximally entangled) Choi-Jamiołkowski operator of the identity channel.

[1] The Choi-Jamiołkowski operator of a quantum channel $\mathcal{E}_{A\to A}(\cdot)$ is defined as $E = d_A \mathcal{E}_{A\to A} \otimes \mathcal{I}|\Phi\rangle\langle\Phi|$, the result of applying it to an un-normalized maximally entangled state $d_A|\Phi\rangle\langle\Phi| = \sum_{i,j} |i_A\rangle\langle j_A| \otimes |i_{A'}\rangle\langle j_{A'}|$ on the Hilbert space of A and a copy A'. Note that the partial transpose is with respect to the same basis as the one chosen for the Choi-Jamiołkowski operator.

Notice that Eq. (7.0.62) only depends on ρ_{AB} and H_{AB} through the operator $C_{AA'}$. In fact, Eq. (7.0.59) guarantees that this operator contains all the information about how much energy can be extracted through local operations. Once it is constructed, the operator inequality can be easily checked to find whether the pair $\{\rho_{AB}, H_{AB}\}$ is CP-local passive or not. If it is not, the semidefinite program can be solved to find the amount of energy that can be extracted, as well as the minimizing CPTP map. The proof can be found in the Supplemental Material of our paper [2], together with details on semidefinite programming duality theory, which we use in a similar manner as in the proof of the Holevo-Yuen-Kennedy-Lax conditions for quantum state discrimination [45, 46, 118, 117].

On top of this characterization, we show that the condition of Theorem 1 is robust to errors, by using a recent result concerning convex channel optimization problems [22]. Roughly, if the operator on the LHS of Eq. (7.0.62) has smallest eigenvalue $-\varepsilon \leq 0$, then the amount of energy that can be extracted is bounded as $\Delta E_{(A)B} \geq -\varepsilon\, d_A$. We give the precise statement and the proof in the Supplemental Material of our paper [2].

Sufficient conditions – The condition of Theorem 1, even though it is simple to verify, makes no direct reference to physical properties of the pair $\{\rho_{AB}, H_{AB}\}$. It is important, however, to find physically relevant situations in which CP-local passivity holds. To that end, we derive sufficient conditions for steady states $\rho_{AB} = \sum_{i=0}^{d_A \times d_B - 1} p_i |E_i\rangle\langle E_i|$ of Hamiltonians $H_{AB} = \sum_{i=0}^{d_A \times d_B - 1} E_i |E_i\rangle\langle E_i|$ of full Schmidt rank with a non-degenerate ground state. Steady states are always trivially CP-local passive for $p_0 = 1$, and Frey et al. [34] found qualitative conditions under which there exists a threshold ground state population p_* such that the pair $\{\rho_{AB}, H_{AB}\}$ remains CP-local passive for all $p_0 \geq p_*$. Here, we provide explicit upper bounds on p_* in terms of ground state entanglement and the energy gap with the first excited state.

Theorem 2. – Threshold ground state population: Let the ground state $|E_0\rangle$ of the Hamiltonian H_{AB} be non-degenerate and with full Schmidt rank. All pairs $\{\rho_{AB}, H_{AB}\}$ with $\rho_{AB} = \sum_i p_i |E_i\rangle\langle E_i|$ and $p_0 \geq p_*$ are CP-local passive with respect to A, with the threshold ground state population bounded from above by

$$p_* \leq \left(1 + \frac{E_1 (q^{AB}_{0,\min})^2}{\max_{i\geq 1} \left[E_i (q^{AB}_{i,\max})^2\right]}\right)^{-1} . \tag{7.0.63}$$

$\{q^{AB}_{i,\alpha}\}_{\alpha=0}^{d_A-1}$ denotes the Schmidt coefficients of $|E_i\rangle$ and $q^{AB}_{i,\min} \equiv \min_\alpha \left[q^{AB}_{i,\alpha}\right]$, $q^{AB}_{i,\max} \equiv$

$\max_\alpha \left[q_{i,\alpha}^{AB}\right]$. See the Supplemental Material of our paper [2] for the proof, and an example illustrating the tightness of the bound. The idea behind it is that, if the ground state population is high enough, the energetic changes caused by any CPTP map will be dominated by the energy gained by exciting the ground state into higher energy levels, making the total change non-negative.

For thermal states, this result implies that, if the ground state has full Schmidt rank, there exists a threshold temperature $T_* > 0$ below which CP-local passivity holds (note that if $T = 0$, CP-local passivity holds trivially). Moreover, this threshold temperature is such that

$$\langle H \rangle_{\beta_*} \geq E_1 p_0 (q_{0,\min}^{AB})^2 \ , \tag{7.0.64}$$

where $\langle H \rangle_{\beta_*}$ is the average energy in the thermal state of inverse temperature β_*.

C2. The PPA protocol on interacting qubits

Here, we show how the fact of having an interacting quantum system will affect the final purity when we want to cool down a single qubit. In particular, we implement the PPA-HBAC method on a system of three qubits, and obtain the final purity for different coupling intensities.

System setup – The system consists of three qubits A, B and C, with Hamiltonian

$$H = H_A + H_B + H_C + V,$$

$$H_A = h_A \sigma_z^A, \qquad H_B = h_B \sigma_z^B, \qquad H_C = h_C \sigma_z^C, \qquad V = k_{AB} \sigma_x^A \sigma_x^B + k_{AC} \sigma_x^A \sigma_x^C + k_{BC} \sigma_x^B \sigma_x^C,$$

where h and κ are positive constants.

Let the system start in the totally mixed state, and implement the PPA protocol for different values of the coupling strength κ. The quantum circuit required to perform the PPA on the three qubits, initially in the totally mixed state, is showed in Fig. 2.8. We are taking A, B and C as the target, the scratch and the reset qubits which are denoted as T, S, and R, respectively, in the circuit.

We simulate the evolution of the state of the system under the PPA method, and we consider that between each two steps of the PPA-HBAC algorithm, there will be a time t for the evolution given for the Hamiltonian. The results are presented in Fig. 7.1, for different coupling parameters. For convenience, we fix $t = 1$ to only control the parameters with k/h.

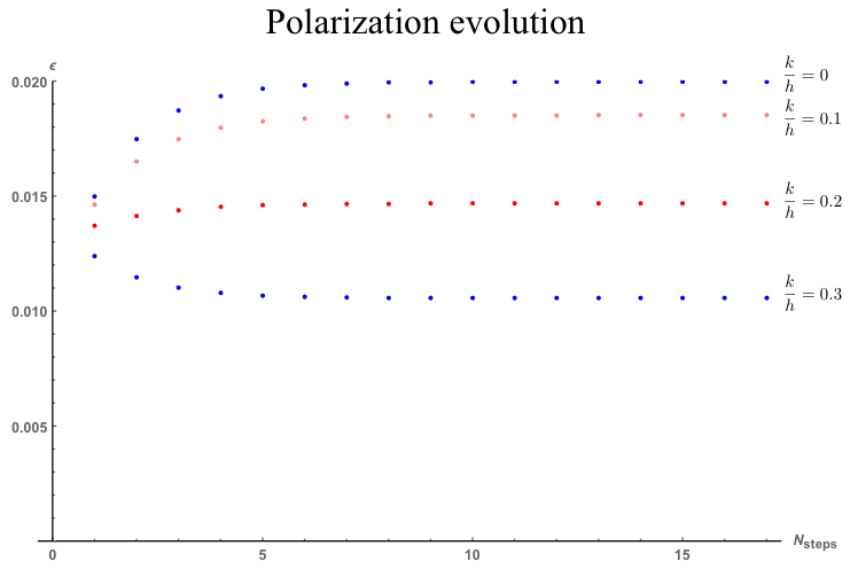

Figure 7.1: Polarization evolution of the target qubit under the application of the PPA-HBAC method on the three qubits, for a heat-bath polarization $\epsilon_b = 0.01$, as a function of the number of iterations of the algorithm (each iteration is shown in the circuit of Figure.5. The results presented correspond to the $k/h = 0, 0.1, 0.2$, and $k/h = 0.3$, and were obtained by simulation. Note that the asymptotic polarization is lower when the coupling of the qubits is stronger.

The results show that even having conventional HBAC methods or very cold thermal reservoirs, the entanglement of the state implies that when we are cooling down the whole system, the subsystem consisting only of the target qubit will remain in a mixed state.Therefore, studying new methods of cooling that take the interaction into account is needed, as QET, which we already demonstrated that it is a potential solution.

C3. Derivation of the QET-HBAC protocols

Here we present the derivation in detail of the QET-HBAC protocols presented in chapter 5.

Step 1: POVM measurement on A, and its energy cost

Alice carries out a POVM on σ_x of A, which commutes with the interaction Hamiltonian V. She obtains the outcome μ (that can take either value $+1$ or -1). The action of the most general measurement on the system is described by the measurement operator

$$M_A(\mu) = e^{i\delta_\mu}\left(m_\mu + e^{i\alpha_\mu} l_\mu \sigma_A^x\right)$$

in a single shot measurement. The coefficients m_μ, l_μ, α_μ and δ_μ are real constants which satisfies

$$\sum_\mu m_\mu^2 + l_\mu^2 = 1,$$

and

$$\sum_\mu m_\mu l_\mu \cos\alpha_\mu = 0.$$

The resulting post-measurement state $|\psi_{\mathrm{PM}}\rangle$ is given by the usual update rule

$$|\psi_{\mathrm{PM}}(\mu)\rangle = \frac{1}{\sqrt{p_A(\mu)}} M_A(\mu)|g\rangle$$

where $p_A(\mu)$ is the probability of outcome μ.

We obtain the following post-measurement average state

$$\rho_1 = \sum_{\mu=\pm1} p_A(\mu)|\psi_{\mathrm{PM}}(\mu)\rangle\langle\psi_{\mathrm{PM}}(\mu)| = \sum_{\mu=\pm1} M_A^\dagger(\mu)|g\rangle\langle g|M_A(\mu).$$

Now remember that $|g\rangle$ had a zero energy expectation. Let us analyze the energy expectation of ρ_1. Let us call it E_{M_A} since it will represent the average energy cost of

carrying out the POVM on qubit A:

$$\begin{aligned} E_{M_A} =& \mathrm{Tr}\left(\rho_1 H\right) = \sum_{\mu=\pm 1} \langle g|M_A^\dagger(\mu) H M_A(\mu)|g\rangle \\ =& \sum_{\mu=\pm 1} \langle g|M_A^\dagger(\mu) H_A M_A(\mu)|g\rangle + \\ & \sum_{\mu=\pm 1} \langle g|M_A^\dagger(\mu) H_B M_A(\mu)|g\rangle + \\ & \sum_{\mu=\pm 1} \langle g|M_A^\dagger(\mu) V M_A(\mu)|g\rangle \end{aligned} \tag{7.0.65}$$

notice that since $M_A(\mu)H_B = M_A(\mu)V = 0$ it is rather easy to prove that

$$\sum_{\mu=\pm 1} \langle g|M_A^\dagger(\mu) H_B M_A(\mu)|g\rangle = \sum_{\mu=\pm 1} \langle g|H_B M_A^\dagger(\mu) M_A(\mu)|g\rangle =$$

$$\frac{1}{2}\sum_{\mu=\pm 1}\left((m_\mu^2 + l_\mu^2)\underbrace{\langle g|H_B|g\rangle}_{0} + 2 l_\mu m_\mu \cos\alpha_\mu \langle g|H_B \sigma_x^A|g\rangle\right) = 0$$

since

$$\langle g|H_B\sigma_x^A|g\rangle \propto \langle g|\sigma_z^B\sigma_x^A|g\rangle = 0.$$

Similarly

$$\sum_{\mu=\pm 1} \langle g|M_A(\mu)^\dagger V M_A(\mu)|g\rangle = \sum_{\mu=\pm 1} \langle g|V M_A^\dagger(\mu) M_A(\mu)|g\rangle =$$

$$\frac{1}{2}\sum_{\mu=\pm 1}\left((m_\mu^2 + l_\mu^2)\underbrace{\langle g|V|g\rangle}_{0} + 2 l_\mu m_\mu \cos\alpha_\mu \langle g|V \sigma_x^A|g\rangle\right) = 0$$

Since

$$\langle g|V\sigma_x^A|g\rangle \propto \langle g|\sigma_x^B|g\rangle = 0.$$

therefore the energy cost of the measurement (on average) is

$$E_{M_A} = \sum_{\mu=\pm 1} \langle g|M_A^\dagger(\mu) H_A M_A(\mu)|g\rangle = \frac{2h^2}{\sqrt{h^2+k^2}} \sum_\mu l_\mu^2 > 0. \tag{7.0.66}$$

Let us remark this: the average cost of the local measurement on A over an ensemble of many measurements is positive and it is 'localized' in H_A (even though, of course, the average energy cost is computed as the difference of the expectation of the full Hamiltonian pre and post-measurement).

Steps 2,3: Classical communication and classically-controlled local unitary on B to improve its polarization

Bob receives the information about Alice's outcome of her measurement. With that information Bob carries out a local unitary operation on B. We assume that the speed of the classical channel is much faster than the inverse of the coupling frequency $1/k$, so the non-local dynamics is frozen during the time it takes from the measurement on A to the unitary operation on B. We will discuss in detail why that scale in a later section. Now Bob carries out the following local operation on B. The operation that maximizes the purity of B is the one that maximizes Bob's energy extraction. Hence, we optimize the parameters to the optimal QET ones.

$$U_B(\mu) = \cos\Omega_\mu \mathbb{1} + i \sin\Omega_\mu \sigma_y^B$$

where μ is the outcome of the POVM $M_A(\mu)$ and Ω_μ is a real constant which satisfies

$$\cos(2\Omega_\mu) = \frac{(h^2+2k^2)\, p_A(\mu)}{\sqrt{(h^2+2k^2)^2 p_A(\mu)^2 + h^2k^2 q_A(\mu)^2}},$$

$$\sin(2\Omega_\mu) = -\frac{hk q_A(\mu)}{\sqrt{(h^2+2k^2)^2 p_A(\mu)^2 + h^2k^2 q_A(\mu)^2}},$$

where $p_A(\mu) = m_\mu^2 + l_\mu^2$ and $q_A(\mu) = 2 l_\mu m_\mu \cos\alpha_\mu$.

In a single shot experiment, the system's state after applying this unitary is

$$U_B(\mu)|\psi_{\rm PM}\rangle = \frac{1}{\sqrt{p_A(\mu)}} U_B(\mu) M_A(\mu)|g\rangle.$$

But, again, we cannot address individual qubits. For an ensemble of qubits, we would get the following average state

$$\rho_2 = \sum_{\mu=\pm 1} U_B(\mu) M_A(\mu)|g\rangle\langle g|M_A^\dagger(\mu) U_B^\dagger(\mu).$$

Notice that on an ensemble of identical setups, on average, Alice's side POVM is not purifying the ensamble system on its own (we are averaging over all possible outcomes of the measurement with their weights) Therefore the entropy decrease on B is completely due to the (averaged effect) of U_B.

C4. Energy yield of the controlled-unitary.

Let us call E_{U_B} the average energy cost of the unitary applied on B. E_{U_B} will be the difference in the expectation of the full Hamiltonian after the unitary and the expectation after the measurement and before the unitary, this is

$$E_{U_B} = \mathrm{Tr}(\rho_2 H) - \mathrm{Tr}(\rho_1 H) = \mathrm{Tr}(\rho_2 H) - E_{M_A}$$

Now,

$$\begin{aligned}
\mathrm{Tr}(\rho_2 H) &= \sum_{\mu=\pm 1} \langle g|M_A(\mu) U_B^\dagger(\mu) H U_B(\mu) M_A(\mu)|g\rangle && (7.0.67)\\
&= \sum_{\mu=\pm 1} \langle g|M_A(\mu) U_B^\dagger(\mu) H_A U_B(\mu) M_A(\mu)|g\rangle && (7.0.68)\\
&+ \sum_{\mu=\pm 1} \langle g|M_A(\mu) U_B^\dagger(\mu) H_B U_B(\mu) M_A(\mu)|g\rangle \\
&+ \sum_{\mu=\pm 1} \langle g|M_A(\mu) U_B^\dagger(\mu) V U_B(\mu) M_A(\mu)|g\rangle && (7.0.69)
\end{aligned}$$

Now since $U_B(\mu)H_A = 0$, the first summand on the right hand side of the equation above is just

$$\sum_{\mu=\pm 1} \langle g|M_A(\mu)U_B^\dagger(\mu)H_A U_B(\mu)M_A(\mu)|g\rangle =$$

$$\sum_{\mu=\pm 1} \langle g|M_A^\dagger(\mu)H_A M_A(\mu)|g\rangle = E_{M_A}$$

therefore, substituting this we get that the average energy cost of the unitary $U_B(\mu)$ is simply

$$E_{U_B} = \mathrm{Tr}(\rho_2 H) - \mathrm{Tr}(\rho_1 H) = \mathrm{Tr}\left[\rho_2(H_B + V)\right] =$$

$$\sum_\mu \langle g|M_A^\dagger(\mu)U_B^\dagger(\mu)[H_B + V]U_B(\mu)M_A(\mu)|g\rangle$$

where we have used that $M_A(\mu)H_B = M_A(\mu)V = 0$. It is moderately lengthy but straightforward to obtain that

$$E_{U_B} = \frac{h^2 + 2k^2}{\sqrt{h^2+k^2}} \sum_\mu p_A(\mu) \left[\sqrt{1 + \frac{h^2k^2}{(h^2+2k^2)^2}\frac{q_A(\mu)^2}{p_A(\mu)^2}} - 1\right].$$

On average, performing the local unitary gives away energy. This energy is always smaller or equal than the energy put there by the local measurement on A.

C5. Purity/Polarization Improvement on B

Here we show the calculations for the improvement on the polarization of applying the minimal QET. The initial polarization of B is $\epsilon_0^B = \frac{h}{\sqrt{h^2+k^2}}$, which is calculated as $Tr\left(\rho_b \sigma_z\right)$, where $\rho_b = Tr_A\left(|g\rangle\langle g|\right)$. The corresponding initial purity, $Tr\left(\rho_b^2\right)$, is $\frac{2h^2+k^2}{2(h^2+k^2)}$.

After doing the measurement on A and applying the unitary operation to extract energy from B, the final polarization of B is going to be given by $\epsilon_2^B = Tr\left(\rho_{2B}\sigma_Z\right)$, where $\rho_{2B} = Tr_A(\rho_2)$, as follows

$$\epsilon_2^{\mathrm{B}} = \frac{1}{\sqrt{h^2+k^2}}(-h\cos 2\Omega_0 + 2kl_1m_1(\sin 2\Omega_0 - \sin 2\Omega_1) + h\left(l_1^2 + m_1^2\right)(\cos 2\Omega_0 - \cos 2\Omega_1)). \quad (7.0.70)$$

The final purity is given by

$$Tr\left(\rho_{2B}^2\right) = \frac{1}{2\left(h^2+k^2\right)}\Big((2h^2+k^2-4hkl_1m_1\sin\left[2\Omega_0-2\Omega_1\right] \\ +4\left[4k^2l_1^2m_1^2+h^2\left(-1+l_1^2+m_1^2\right)\left(l_1^2+m_1^2\right)\right]\sin^2\left[\Omega_0-\Omega_1\right]\Big).$$

Here, we have assumed $\alpha_\mu = 0$ for simplicity, but it could be another parameter subject to optimization.

References

[1] Álvaro M Alhambra, Matteo Lostaglio, and Christopher Perry. Heat-bath algorithmic cooling with optimal thermalization strategies. *Quantum*, 3:188, 2019.

[2] Álvaro M Alhambra, Georgios Styliaris, Nayeli A Rodriguez-Briones, Jamie Sikora, and Eduardo Martín-Martínez. Fundamental limitations to local energy extraction in quantum systems. *Physical review letters*, 123(19):190601, 2019.

[3] Andris Ambainis, Leonard J Schulman, and Umesh V Vazirani. Computing with highly mixed states. In *Proceedings of the thirty-second annual ACM symposium on Theory of computing*, pages 697–704. ACM, 2000.

[4] Yosi Atia, Yuval Elias, Tal Mor, and Yossi Weinstein. Algorithmic cooling in liquid-state nuclear magnetic resonance. *Physical Review A*, 93(1):012325, 2016.

[5] Yosi Atia and Tal Mor. *Algorithmic Cooling of Spins by Optimal Control*. PhD thesis, Computer Science Department, Technion, 2012.

[6] Murray D Barrett, B DeMarco, T Schaetz, V Meyer, D Leibfried, J Britton, J Chiaverini, WM Itano, B Jelenković, JD Jost, et al. Sympathetic cooling of 9 be+ and 24 mg+ for quantum logic. *Physical Review A*, 68(4):042302, 2003.

[7] Jonathan Baugh, Osama Moussa, Colm A Ryan, Ashwin Nayak, and Raymond Laflamme. Experimental implementation of heat-bath algorithmic cooling using solid-state nuclear magnetic resonance. *Nature*, 438(7067):470–473, 2005.

[8] Charles H Bennett, Herbert J Bernstein, Sandu Popescu, and Benjamin Schumacher. Concentrating partial entanglement by local operations. *Physical Review A*, 53(4):2046, 1996.

[9] Rajendra Bhatia. *Matrix analysis*, volume 169. Springer Science & Business Media, 2013.

[10] Stephen Boyd, Stephen P Boyd, and Lieven Vandenberghe. *Convex optimization*. Cambridge university press, 2004.

[11] P Oscar Boykin, Tal Mor, Vwani Roychowdhury, Farrokh Vatan, and Rutger Vrijen. Algorithmic cooling and scalable NMR quantum computers. *Proceedings of the National Academy of Sciences*, 99(6):3388–3393, 2002.

[12] Fernando Brandao, Michał Horodecki, Nelly Ng, Jonathan Oppenheim, and Stephanie Wehner. The second laws of quantum thermodynamics. *Proceedings of the National Academy of Sciences*, 112(11):3275–3279, 2015.

[13] Fernando GSL Brandao, Michał Horodecki, Jonathan Oppenheim, Joseph M Renes, and Robert W Spekkens. Resource theory of quantum states out of thermal equilibrium. *Physical review letters*, 111(25):250404, 2013.

[14] Gilles Brassard, Yuval Elias, José M Fernandez, Haggai Gilboa, Jonathan A Jones, Tal Mor, Yossi Weinstein, and Li Xiao. Experimental heat-bath cooling of spins. *The European Physical Journal Plus*, 129(12):266, 2014.

[15] Gilles Brassard, Yuval Elias, Tal Mor, and Yossi Weinstein. Prospects and limitations of algorithmic cooling. *The European Physical Journal Plus*, 129(11):1–16, 2014.

[16] Nicolas Brunner, Marcus Huber, Noah Linden, Sandu Popescu, Ralph Silva, and Paul Skrzypczyk. Entanglement enhances cooling in microscopic quantum refrigerators. *Physical Review E*, 89(3):032115, 2014.

[17] DE Chang, LMK Vandersypen, and M Steffen. NMR implementation of a building block for scalable quantum computation. *Chemical physics letters*, 338(4-6):337, 2001.

[18] Bob Coecke, Tobias Fritz, and Robert W Spekkens. A mathematical theory of resources. *Information and Computation*, 250:59–86, 2016.

[19] David G Cory, Amr F Fahmy, and Timothy F Havel. Ensemble quantum computing by NMR spectroscopy. *Proceedings of the National Academy of Sciences*, 94(5):1634–1639, 1997.

[20] David G Cory, R Laflamme, E Knill, L Viola, TF Havel, N Boulant, G Boutis, E Fortunato, S Lloyd, R Martinez, et al. NMR based quantum information processing: Achievements and prospects. *Fortschritte der Physik*, 48(9-11):875–907, 2000.

[21] David G Cory, MD Price, W Maas, E Knill, Raymond Laflamme, Wojciech H Zurek, Timothy F Havel, and SS Somaroo. Experimental quantum error correction. *Physical Review Letters*, 81(10):2152, 1998.

[22] Bryan Coutts, Mark Girard, and John Watrous. Certifying optimality for convex quantum channel optimization problems. *arXiv preprint arXiv:1810.13295*, 2018.

[23] Raoul Dillenschneider and Eric Lutz. Energetics of quantum correlations. *EPL (Europhysics Letters)*, 88(5):50003, 2009.

[24] David P Divincenzo. The physical implementation of quantum computation. *Fortschritte der Physik*, 48:771–783, 2000.

[25] Dario Egloff, Oscar CO Dahlsten, Renato Renner, and Vlatko Vedral. A measure of majorization emerging from single-shot statistical mechanics. *New Journal of Physics*, 17(7):073001, 2015.

[26] Yuval Elias, José M Fernandez, Tal Mor, and Yossi Weinstein. Optimal algorithmic cooling of spins. *Israel Journal of Chemistry*, 46(4):371–391, 2006.

[27] Yuval Elias, Haggai Gilboa, Tal Mor, and Yossi Weinstein. Heat-bath cooling of spins in two amino acids. *Chemical Physics Letters*, 517(4):126–131, 2011.

[28] Yuval Elias, Tal Mor, and Yossi Weinstein. Semioptimal practicable algorithmic cooling. *Physical Review A*, 83(4):042340, 2011.

[29] Jose M Fernandez, Seth Lloyd, Tal Mor, and Vwani Roychowdhury. Algorithmic cooling of spins: A practicable method for increasing polarization. *International Journal of Quantum Information*, 2(04):461–477, 2004.

[30] Jose M Fernandez, Tal Mor, and Yossi Weinstein. Paramagnetic materials and practical algorithmic cooling for NMR quantum computing. *International Journal of Quantum Information*, 3(1):281–285, 2005.

[31] Richard P Feynman. Simulating physics with computers. *International journal of theoretical physics*, 21(6):467–488, 1982.

[32] P. Forn-Diaz, J. J. Garcia-Ripoll, B. Peropadre, J. L. Orgiazzi, M. A. Yurtalan, R. Belyansky, C. M. Wilson, and A. Lupascu. Ultrastrong coupling of a single artificial atom to an electromagnetic continuum in the nonperturbative regime. *Nat Phys*, 13(1):39–43, 2017.

[33] Nahuel Freitas, Rodrigo Gallego, Lluís Masanes, and Juan Pablo Paz. Cooling to absolute zero: The unattainability principle. In *Thermodynamics in the Quantum Regime*, pages 597–622. Springer, 2018.

[34] Michael Frey, Ken Funo, and Masahiro Hotta. Strong local passivity in finite quantum systems. *Physical Review E*, 90(1):012127, 2014.

[35] Michael R Frey, Karl Gerlach, and Masahiro Hotta. Quantum energy teleportation between spin particles in a gibbs state. *Journal of Physics A: Mathematical and Theoretical*, 46(45):455304, 2013.

[36] Nicolai Friis, Marcus Huber, and Martí Perarnau-Llobet. Energetics of correlations in interacting systems. *Phys. Rev. E*, 93:042135, 2016.

[37] R Gallego, A Riera, and J Eisert. Thermal machines beyond the weak coupling regime. *New Journal of Physics*, 16(12):125009, 2014.

[38] Neil A Gershenfeld and Isaac L Chuang. Bulk spin-resonance quantum computation. *science*, 275(5298):350–356, 1997.

[39] Robin Giles. *Mathematical foundations of thermodynamics: International series of monographs on pure and applied mathematics*, volume 53. Elsevier, 2016.

[40] John Goold, Marcus Huber, Arnau Riera, Lídia del Rio, and Paul Skrzypczyk. The role of quantum information in thermodynamics—a topical review. *Journal of Physics A: Mathematical and Theoretical*, 49(14):143001, 2016.

[41] Gilad Gour, Markus P Müller, Varun Narasimhachar, Robert W Spekkens, and Nicole Yunger Halpern. The resource theory of informational nonequilibrium in thermodynamics. *Physics Reports*, 583:1–58, 2015.

[42] Lov K Grover. A fast quantum mechanical algorithm for database search. In *Proceedings of the twenty-eighth annual ACM symposium on Theory of computing*, pages 212–219, 1996.

[43] Yelena Guryanova, Nicolai Friis, and Marcus Huber. Ideal projective measurements have infinite resource costs. *Quantum*, 4:222, 2020.

[44] Jonathan S Hodges, Jamie C Yang, Chandrasekhar Ramanathan, and David G Cory. Universal control of nuclear spins via anisotropic hyperfine interactions. *Physical Review A*, 78(1):010303, 2008.

[45] Alexander S Holevo. Statistical decision theory for quantum systems. *Journal of multivariate analysis*, 3(4):337–394, 1973.

[46] Alexander S Holevo. Statistical problems in quantum physics. In *Proceedings of the second Japan-USSR Symposium on probability theory*, pages 104–119. Springer, 1973.

[47] Michał Horodecki and Jonathan Oppenheim. Fundamental limitations for quantum and nanoscale thermodynamics. *Nature communications*, 4(1):1–6, 2013.

[48] Masahiro Hotta. A protocol for quantum energy distribution. *Physics Letters A*, 372(35):5671–5676, 2008.

[49] Masahiro Hotta. Quantum measurement information as a key to energy extraction from local vacuums. *Physical Review D*, 78(4):045006, 2008.

[50] Masahiro Hotta. Quantum energy teleportation in spin chain systems. *Journal of the Physical Society of Japan*, 78(3):034001, 2009.

[51] Masahiro Hotta. Controlled hawking process by quantum energy teleportation. *Physical Review D*, 81(4):044025, 2010.

[52] Masahiro Hotta. Energy entanglement relation for quantum energy teleportation. *Physics Letters A*, 374(34):3416–3421, 2010.

[53] Masahiro Hotta, Jiro Matsumoto, and Go Yusa. Quantum energy teleportation without a limit of distance. *Physical Review A*, 89(1):012311, 2014.

[54] Dominik Janzing, Pawel Wocjan, Robert Zeier, Rubino Geiss, and Th Beth. Thermodynamic cost of reliability and low temperatures: tightening landauer's principle and the second law. *International Journal of Theoretical Physics*, 39(12):2717–2753, 2000.

[55] Phillip Kaye. Cooling algorithms based on the 3-bit majority. *Quantum Information Processing*, 6(4):295–322, 2007.

[56] Navin Khaneja. Switched control of electron nuclear spin systems. *Physical Review A*, 76(3):032326, 2007.

[57] Emanuel Knill and Raymond Laflamme. Power of one bit of quantum information. *Physical Review Letters*, 81(25):5672, 1998.

[58] Emanuel Knill, Raymond Laflamme, and Lorenza Viola. Theory of quantum error correction for general noise. *Physical Review Letters*, 84(11):2525, 2000.

[59] Kamil Korzekwa. Coherence, thermodynamics and uncertainty relations. *Imperial College London*, 2016.

[60] Kamil Korzekwa. Structure of the thermodynamic arrow of time in classical and quantum theories. *Physical Review A*, 95(5):052318, 2017.

[61] Thaddeus D Ladd, Fedor Jelezko, Raymond Laflamme, Yasunobu Nakamura, Christopher Monroe, and Jeremy L O'Brien. Quantum computers. *Nature*, 464(7285):45–53, 2010.

[62] Andrew Lenard. Thermodynamical proof of the gibbs formula for elementary quantum systems. *Journal of Statistical Physics*, 19(6):575–586, 1978.

[63] Malcolm H Levitt. *Spin dynamics: basics of nuclear magnetic resonance*. John Wiley & Sons, 2001.

[64] Amikam Levy, Robert Alicki, and Ronnie Kosloff. Quantum refrigerators and the third law of thermodynamics. *Physical Review E*, 85(6):061126, 2012.

[65] Jun Li, Dawei Lu, Zhihuang Luo, Raymond Laflamme, Xinhua Peng, and Jiangfeng Du. Maximally accessible purity in coherently controlled open quantum systems: application to quantum state engineering. *Phys. Rev. A*, 94(3):032316, 2016.

[66] Pietro Liuzzo-Scorpo, Luis A Correa, Rebecca Schmidt, and Gerardo Adesso. Thermodynamics of quantum feedback cooling. *Entropy*, 18(2):48, 2016.

[67] Iman Marvian and Robert W Spekkens. Asymmetry properties of pure quantum states. *Physical Review A*, 90(1):014102, 2014.

[68] Lluis Masanes and Jonathan Oppenheim. A derivation (and quantification) of the third law of thermodynamics. *arXiv:1412.3828*, 2014.

[69] Lluis Masanes and Jonathan Oppenheim. A general derivation and quantification of the third law of thermodynamics. *Nature communications*, 8:14538, 2017.

[70] Emma McKay, Nayeli A Rodríguez-Briones, and Eduardo Martín-Martínez. Fluctuations of work cost in optimal generation of correlations. *Physical Review E*, 98(3):032132, 2018.

[71] Tal Mor, Vwani Roychowdhury, Seth Lloyd, Jose Manuel Fernandez, and Yossi Weinstein. Algorithmic cooling, 2004. US Patent 20,040,051,528.

[72] Tal Mor, Vwani Roychowdhury, Seth Lloyd, Jose Manuel Fernandez, and Yossi Weinstein. Algorithmic cooling, 2005. US Patent 6,873,154.

[73] Osama Moussa. On heat-bath algorithmic cooling and its implementation in solid-state NMR. Master of science in physics thesis, University of Waterloo, 2005.

[74] Michael A Nielsen and Isaac Chuang. Quantum computation and quantum information, 2002.

[75] T. Niemczyk, F. Deppe, H. Huebl, E. P. Menzel, F. Hocke, M. J. Schwarz, J. J. Garcia-Ripoll, D. Zueco, T. Hummer, E. Solano, A. Marx, and R. Gross. Circuit quantum electrodynamics in the ultrastrong-coupling regime. *Nat Phys*, 6(10):772–776, 2010.

[76] Albert W Overhauser. Paramagnetic relaxation in metals. *Physical Review*, 89(4):689, 1953.

[77] Daniel K Park, Guanru Feng, Robabeh Rahimi, Stéphane Labruyère, Taiki Shibata, Shigeaki Nakazawa, Kazunobu Sato, Takeji Takui, Raymond Laflamme, and

Jonathan Baugh. Hyperfine spin qubits in irradiated malonic acid: heat-bath algorithmic cooling. *Quantum Information Processing*, 14(7):2435–2461, 2015.

[78] Daniel K Park, Nayeli A Rodriguez-Briones, Guanru Feng, Robabeh Rahimi, Jonathan Baugh, and Raymond Laflamme. Heat bath algorithmic cooling with spins: review and prospects. In *Electron Spin Resonance (ESR) Based Quantum Computing*, pages 227–255. Springer, 2016.

[79] Daniel K Park, Nayeli A Rodriguez-Briones, Guanru Feng, Robabeh Rahimi, Jonathan Baugh, and Raymond Laflamme. Heat bath algorithmic cooling with spins: review and prospects. In *Electron Spin Resonance (ESR) Based Quantum Computing*, pages 227–255. Springer, 2016.

[80] Om Patange. On an instrument for the coherent investigation of nitrogen-vacancy centres in diamond. Master of science in physics thesis, University of Waterloo, 2013.

[81] Martí Perarnau-Llobet, Karen V Hovhannisyan, Marcus Huber, Paul Skrzypczyk, Nicolas Brunner, and Antonio Acín. Extractable work from correlations. *Physical Review X*, 5(4):041011, 2015.

[82] Martí Perarnau-Llobet, H Wilming, A Riera, R Gallego, and J Eisert. Strong coupling corrections in quantum thermodynamics. *Physical review letters*, 120(12):120602, 2018.

[83] Yuval Peres. Iterating von neumann's procedure for extracting random bits. *The Annals of Statistics*, 20(1):590–597, 1992.

[84] B. Peropadre, P. Forn-Díaz, E. Solano, and J. J. García-Ripoll. Switchable ultrastrong coupling in circuit qed. *Phys. Rev. Lett.*, 105:023601, 2010.

[85] Christopher Perry, Piotr Ćwikliński, Janet Anders, Michał Horodecki, and Jonathan Oppenheim. A sufficient set of experimentally implementable thermal operations for small systems. *Physical Review X*, 8(4):041049, 2018.

[86] David Poulin, Robin Blume-Kohout, Raymond Laflamme, and Harold Ollivier. Exponential speedup with a single bit of quantum information: Measuring the average fidelity decay. *Physical review letters*, 92(17):177906, 2004.

[87] J. F. Poyatos, J. I. Cirac, and P. Zoller. Quantum reservoir engineering with laser cooled trapped ions. *Phys. Rev. Lett.*, 77:4728–4731, 1996.

[88] Sadegh Raeisi and Michele Mosca. Asymptotic bound for heat-bath algorithmic cooling. *Physical Review Letters*, 114(10):100404, 2015.

[89] Nayeli A Rodriguez-Briones, Jun Li, Xinhua Peng, Tal Mor, Yossi Weinstein, and Raymond Laflamme. Heat-bath algorithmic cooling with correlated qubit-environment interactions. *New Journal of Physics*, 19(11):113047, 2017.

[90] Nayeli A Rodríguez-Briones, Eduardo Martín-Martínez, Achim Kempf, and Raymond Laflamme. Correlation-enhanced algorithmic cooling. *Physical review letters*, 119(5):050502, 2017.

[91] Nayeli Azucena Rodriguez Briones. Achievable polarization for heat-bath algorithmic cooling. Master's thesis, University of Waterloo, 2015.

[92] Nayeli Azucena Rodríguez Briones. Computación cuántica. *Eek – Science outreach – Council for Science, Technology and Innovation of Zacatecas*, 2017.

[93] Nayeli Azucena Rodríguez-Briones and Raymond Laflamme. Achievable polarization for heat-bath algorithmic cooling. *Physical review letters*, 116(17):170501, 2016.

[94] Nayeli Azucena Rodriguez-Briones, Jun Li, Xinhua Peng, Tal Mor, Yossi Weinstein, and Raymond Laflamme. Comments on: Asymptotic bound for heat-bath algorithmic cooling. *arXiv preprint arXiv:1506.01778*, 2015.

[95] Ernst Ruch, Rudolf Schranner, and Thomas H Seligman. Generalization of a theorem by hardy, littlewood, and pólya. *Journal of Mathematical Analysis and Applications*, 76(1):222–229, 1980.

[96] C. A. Ryan, O Moussa, J Baugh, and R Laflamme. Spin based heat engine: demonstration of multiple rounds of algorithmic cooling. *Physical review letters*, 100(14):140501, 2008.

[97] L. J. Schulman and U. Vazirani. Scalable NMR quantum computation. In *Proceedings of the 31th Annual ACM Symposium on the Theory of Computation (STOC)*, pages 322–329, El Paso, Texas, 1998. ACM Press.

[98] Leonard J Schulman, Tal Mor, and Yossi Weinstein. Physical limits of heat-bath algorithmic cooling. *Physical review letters*, 94(12):120501, 2005.

[99] Leonard J Schulman, Tal Mor, and Yossi Weinstein. Physical limits of heat-bath algorithmic cooling. *SIAM Journal on Computing*, 36(6):1729–1747, 2007.

[100] Leonard J Schulman and Umesh V Vazirani. Molecular scale heat engines and scalable quantum computation. In *Proceedings of the thirty-first annual ACM symposium on Theory of computing*, pages 322–329. ACM, 1999.

[101] Peter W Shor. Algorithms for quantum computation: discrete logarithms and factoring. In *Proceedings 35th annual symposium on foundations of computer science*, pages 124–134. Ieee, 1994.

[102] Peter W Shor. Polynomial-time algorithms for prime factorization and discrete logarithms on a quantum computer. *SIAM journal on computing*, 26(5):1484–1509, 1997.

[103] Paul Skrzypczyk, Anthony J Short, and Sandu Popescu. Work extraction and thermodynamics for individual quantum systems. *Nature communications*, 5:4185, 2014.

[104] I. Solomon. Relaxation processes in a system of two spins. *Phys. Rev.*, 99:559, 1955.

[105] O. W. Sørensen. A universal bound on spin dynamics. *Journal of Magnetic Resonance (1990)*, 86:435–440, 1990.

[106] Ole W Sørensen. The entropy bound as a limiting case of the universal bound on spin dynamics. polarization transfer in $i_n s_m$ spin systems. *Journal of Magnetic Resonance (1969)*, 93(3):648–652, 1991.

[107] Ole Winneche Sørensen. Polarization transfer experiments in high-resolution NMR spectroscopy. *Progress in Nuclear Magnetic Resonance Spectroscopy*, 21(6):503–569, 1989.

[108] Philip Taranto, Faraj Bakhshinezhad, Philipp Schüttelkopf, and Marcus Huber. Exponential improvement for quantum cooling through finite memory effects. *arXiv preprint arXiv:2004.00323*, 2020.

[109] Jose Trevison and Masahiro Hotta. Quantum energy teleportation across a three-spin ising chain in a gibbs state. *Journal of Physics A: Mathematical and Theoretical*, 48(17):175302, 2015.

[110] Lieven MK Vandersypen and Isaac L Chuang. NMR techniques for quantum control and computation. *Reviews of modern physics*, 76(4):1037, 2005.

[111] Guillaume Verdon-Akzam, Eduardo Martín-Martínez, and Achim Kempf. Asymptotically limitless quantum energy teleportation via qudit probes. *Phys. Rev. A*, 93:022308, 2016.

[112] John Von Neumann. Various techniques used in connection with random digits. *National Bureau of Standards Applied Mathematics Series*, pages 12:36–38, 1951.

[113] George Proctor Wadsworth, Joseph G Bryan, and A Cemal Eringen. Introduction to probability and random variables, 1961.

[114] HengYan Wang, Jian Pan, WenQiang Zheng, and XinHua Peng. Algorithmic cooling based on cross-relaxation and decoherence-free subspace. *Science China-Physics mechanics and Astronomy*, 63(7), 2020.

[115] John Watrous. *The theory of quantum information*. Cambridge University Press, 2018.

[116] Jin-Shi Xu, Man-Hong Yung, Xiao-Ye Xu, Sergio Boixo, Zheng-Wei Zhou, Chuan-Feng Li, Alán Aspuru-Guzik, and Guang-Can Guo. Demon-like algorithmic quantum cooling and its realization with quantum optics. *Nature Photonics*, 8(2):113–118, 2014.

[117] Horace Yuen, Robert Kennedy, and Melvin Lax. Optimum testing of multiple hypotheses in quantum detection theory. *IEEE transactions on information theory*, 21(2):125–134, 1975.

[118] Horace P Yuen, Robert S Kennedy, and Melvin Lax. On optimal quantum receivers for digital signal detection. *Proceedings of the IEEE*, 58(10):1770–1773, 1970.

[119] Yingjie Zhang, Colm A Ryan, Raymond Laflamme, and Jonathan Baugh. Coherent control of two nuclear spins using the anisotropic hyperfine interaction. *Physical review letters*, 107(17):170503, 2011.

Chapter 8

List of publications

The work presented in this thesis contains material from the following publications and preprints:

- N. Rodríguez Briones, and R. Laflamme, "Achievable polarization for Heat-Bath Algorithmic Cooling", Phys. Rev. Lett. 116, 170501 (2016) [93, 91]
- N. Rodríguez Briones, E. Martín-Martínez, A. Kempf, and R. Laflamme, "Correlation-Enhanced Algorithmic Cooling", Phys. Rev. Lett. 119 (5), 050502 (2017) [90]
- N. Rodríguez Briones, J. Li, X. Peng, T. Mor, Y. Weinstein, and R. Laflamme, "Heat-Bath Algorithmic Cooling with correlated qubit-environment interactions", New Journal of Physics 19 (11), 113047, (2017) [89]
- A. Alhambra, G. Styliaris, N. Rodríguez Briones, J. Sikora, and E. Martín-Martínez, "Fundamental limitations to local cooling of quantum systems", Phys. Rev. Lett. 123, 190601 (2019) [2]
- N. Rodríguez Briones, R. Spekkens, "N-to-1 distillation of athermality for two-level systems", in progress

Other publications completed during the duration of my PhD but not included in this thesis are:

- E McKay, N. Rodríguez-Briones, and E. Martín-Martínez, "Fluctuations of work cost in optimal generation of correlations", Phys. Rev. E 98, 032132 (2018) [70]
- N. Rodríguez Briones, "Computación cuántica", Science Outreach article. Eek Magazine. Consejo Zacatecano de Ciencia, Tecnología e Innovación (2017) [92]
- D. K. Park, N. Rodríguez Briones, G. Feng, R. Rahimi, J. Baugh, and R. Laflamme, "Heat Bath Algorithmic Cooling with Spins: Review and Prospects", Book Chapter in L. Berliner et al. (eds.), Electron Spin Resonance (ESR) Based Quantum Computing, Biological Magnetic Resonance 31, DOI 10.1007/978-1-4939-3658-8-8, Springer New York 2016) [78]